Functions of the ubiquitin system in mammalian spermatogenesis and skeletal muscle

Zhiyu Pang
Division of Experimental Medicine
Department of Medicine
McGill University
Montreal, Canada
September 2010

A thesis submitted to McGill University in partial fulfillment of the requirements of the degree of Doctor of Philosophy

© Zhiyu Pang, 2010

Abstract

The conjugation of ubiquitin to proteins is catalyzed sequentially by a cascade of members of three classes of enzymes – ubiquitin activating enzyme (E1), ubiquitin conjugating enzyme (E2), and ubiquitin protein ligase (E3). Polyubiquitinated protein substrates are selectively targeted for degradation by the proteasome. Removal of ubiquitin from ubiquitinated substrates is catalyzed by deubiquitinating enzymes (DUB). In this thesis, I have explored functions of three specific enzymes of the ubiquitin system, the E2 UBC4-testis, the HECT E3 EDD/Rat100 and the deubiquitinating enzyme USP19, in mammalian spermatogenesis or muscle wasting.

UBC4-testis is a rodent testis specific E2 enzyme that is induced in round spermtids. Mice lacking the UBC4-testis gene had a delay in postnatal development during the first wave of spermatogenesis but ultimately had in adulthood normal fertility and testis weights, spermatid number, protein content, rate of ubiquitination and quantity and quality of sperm. When subjected to the heat stress of experimental cryptorchidism, the profile of germ cell degeneration was not significantly different from that of wild type mice. Our data suggest that UBC4-testis has a specific function in promoting the evolution of the first wave of spermatogenesis; however, some coexisting isoforms of UBC4 may serve redundant complementary functions in later stages of spermatogenesis.

EDD/Rat100 is a UBC4 dependent E3 that is highly expressed in rat testis. The poly(A)-binding protein (PABP) is a translation initiation factor that is negative regulated by the

PABP-interacting protein 2 (Paip2). Both PABP and EDD/Rat100 share a PABC domain, through which they can interact with Paip2. EDD/Rat100 can ubiquitinate Paip2 in vitro. Under normal *in vivo* conditions, the abundant PABP may sequester Paip2 from ubiquitination by EDD/Rat100. In PABP-depleted cells, Paip2 is free to interact with EDD/Rat100, which leads to Paip2 ubiquitination and degradation by the proteasome. Degradation of Paip2 may then restore the activity of PABP and therefore maintain its homeostasis. Thus, the turnover of Paip2 in the cell is mediated by EDD/Rat100 but is regulated by PABP. In addition, six proteins that were copurified from immunoprecipitation of EDD/Rat100 in rat testis have been elaborately studied, but none of them was identified as a *bona fide* substrate of EDD/Rat100.

Finally, I studied USP19, a 150 kDa DUB that is induced in atrophying skeletal muscle. A modest increase of expression of USP19 was observed in early differentiation of L6 cells. TNF- α can increase expression of USP19 in L6 myotubes. SiRNA mediated silencing of USP19 expression can increase expression of MHC in L6 myotubes in a myogenin dependent manner. And silencing of USP19 can partially reverse the TNF- α or DEX stimulated catabolism of MHC. Thus, USP19 can regulate synthesis of myofibrillar proteins through modulating transcriptional factor in myotubes. These data demonstrate that the ubiquitin system not only mediates the increased protein breakdown but is also involved in the decreased protein synthesis in atrophying skeletal muscle.

Résumé

L'attachement de l'ubiquitine à un substrat protéique est catalysé par une série de réactions en chaîne impliquant trois classes d'enzymes- l'enzyme d'activation de l'ubiquitine (E1), l'enzyme de conjugaison de l'ubiquitine (E2) et l'enzyme de ligation de l'ubiquitine (E3). Les substrats protéiques polyubiquitinés sont spécifiquement reconnus par le protéasome pour être dégradés. L'enlèvement de l'ubiquitine présent sur les substrats ubiquitinés est catalysé par les enzymes de déubiquitination (DUB). Dans cette thèse, j'ai étudié les fonctions de trois enzymes du système ubiquitine : l'enzyme E2 UBC4-testis, l'enzyme E3 EDD/Rat100 et l'enzyme de déubiquitination USP19. Leurs rôles dans la spermatogénèse et l'atrophie musculaire ont été étudiés chez les mammifères

UBC4-testis est une enzyme spécifiquement exprimée dans les testicules de rongeurs et est induite dans les spermatides ronds. Des souris ayant le gène UBC4-testis inactivé démontrent un délai dans le développement postnatal durant la première vague de spermatogénèse. Par contre, arrivées à l'âge adulte, ces mêmes souris démontrent une fertilité et un poids testiculaire normal. Aussi, nous avons observé des données normales pour le nombre de spermatides, le contenu protéique, le taux d'ubiquitination ainsi que pour la quantité et la qualité des spermatozoïdes. Lorsque les testicules de ces souris sont soumis à un stress de température en effectuant une cryptorchidie expérimentale, le profil de dégénérescence des cellules germinales n'était pas significativement différent de celui de souris normales ayant subit le même traitement. Nos résultats suggèrent donc que UBC4-testis exerce un rôle dans l'évolution de la première vague de la spermatogénèse

mais il est possible que d'autres isoformes UBC4 puissent exercer des fonctions redondantes dans les étapes tardives de la spermatogénèse.

EDD/Rat100 est une enzyme E3 qui est dépendante de l'enzyme E2 UBC4 et qui est fortement exprimée dans les testicules de rat. La protéine de liaison au Poly(A) (PABP) est un facteur d'initiation à la traduction qui est négativement régulé par une protéine interagissant avec PABP appelée Paip2. PABP et EDD/Rat100 ont en commun un domaine appelé PABC qui peut interagir avec Paip2. EDD/Rat100 est capable d'ubiquitiner Paip2 in vitro. Dans des conditions normales in vivo, PABP, qui est en abondance, pourrait séquestrer Paip2 pour être ubiquitiné par EDD/Rat100. Dans des cellules qui ont des niveaux de PABP réduits, Paip2 est libre d'interagir avec EDD/Rat100 et est donc ubiquitiné et dégradé par le protéasome. La dégradation de Paip2 peut finalement rétablir l'activité de PABP et par conséquent maintenir son homéostasie. Ainsi, le taux de renouvellement de Paip2 dans la cellule est géré par EDD/Rat100 mais est régulé par PABP. De plus, six protéines copurifiées par immunoprécipitation avec EDD/Rat100 dans des extraits de testicules de rat ont été minutieusement étudiées mais aucune d'entre elle n'a été identifiée comme étant un substrat bona fide de EDD/Rat100.

Finalement, j'ai analysé USP19, une enzyme de déubiquitination qui est induite dans les muscles squelettiques dans des conditions d'atrophie musculaire. Une modeste augmentation de l'expression de USP19 a été observée dans des cellules L6 en début de différentiation. TNF-α peut augmenter l'expression de USP19 dans les cellules L6.

Lorsque les niveaux d'USP19 sont réduits par ARN interférent dans les myotubes L6, l'expression de MHC est augmentée de façon dépendante de la myogénine. Aussi, en diminuant les niveaux d'USP19, la dégradation de MHC stimulée par TNF-α ou par DEX peut partiellement être renversée. Donc, USP19 peut réguler la synthèse de protéines myofibrillaires en modulant la transcription dans des cellules musculaires L6. Ces résultats démontrent que le système ubiquitine n'agit non seulement sur la dégradation protéique dans les muscles squelettiques atrophiés mais aussi en diminuant la synthèse protéique.

Acknowledgements

I would first like to thank my supervisor Dr. Simon Wing for his heuristic guidance, continuous encouragement and support throughout my PhD studies.

I would also like to thank Nathalie Bedard for her indispensable technical assistance and excellent French translation of the abstract, Dr. Olasunkanmi Adegoke, a postdoctoral researcher in Dr. Simon Wing's laboratory, for constructive discussions and technical support, and Dr. Yu Lu for sharing her experience with siRNA mediated silencing of USP19.

I thank the members of my thesis committee - Dr. J. J. Lebrun, Dr. Ted Fon and Dr. Carlos Morales for their professional advice on my research project.

Finally, I would like to express my most sincere thanks to my wife for her constant support and to the staff in the Polypeptide Laboratory for their enthusiasm, emotional support and friendship.

I began my PhD studies in 2001 and completed my research and entered medical school in 2006. Since then, I have been writing this thesis, but its completion has been interrupted by a series of major changes in my life. My son was born in 2007. Coincidentally, my father in China was diagnosed with cancer and died 6 months later. He did a great favor to me by looking after my mother who was ill from diabetes and its

complications, allowing me to devote my time to my doctoral studies. I took a year leave of absence from medical school to spend 2008 in China taking care of my father and then consoling my mother and arranging for her care. Then I had to return to Canada to continue my medical studies. These experiences filled with mixed emotions have become precious parts of my life.

Mencius said, "When heaven is about to place a great responsibility on a great man, it always first frustrates his spirit and will, exhausts his muscles and bones, exposes him to starvation and poverty, harasses him by troubles and setbacks so as to stimulate his spirit, toughen his nature and enhance his abilities."

Table of Contents

Abstract	i
Résumé	iii
Acknowledgements	vi
Table of Contents	viii
List of Tables.	X
List of Figures and Illustrations	xi
List of Abbreviations	xiii
CHAPTER 1: Introduction	1
The ubiquitin activating enzyme (E1)	3
The ubiquitin conjugating enzyme (E2)	4
The ubiquitin protein ligase (E3)	6
Deubiquitinating enzymes (DUB)	14
Spermatogenesis and ubiquitin dependent proteolysis	21
Muscle wasting and the ubiquitin system	38
CHAPTER 2: Function of the E2 enzyme UBC4-testis in mammalian	
spermatogenesis	48
Materials and methods	50
Results	51
Discussion	53

CHAPTER 3: Identification of substrates for EDD/Rat100, a 300 KDa ubiqutin	
protein ligase	55
Materials and methods	60
Results	69
Discussion	79
CHAPTER 4: Function of USP19, a deubiquitinating enzyme, in skeletal muscle	86
Materials and methods	88
Results	91
Discussion	95
CHAPTER 5: General discussion	99
CONTRIBUTION TO NEW KNOWLEDGE	105
CONTRIBUTION TO MANUSCRIPTS	107
FIGURE LEGENDS	108
FIGURES AND TABLES	119
REFERENCES	142

List of tables

1(A). E2 of S. cerevisiae	139
1(B). E2 of mammalian cells	140
2. Proteins identified from mass spectrometry	141

List of figures and legends

Figure 1	119
Figure 2	120
Figure 3	121
Figure 4	122
Figure 5	123
Figure 6	124
Figure 7	126
Figure 8	128
Figure 9	129
Figure 10	130
Figure 11	131
Figure 12	132
Figure 13	133
Figure 14	135
Figure 15	136
Figure 16	137
Figure 17	138
Legend 1	108
Legend 2	108
Legend 3	109
Legend 4	110

Legend 5	110
Legend 6	111
Legend 7	111
Legend 8	112
Legend 9	112
Legend 10	114
Legend 11	114
Legend 12	115
Legend 13	115
Legend 14.	116
Legend 15	117
Legend 16.	117
Legend 17	118

List of abbreviations

E1: the ubiquitin activating enzyme.

E2: the ubiquitin conjugating enzyme.

E3: the ubiquitin protein ligase.

DUB: the deubiquitinating enzyme.

RING: really interesting new gene.

HECT: homologous to E6-AP C terminus.

xiii

Chapter 1

Introduction

Enzymes of the ubiquitin system and their functions in mammalian spermatogenesis and muscle atrophy

Ubiquitin is a highly conserved 76-amino acid peptide expressed in eukaryotic cells. Protein substrates that are covalently conjugated with a polymer of ubiquitin are selectively targeted for degradation by the proteasome, an ATP-dependent protease complex. In addition, mono or oligoubiquitination of a substrate can modify the function of the substrate or target it for endocytosis or intracellular trafficking to the lysosome. The ubiquitin-proteasome pathway is involved in many critical functions of mammalian cells, which include the progression of cell cycle, antigen presentation, ER associated degradation, muscle protein turnover and spermatogenesis. With our expanding knowledge of the ubiquitin system, an increasing number of clinical disorders, including cancer, Parkinson's disease and muscle wasting, are found to be related to dysregulated activity of the ubiquitin proteasome system.

Ubiquitination is catalyzed sequentially by a cascade of three enzymes - the ubiquitin activating enzyme (E1), the ubiquitin conjugating enzyme (E2) and the ubiquitin protein ligase (E3) (Fig. 1). During activation of ubiquitin, E1 forms a high energy thiol ester bond with the carboxyl terminal glycine (G76) of ubiquitin, using ATP as an energy source. Then the activated ubiquitin is transmitted to an E2, forming an E2-ubiquitin thiol ester. The function of an E3 is to recognize a substrate and transfer the activated ubiquitin

from an E2 to the substrate. Ubiquitination usually results in the formation of an isopeptide bond between the G76 of ubiquitin and the ε -amino group of a substrate's internal lysine residue. Recently, ubiquitin conjugation to the N terminal α -amino group of several substrates, such as ERK3, P21 and MyoD, has also been reported [1, 2]. In a rare case, ubiquitination can occur on a cysteine residue as has been demonstrated to occur on the intracytoplasmic tail of the major histocompatibility complex class I protein [3].

To date, there are two E1 genes (Ube1, Uba6/UBE1L2) identified [4, 5] and a limited number of genes in the E2 family (13 in yeast and approximately 30 in mammalian cells). All of the E2 enzymes have a conserved globular core domain and an essential cysteine residue in the active site. The number of genes in the E3 family is much larger. The recognition of substrate for ubiquitination is governed by presence or accessibility of specific structures in the substrate, namely ubiquitination signals, which are recognized by cognate E3s. Therefore, E3s are the central determinants of specificity in ubiquitination. E3s are classified into two subfamilies based on their structures. One has a conserved Homologous to E6-AP Carboxyl Terminus (HECT) domain, which forms a thiol ester bond with ubiquitin during catalysis. The other shares a Really Interesting New Gene (RING) finger domain. Instead of forming a covalent bond with ubiquitin, a RING finger E3 catalyzes ubiquitination by bringing together and orienting an E2 and a substrate to facilitate the transmission of ubiquitin from the E2 to the substrate. Function of a RING finger E3 as an allosteric activator of E2 has also been reported [6].

Removal of ubiquitin from a ubiquitinated substrate is catalyzed by deubiquitinating enzymes (DUB), which play an important role in ubiquitin-dependent proteolysis. DUBs include five subfamilies: ubiquitin carboxy-terminal hydrolase (UCH), ubiquitin specific protease (UBP/USP), Otubain (Ovarian tumor (OTU)-domain Ub-aldehyde-binding protein), Josephine and JAMM (Jab1/Pad1/MPN-domain metallo-enzyme). To date, more than 70 DUB genes are identified. The majority are of the UBP/USP subfamily, and the remainder are dispersed amongst the four other subfamilies.

In this review, I will discuss primarily the mechanism of E1, E2, E3 and DUB. I will also focus on the functions of the ubiquitin system in spermatogenesis and muscle wasting.

1.1 The ubiquitin activating enzyme (E1)

The ubiquitin E1 is a 110 kDa essential enzyme of eukaryotic cells. In most organisms, a single E1 (Ube1 in mammals) activates ubiquitin for the entire downstream ubiquitin conjugation pathway. Although the ubiquitin E1 has not been crystallized, structures of E1s for other ubiquitin-like modifiers (Ubl), such as NEDD8 and SUMO, are available. Both the NEDD8-E1 (APPBP-1/UBA3) and the SUMO-E1 (Sae1/Sae2) are multidomain heterodimers, while the ubiquitin E1 is encoded on a single polypeptide chain with sequence similarity to APPBP-1 and Sae1 in its N-terminal part and to UBA3 and Sae2 in its C-terminal part. Based on sequence similarity to these proteins, the structure of the ubiquitin E1 is thought to contain three functional domains: 1) the adenylation domain, which contains the Gly-X-Gly-X-X-Gly ATP binding motif conserved in Ubl activating

enzymes throughout evolution; 2) the catalytic cysteine domain, which forms the ubiquitin-thiol ester intermediate with the catalytic cysteine residue; and 3) the C-terminal ubiquitin-like domain, which is involved in E2 recognition [7].

E1 activates ubiquitin in four steps [8, 9]. The first step is the adenylation of the carboxy-terminus of ubiquitin, in which one ATP is consumed and one ubiquitin adenylate and one pyrophosphate are produced. Mg²⁺ is required for this step. The adenylated ubiquitin forms a tight noncovalent complex with the E1. In the second step, the E1's catalytic cysteine attacks the adenylate and forms a thiol ester bond with ubiquitin's carboxy terminal glycine residue. Next the E1 adenylates another molecule of ubiquitin and associates with it noncovalently. Now the E1 is carrying two molecules of ubiquitin, one through a covalent thiol ester bond, the other through a noncovalent bond. The noncovalently associated ubiquitin not only promotes transfer of the thiol ester-linked ubiquitin molecule to E2 but also primes the E1 for another round of catalysis immediately. The final step is transfer of ubiquitin to E2, which will be discussed subsequently.

1.2 The ubiquitin conjugating enzyme (E2)

Although a major E1 activates ubiquitin, many E2 enzymes have been identified in every eukaryotic organism. There are 13 in yeast (Table 1A) and over 25 in mammals (Table 1B). Structures of ten E2 enzymes from different species have been solved, nine by X-ray crystallography and two by NMR. All E2 structures share a highly homologous compact

core domain, which includes approximately 150 amino acids. This core catalytic domain contains the active site cysteine residue required for thiol ester formation with ubiquitin. Some E2 proteins also have N or C-terminal extensions, which may endow E2 with further functions. For instance, the C terminal extension of UBC2 (Rad6) is important for ubiquitination of Histone H2B in vitro; and the C-terminal extension of UBC6, including a hydrophobic signal-anchor sequence, is responsible for anchoring UBC6 to the ER membrane [10, 11].

The mechanism of E1-E2 interaction has been revealed based on the crystal structure of a trapped activation complex containing the NEDD8 activating enzyme bound to NEDD8 and its conjugating enzyme Ubc12 [12]. This structure suggests a model for ubiquitin transfer from E1 to E2 [13, 14]. Briefly, E1 loaded with ubiquitin (or a UBL) has dramatically increased affinity for E2. A conformational change in the complex brings the catalytic cysteine residues of E1 and E2 close enough to allow the transfer of the ubiquitin. Transthiolation facilitates release of the E2-ubiquitin/UBL product. Thus, E1–E2 interactions depend on whether E1 or E2 is thiol ester-bound to the ubiquitin/UBL. Formation of the E1-ubiquitin/UBL thiol ester favours binding with free E2, whereas formation of the E2-ubiquitin/UBL thiol ester leads to release.

Because all of the ubiquitin E2s of *S. cerevisiae* interact with ubiquitin and the E1 enzyme, it is expected that there will be conserved binding surfaces found on E2 proteins. Indeed, conserved residues of the 13 *S. cerevisiae* E2s are localized predominantly on the face of the molecule in the vicinity of the active site cysteine. This surface is therefore

likely to participate in binding E1, ubiquitin, or both. On the other hand, because each UBC has a distinct group of substrates that are either recognized directly by the E2-ubiquitin complex or via an E3, it is expected that E3 and substrate-binding surfaces will be comprised of residues that are not conserved between different E2s. Most of these poorly conserved residues cluster on the face of the molecule opposite to the active site [15]. In addition, the C terminal acidic extension of UBC2 can confer substrate specificity as deletion of the C terminal extension makes UBC2 unable to efficiently ubiquitinate histones in vitro [10]. The interacting surface between E2 and E3 is further confirmed by crystal structures of E2-E3 complexes, which will be discussed later.

1.3 The ubiquitin ligase (E3)

E3 confers substrate specificity and is the largest enzyme family of the ubiquitin system. Ubiquitin E3 ligases can be classified into two groups according to their mode of action: (1) HECT domain E3 ligases are true enzymes, because they form a thiol ester bond with ubiquitin before they transfer it to a substrate; (2) RING type E3s, defined by the RING (Really Interesting New Gene) finger domain contained in this kind of protein, serve as adaptors between E2 and its substrate and allosteric activators of E2. These E3s are either in the form of single proteins or as multisubunit complexes. RING finger domain E3s represent the largest group of E3s.

1.3.1 HECT domain E3s

HECT domain E3s are defined by an approximately 350 amino acid HECT domain (Homologous to E6-AP C terminus), originally identified in E6-AP [16]. E6-AP is a cellular ubiquitin ligase. It can associate with the human papilloma virus E6 oncoprotein, and this association allows it to target the tumor suppressor p53 for degradation in infected cells [17, 18]. The HECT domain is located in the C terminus of E3s. The conserved active site cysteine, which forms a thiol ester bond with ubiquitin during the cascade of ubiquitin thiol ester transfers, is usually within the C terminal ~50 amino acids of the HECT domain. Amino acids on the C terminal end of the HECT domain are critical for isopeptide bond catalysis. A key requirement for ubiquitin transfer from the active site cysteine to the substrate is a phenylalanine residue located about four amino acids from the end of the protein. It may function to properly orient the ubiquitin molecule that is tethered to the active site cysteine [19]. The extensive variable N terminus of HECT domain E3s accounts for the wide range of molecular weights (90 to 500 kDa) of this E3 family. It appears that the N-terminus of HECT domain E3s confers the ability of substrate binding and subcellular localization, and the HECT domain itself serves to interact with E2 and directly transfer ubiquitin from a thiol ester linkage to the substrate.

1.3.1.1 Interaction between E2 and the HECT domain E3

The structure of the HECT domain of human E6AP and the structure of this domain bound to the human E2 UbcH7 have shed some light on the cooperation between E2 and the HECT domain E3 (Fig. 2A). The E6AP HECT domain/UbcH7 complex has a Ushaped structure, with the E6AP HECT domain representing the base and one side and UbcH7 representing the other side. The HECT domain consists of a larger N terminal lobe that contains the E2 binding site, and a smaller C terminal lobe that contains the active site cysteine. The two lobes are packed loosely across a small interface and are connected by a three residue hinge. The E6AP and UbcH7 active-site cysteine side chains are 41 Å apart from each other. Therefore, it appears that conformational flexibility about this hinge is critical for juxtaposing the active site cysteines of the E2 and E3 in order to facilitate the transfer of ubiquitin from the E2 to the E3. UbcH7 binds in a large hydrophobic groove on the N terminal lobe of the E6AP HECT domain, using loops at one end of its β sheet and a portion of its N terminal α helix. A phenylalanine (Phe63) of UBCH7 binds in the center of the hydrophobic groove of the HECT domain, making a critical contact between UBCH7 and E6AP [20].

The HECT domain of the human ubiquitin E3 WWP1/AIP5 also maintains a two-lobed structure. While the individual N and C terminal lobes of WWP1 possess very similar folds to those of E6AP, the distance between cysteines of WWP1 and a docked E2 UBCH5 is only 16.5Å due to rotation about a polypeptide hinge linking the N and C terminal lobes. Further rotation is speculated to occur during the transthiolation reaction. Indeed, mutational analyses in this region suggest that a range of conformations achieved by rotation about this flexibile hinge region is essential for catalytic activity [21].

Based on these crystal structures, two working models of HECT domains have been proposed. (1) The HECT domain adds ubiquitin moieties in a sequential manner to substrates. The C terminal lobe first rotates to pick up ubiquitin from a bound E2ubiquitin conjugate, tethers it to the C terminal lobe cysteine through a thiol ester bond, and ultimately transfers it to a bound target through isopeptide bond formation. This cycle is repeated with subsequent ubiquitin molecules attached to the previously transferred ones on the target protein-ubiquitin conjugate, thus elongating the ubiquitin chain. (2) In an alternative model, a ubiquitin chain is formed on the C terminal lobe cysteine through a thiol ester bond. The C terminal lobe adjusts its orientation during elongation of the ubiquitin chain so that the target lysine residue of the most recently added ubiquitin is repositioned every cycle to accept a subsequent ubiquitin molecule. As the chain length increases, it may interfere with E2 binding as well as rotations of the C terminal lobe, therefore preventing its own elongation. Conjugation of a polyubiquitin chain to a substrate could occur in a single final step as the reactive thiol ester bond linking the HECT domain catalytic cysteine and the C terminus of the polyubiquitin chain is in position for transfer of the chain to the substrate. Functionally, HECT domains are capable of substrate-independent polyubiquitin chain synthesis in vitro, which is consistent with this model [21, 22].

1.3.1.2 Substrate recognition by HECT domain E3s

The N terminus of HECT domain E3s is responsible for substrate identification and regulation. For instance, the C2-WW-HECT E3s, such as yeast Rsp5 and human Nedd4, contain an N-terminal C2 phospholipid binding domain and two to four WW domains in the central portion of the protein that mediate enzyme-substrate interactions [23-25]. (1) The C2 domain can, under the regulation of Ca²⁺, interact with membrane phospholipids, inositol polyphosphates and proteins. It is involved in targeting membrane protein substrates of Rsp5, either by localizing Rsp5 to the plasma membrane or by directly mediating the interaction with membrane-associated substrates. (2) The WW domains are protein-protein interaction modules that have an affinity for proline-rich sequences, with the consensus binding site containing a PPXY sequence. These WW domains consist of 38 to 40 amino acids, have two absolutely conserved tryptophan residues, and form a three-stranded antiparallel β-sheet with a hydrophobic binding pocket for the PPXY ligand. Functionally, the WW domains are somewhat analogous to SH3 domains in that they both have affinities for proline-rich ligands, and in some cases, WW and SH3 domains can compete for binding to the same ligands in vitro [26]. Substrate recognition is commonly mediated by the WW domains. Rsp5 has three WW domains; the second and the third ones are responsible for binding of Rsp5 with its substrate Rpb1. Substrates without WW-domain interacting motifs are recruited through either the C2 domain or adaptor proteins that can associate simultaneously with the substrate and the WW domain of E3s [27].

HECT E3s without the WW and C2 domains may use other mechanisms to recognize their substrates. For instance, the human papillomavirus oncoprotein E6 can function as

an adaptor to facilitate ubiquitination of p53 by E6AP for proteasomal degradation, which contributes to epithelial transformation by papillomavirus [28]. Another human HECT E3 EDD (E3 isolated by differential display) has a PABC domain, which is similar to the C terminus of Poly(A) binding protein (PABP) and is located N terminal to the HECT domain of EDD. It has been found that EDD can interact with its substrate the PABP interacting protein (Paip) through the PABC domain [29, 30].

1.3.2 RING finger domain E3s

RING fingers have been defined by the consensus sequence Cys¹-X2-Cys²-X(9–39)-Cys³(1–3)-His⁴-X(2–3)-Cys/His⁵-X2-Cys⁶-X(4–48)-Cys⁻-X2-Cys⁶. X can be any amino acid. Two zinc atoms are complexed by the cysteine/ histidine residues in a cross-brace manner, to provide correct folding and biological activity of the RING domain. RING fingers are subcategorized into RING-HC and RING-H2 depending of whether a cysteine or histidine occupies the fifth coordination site, respectively [31]. A subset of RING finger E3s, such as c-CBL, Hrd1 and EL5, have a conserved tryptophan within the RING domain, which is important for ubiquitination [32, 33]. Replacement of the RING tryptophan of c-CBL by alanine reduced its ability in ubiquitin ligation and Ubc4 activation [34]. To date, hundreds of proteins containing a RING finger domain have been identified in the mammalian genomic database. However, only a portion of them have been proven to have E3 activity in vivo.

1.3.2.1 Interaction of E2 and the RING finger E3:

Cbl is a single subunit RING finger domain E3 that functions in endocytosis and degradation of RTK (receptor tyrosine kinases). The mechanism of how RING E3s promote the ubiquitination of substrates by E2s has been studied by using the crystal structure of a c-Cbl-UbcH7-ZAP70 protein kinase peptide substrate ternary complex (Fig. 2B). c-CBL consists of a tyrosine kinase binding (TKB) domain and a RING domain connected by an ~40-residue conserved α helix sequence (linker helix), which is an integral part of the TKB domain. UbcH7 binds to the RING domain of c-Cbl through contacts between a groove within the RING domain of c-Cbl and two loops (L1 and L2) in the E2 fold of UbcH7. The interactions between UbcH7 and the c-Cbl RING are largely due to van der Waals interactions involving aromatic hydrophobic residues in UbcH7 and the c-Cbl RING. The nature of the residues in the site of E2-RING E3 interactions may play a significant role in determining cognate E2-RING pairs. In addition, the interaction between the linker helix of the TKB domain and UbcH7 determines the relative arrangement of UbcH7, which is important for the E3 activity [35].

To date, there is no evidence that RING finger E3s catalyze ubiquitination by forming a thiol ester bond with ubiquitin. The current model indicates that RING finger E3s function as molecular scaffolds. They can simultaneously associate with an E2 molecule through the RING finger domain and interact with a substrate through a substrate binding motif, such as the SH2 (Src homology 2) domain of Cbl. By this means, they facilitate the direct transfer of ubiquitin from E2 to substrates. The interaction of various RING

finger domains with E2s is the central event in catalysis because mutations of the RING finger or addition of zinc chelators can abrogate E2 binding and E2-dependent ubiquitination. Indeed, the majority of RING finger E3s including Cbl do not bind to E2s if they lack a RING finger. By contrast, there is evidence that the role of the RING finger is not merely to recruit E2s to the vicinity of substrates for ubiquitination. For instance, Ubr1 binds its cognate E2, Rad6, predominantly via the BRR region outside the RING finger, yet mutations in the BRR region only weakly reduce E3 activity. While a RING mutation did not affect binding to E2 or substrates, it abolished ubiquitination. In this case, the function of the RING finger domain of Ubr1 is possibly to promote E2 catalytic activity [15].

1.3.2.2 .Substrate recognition by RING finger domain E3s

RING finger E3s recognize substrates that are modified with signals for ubiquitination. As a single subunit RING finger E3, Cbl can interact through its N-terminal SH2 domain with phosphorylated RTKs and regulate their recycling by monoubiquitination. For multiple subunit RING finger E3s, such as SCF (Skp1, cullin, F-box) complexes, VBC (the von Hippel-Lindau (VHL)–Elongin B–Elongin C) and APC (anaphase-promoting complex), a distinct subunit of the complex plays the role of the substrate receptor. For instance, the SCF complex contains at least four subunits: Skp1, Cul1, Roc1/Rbx1/Hrt1 and an F-box protein. Human Roc1/Rbx1 (Hrt1 in yeast) is a RING-H2 finger protein that appears to promote association of the Cul1 protein with the E2 enzyme and to enhance ubiquitin ligase activity [36]. The F-box protein determines substrate specificity.

It binds Cul1 through the F-box domain and therefore acts as an adaptor approximating substrates and the rest of the E3 [37]. Due to the broad range of F-box proteins, the number of SCF substrates is predicted to be large. Based on the protein-protein interaction domains, F-box proteins are classified into three categories: Fbw, F-box proteins containing WD40-repeat domains; Fbl, containing leucine-rich repeats (LRR) domains; and Fbx, containing other structures (x) [38].

In the well studied SCF F-box complexes, SCF^{Cdc4}, SCF^{Grr1}, SCF^{Skp2} and SCF^{β-TrCP}, substrate phosphorylation is required for binding the F-box protein. In the yeast SCF^{Cdc4} F-box complex (Fbw), each of the known substrates, Sic1p, Cdc6p, Gcn4p and Far1p, has been shown to require phosphorylation for ubiquitination. SCF^{β-TrCP} (Fbw) also recognizes phosphorylated proteins, such as IκB- α and β -catenin. The known substrates of the LRR-containing F-box Grr1 (Fbl) must be phosphorylated before being ubiquitinated. Skp2, an LRR F-box protein similar to Grr1, also recognizes only the phosphorylated form of the cyclin-dependent kinase (CDK) inhibitor p27^{Kip1} [39].

1.4 Deubiquitinating enzymes (DUB)

Ubiquitination is a reversible process. While ubiquitin can be conjugated onto substrates by the E1, E2 and E3 enzymes, it can be removed from the conjugates by deubiquitinating enzymes. Therefore, the extent of ubiquitination of a substrate in vivo is determined by the balance between the activities of these two groups of enzymes. There are four main functions of DUBs. (1) When deubiquitination occurs before the

commitment of a substrate to proteasomal proteolysis, it negatively regulates protein degradation. For efficient binding of polyubiquitinated proteins by proteasome, it generally requires polymers of at least four ubiquitin moieties [40]. By shortening the conjugated ubiquitin chain lower than this threshold, DUBs work as editing or proofreading enzymes to rescue inappropriately ubiquitinated proteins [41]. (2) However, once a substrate is targeted to the proteasome and is committed to degradation by unfolding, deubiquitination of the substrate by chain cleavage facilitates its proteolysis. The cleaved polyubiquitin chain is further disassembled by DUBs. This helps to maintain a sufficient pool of free ubiquitin in vivo, which is necessary for sustaining a normal rate of proteolysis. Indeed, removal of ubiquitin is so important for proteasomal proteolysis that some DUBs, such as Ubp6 and Rpn11/POH1, are subunits of the proteasome regulatory particle [42]. Failure to detach polyubiquitin can result in either inappropriate degradation of ubiquitin along with the substrate or interference with entry of the substrate into the narrow opening of the central proteolytic chamber of the proteasome. (3) In addition, DUBs are responsible for processing ubiquitin precursors. Ubiquitin molecules are encoded in the genome and produced as ubiquitin-ribosomal fusion proteins or as head-to-tail-linked linear ubiquitin polymers [43, 44]. Some DUBs have peptidase acitivity, which is required for cleaving the peptide bond linking ubiquitin to various C-terminal peptide extensions to generate free ubiquitin monomers. Ubiquitin precursor processing is rapid and can happen cotranslationally [45]. (4) Membrane proteins, mostly cell surface proteins, are generally targeted to the vacuole or lysosome rather than the proteasome for degradation. Monoubiquitination or lysine 63 linked oligoubiquitination of cell surface proteins can enhance their internalization. Once

internalized, these proteins are sorted through the late endosome, the multivesicular body (MVB) and finally into the vacuole for degradation. A yeast DUB, Doa4 acts at the late endosome/prevacuolar compartment to recover ubiquitin from ubiquitinated membrane proteins en route to the vacuole [46]. The AMSH DUB appears to act similarly in mammalian cells [47].

1.4.1 Classification and structures of DUBs

DUBs are grouped on the basis of sequence into five classes. Ubiquitin specific processing proteases (UBPs) and ubiquitin C-terminal hydrolases (UCHs) are traditional DUBs, which are cysteine proteases and are sensitive to inhibition by thiol reagents, such as *N*-ethylmaleimide [48-50]. In mammals, UBP is also called USP (ubiquitin-specific protease) [51]. In most organisms, the UBP/USP family is the predominant and the most diversified type of DUB. More recently described DUB families, including the Otubain (Ovarian tumor (OTU)-domain Ub-aldehyde-binding protein), Josephine and JAMM (Jab1/Pad1/MPN-domain metallo-enzyme) families, do not show any sequence homology to the UCH or UBP family. Except for the JAMM motif metallo-enzyme, the other DUBs are also cysteine proteases.

1.4.1.1 The UBP/USP family

UBPs have a ~350 amino acid core catalytic domain. The yeast UBP family members share 4-6 homologous regions including the Cys box (~19 amino acids) and the His box

(60–90 amino acids) [49]. UBPs vary in size from 50 to 300 kDa with a variety of N terminal extensions, occasional C-terminal extensions, and insertions in the catalytic domains. The extensions and insertions have been suggested to function in substrate recognition, subcellular localization of the enzymes, and protein-protein interactions. In addition to processing of ubiquitin precursors, UBPs are responsible for removing ubiquitin from polyubiquitinated proteins and for disassembly of free polyubiquitin chains [52].

The crystal structures for the 40 kDa catalytic core domain (residues 208-560) of HAUSP/USP7 alone and in complex with the substrate analogue inhibitor Ub-aldehyde (Ubal) have been determined [53]. The HAUSP/USP7 catalytic core domain is composed of three domains: Fingers, Palm, and Thumb. The general conservation of the residues that comprise the secondary structural elements in the three domains suggests the conservation of the Fingers-Palm-Thumb architecture among other UBP proteins. The highly conserved Cys and His boxes are positioned on the opposite sides of the catalytic cleft created by the Palm and Thumb scaffold (Fig. 2C). This open cleft structure of the HAUSP/USP7 catalytic domain and the three-domain architecture are suitable for deubiquitination of large substrates, such as polyubiquitinated proteins and free polyubiquitin chains. Ubal binds to the putative substrate binding surface of HAUSP/USP7 and makes extensive contacts with both the Fingers and the Palm-Thumb scaffold. The Ubal C terminus is bound in the deep catalytic cleft between the Palm and the Thumb, with a thiohemiacetal linkage formed between the aldehyde group and the side chain of Cys223.

The HAUSP/USP7 catalytic core by itself may be insufficient for recognition of ubiquitinated substrates *in vivo*. Interestingly, the C-terminal segment of p53 (residues 357–382) contains five of the six putative ubiquitination sites. It is possible that the N-terminal domain of HAUSP/USP7 recognizes the ubiquitinated region of p53, thus recruiting it to the HAUSP/USP7 catalytic core domain. Likewise, the highly divergent N- and/or C terminal extensions of UBPs may contribute to the recruitment of specific substrates to the catalytic domains of the enzymes [54].

1.4.1.2 The UCH family

UCHs are generally small proteins (20–30 kDa). They have a core catalytic domain (~230 amino acids) that is structurally defined by the presence of a catalytic triad consisting of positionally conserved Cys, His, and Asp residues [55]. *In vitro*, UCHs can remove peptides and small molecules, such as glutathione, from the C-terminus of ubiquitin, some of which may become attached non-specifically by reacting with activated ubiquitin linked in thiol ester forms to the enzymes involved in conjugation [56]. Most UCHs cannot in *in vitro* assays release ubiquitin from ubiquitin-protein conjugates or disassemble polyubiquitin chains. Thus, UCHs appear to play a role in elimination of small adducts from ubiquitin and in generation of free monomeric ubiquitin from its precursors. Crystal structures of the yeast UCH-Yuh1, and the human UCH-L3 are now available. In contrast to the open active-site cleft structure of HAUSP/USP7, both UCHs have a crossover loop of remarkably similar conformation that blocks the active-site cleft

in absence of substrates. Constraints on this loop conformation may function to control UCH specificity [57, 58].

1.4.1.3 The Otubain family

The Otubain family has no sequence homology to other DUBs. Instead, it belongs to the OTU (ovarian tumor) superfamily of proteins, a group of putative cysteine proteases that are homologous to the *ovarian tumor* gene product of *Drosophila* [59]. Two members of this family, otubain-1 and otubain-2, were isolated from HeLa cells by Ub-aldehyde affinity purification [60]. Both can cleave the isopeptide bond in polyubiquitin chains, but not the peptide bond in the Ub-GFP fusion protein. Another member of the OTU family, Cezanne (cellular zinc finger anti-NF-κB) can also cleave the isopeptide bond in polyubiquitin chains. Proteins in the Otubain family contain conserved Cys, His, and Asp residues that define the catalytic triad of cysteine protease, and the enzyme activity is sensitive to Ub-aldehyde [61]. However, the crystal structure of otubain shows differences from other DUBs. A novel loop conformation sterically occludes the active-site cleft, and the residues that orient and stabilize the active-site histidine of otubain 2 are different from other cysteine proteases. This reorganization of the active-site topology may possibly contribute to the low turnover and substrate specificity of the otubains [62].

1.4.1.4 The Josephin family

Ataxin-3 is a 42 kDa polyglutamine containing protein responsible for the genetic neurodegenerative Machado-Joseph disease. When the polyglutamine track within Ataxin-3 expands over a specific threshold, it can aggregate and deposit as nuclear inclusions, causing neurodegenerative disorders characterised by progressive dysfunction and necrosis of neurons. Ataxin-3 contains an N-terminal Josephin domain followed by tandem ubiquitin (Ub)-interacting motifs (UIMs) and a polyglutamine stretch. The Josephin domain, which belongs to the family of papain-like cysteine proteases, is conserved within a novel family of DUB with wide phylogenic distribution [63]. This domain folds into a globular conformation and confers ubiquitin protease activity. Similar to other DUBS, the Josephin domain also contains a catalytic triad including Cys, His and Arg. The crystal structure of Josephin features a flexible helical hairpin formed by a 32residue insertion, which resembles a papain-like fold in other DUBs [64, 65]. The current model of Ataxin-3 indicates that it binds ubiquitin chains through the C-terminal UIMs and cleaves ubiquitin chains through the Josephin domain. Though Ataxin-3 can bind either Lys48 or Lys63-linked polyubiquitin chains, it preferentially cleaves Lys63 linkages. It cleaves Lys63 linkages with an even higher activity in Lys48-Lys63-mixed linkage polyubiquitin chains. The specificity of restrictive cleavage by the Josephin domain is regulated by the UIMs, which confer ability of Ataxin-3 to edit topologically complex chains [66].

1.4.1.5 The JAMM family

It has been found that a motif within the MPN (Mpr1, Pad1 N-terminal) domain of Rpn11 in the proteasome lid complex is responsible for a deubiquitinating activity associated with the 26S proteasome [67-69]. The MPN domain is also present in COP9 signalosome (CSN) and eIF3 complex. A number of polar residues are conserved in a highly coordinated fashion in a subset of MPN domains. This EXnHXHX10D motif, referred to as JAMM [68] or MPN+ [70], is frequently found in the active site of metallo enzymes or as the coordinating ligands in metal-binding proteins. Moreover, the deubiquitinating activity of Rpn11 is insensitive to classical DUB inhibitors, such as Ub-aldehyde, but is destroyed by the Zn²⁺-specific chelator TPEN (*N,N,N',N'*-tetrakis(2-pyridylmethyl)-ethylenediamine) as well as by other metal chelators, such as *o*-phenanthroline [68, 69]. Thus, Rpn11 and other eukaryotic proteins containing the JAMM motif constitute a new DUB family that has a metal-binding site.

1.5 Spermatogenesis and Ubiquitin Dependent Proteolysis

1.5.1 Mammalian Spermatogenesis

1.5.1.1 Histology of testis

The testis has a thick capsule of dense connective tissue, the tunica albuginea. It is thickened on the posterior surface of the testis to form the mediastinum testis, from which fibrous septa penetrate the gland, dividing it into hundreds of testicular lobules. Each lobule contains several seminiferous tubules enmeshed in a web of loose connective

tissue rich in blood and lymphatic vessels, nerves and the Leydig cells. Seminiferous tubules produce male reproductive cells, the spermatozoa. The Leydig cell is the major source of testosterone and a variety of other steroids.

The seminiferous tubules consist of a tunic of fibrous connective tissue, a well-defined basal lamina and a complex seminiferous epithelium. The epithelium consists of two types of cells: supporting cells (Sertoli cells) and cells that constitute the spermatogenic lineage. The spermatogenic cells are stacked in 4-8 layers that occupy the space between the basal lamina and the lumen of the tubule. These cells divide several times and finally differentiate, producing spermazoa (Fig. 3A).

1.5.1.2 Spermatogenesis

Spermatogenesis is the complex process in which spermatogonia develop into mature spermatozoa. There are three types of spermatogenic cells: spermatogonia, spermatocytes and spermatids. Spermatogonia rest on the basement membrane, spermatocytes are generally located in the middle of the seminiferous epithelium and spermatids are located in the abluminal region. Spermatogonia divide and differentiate into spermatocytes, which undergo meiosis to generate spermatids. Spermatids enter a long process of metamorphosis and maturation that ends with the formation of spermatozoa. The whole process is divided into three phases: (1) Spermatogonial phase (Mitosis), (2) Spermatocyte phase (Meiosis), and (3) Spermatid phase (Spermiogenesis).

(1) Spermatogonial phase (Mitosis): Spermatogonia undergo mitotic divisions to replace themselves and to produce successive cells that begin differentiation, and finally give rise to spermatocytes. The isolated type A ($A_{isolated}$) spermatogonia are thought to be stem cells, whereas other types of spermatogonia are proliferative (A_{paired} and $A_{aligned}$) and differentiated (A_1 , A_2 , A_3 , A_4 , Intermediate and Type B) spermatogonia. An $A_{isolated}$ spermatogonium can divide into two daughter cells, one remains a stem cell, the other is destined to differentiate into A_{paired} spermatogonia. A_{paired} spermatogonia divide into $A_{aligned}$ spermatogonia, which are able to self-renew. A fraction of $A_{aligned}$ spermatogonia morphologically change into A_1 spermatogonia, which then give rise to subsequent cell types by mitosis. A_{paired} spermatogonia as well as all their offspring cells are connected to other cells of the same type by intercellular bridges, which are thought to promote the synchronous development of spermatogonial cell clones and the synchronous development of all other types of germ cells.

Spermatogonia reside on the basal level of the seminiferous tubules (Fig. 3A). They are relatively small cells and generally have a flattened surface along the basal lamina and a round surface on the other side in contact with Sertoli cells. In mouse, undifferentiated spermatogonia (A_{aligned}, A_{paired} and possibly A_{isolated}) are preferentially located in regions of seminiferous tubules that are adjacent to blood vessels surrounded with interstitial cells [71]. This vascular/interstitial stem cell niche is thought to be responsible for stem cell maintenance and differentiation during mammalian spermatogenesis [72]. A₁, A₂, A₃ and A₄ spermatogonia are quite similar in morphology and therefore can only be identified

according to the stage of seminiferous tubules. Only some of the spermatogonial cell types can be distinguished from each other based on morphological criteria. Generally, from Type A to Type B spermatogonia, there is an increasing accumulation of heterochromatin under the nuclear envelope. Type A spermatogonia possess essentially none, Intermediate spermatogonia display a moderate amount, and Type B spermatogonia have a large amount. Type B spermatogonia are committed to differentiate into more mature germ cells, spermatocytes.

(2) Spermatocyte phase (Meiosis): Spermatocytes replicate their DNA shortly after they form, thus, primary spermatocytes contain 4N amount of DNA (44 autosomes and an X and a Y choromsomes each having 2 chromatids). During this phase, the spermatocyte goes through two successive divisions. The prophase of the first division is divided into the following stages: Preleptotene and Leptotene stage characterized by chromatin condensation into visible chromosomes. Zygotene and Pachytene stage, during which homologous chromosomes are paired. Diplotene stage, the pairs of homologous chromosomes (also known as tetrads, because now each pair of homologous chromosomes are consisting of totally 4 chromatids) exchange genetic materials by crossing-over. After the prophase the primary spermatocyte divides into two secondary spermatocytes, the tetrads meanwhile separate to become diads (two-chromatid chromosomes) in the daughter cells. Although secondary spermatocytes have 2N amount of DNA, they are haploid cells (22 autosomes and an X or a Y chromosome). During the

metaphase of the second meiosis, the sister chromatids separate. Two haploid spermatids containing 1N amount of DNA are formed from each secondary spermatocyte.

(3) Spermiogenesis: a process of metamorphosis from round spermatids with typical organelles to highly specialized, elongated spermatozoa well adapted for traversing the male and female reproductive tracts and achieving fertilization of an egg. No further cell division occurs in this phase. During spermiogenesis, the acrosome and the flagella apparatus form, the nuclear material becomes compact in one part of the cell forming the sperm head. Most excess cytoplasm (the residual body) is separated and taken up by the Sertoli cell. Spermatozoa are released into the lumen of the seminiferous tubule. A small amount of excess cytoplasm (the cytoplasmic droplet) is shed later in the epididymis [73].

1.5.1.3 Roles of Sertoli cells in spermatogenesis

Sertoli cells serve a number of functions during spermatogenesis, supporting the developing gametes in the following ways: maintenance of the integrity of the seminiferous epithelium via desmosomes, hemidesmosomes, gap junctions and tight junctions; constitution of the environment necessary for development and maturation of germ cells via compartmentalization of the seminiferous epithelium; secretion of substances initiating meiosis; secretion of androgen-binding protein which concentrates testosterone in close proximity to the germ cells; secretion of hormones particularly inhibin, which feeds back on the pituitary gland and its control of spermatogenesis [74],

delivery of nutrients to germ cells; phagocytosis of residual cytoplasm left over from spermiogenesis [75].

1.5.1.4 The seminiferous cycle and the spermatogenic wave

New spermatozoa are being formed and released constantly. To have this constant sperm production, spermatogenesis needs to be staggered in timing throughout the seminiferous tubules. Certain developmental cell types of spermatogenesis have been observed at a given time via examination of normal, cross-sectioned seminiferous tubules. The grouping of cell types at a specific developmental progression is called a stage. A complete series of changes in cell stages arranged in the logical sequence of developmental progression is called the cycle of the seminiferous epithelium. A cycle represents the time required for one cell to go through all the stages. Stages of the cycle may be recognized by the developmental changes in the acrosomal system of the spermatids and their nuclear shape. This has been studied most extensively in the rat and mouse, in which 14 and 12 distinct stages can be recognized respectively (Fig. 3B). The seminiferous tubules are a series of loops in the testis with each loop entering the rete testis. There is an orderly progression of stages along the tubule. The progression of stages is called a wave and ensures that a portion of the seminiferous tubule is releasing sperm at any given time [76].

1.5.2 Ubiquitin-Dependent Proteolysis in Mammalian Male Reproduction

Ubiquitin and its related proteins are involved in many mammalian reproductive processes such as spermatogenesis, sperm quality control, fertilization and mitochondrial inheritance.

1.5.2.1 The ubiquitin system is implicated in different aspects of spermatogenesis

Spermatogenesis is a critical and complex developmental process during which a high turnover of proteins occurs, such as the turnover of nuclear proteins during the postmeiotic histone-protamine transition. Such transition probably requires rapid and massive downregulation of the cellular concentration of a number of proteins and could pose a high demand on ubiquitin dependent proteolysis. For instance, a great amount of cellular protein is degraded as the spermatids become remodelled into their elongated mature forms. Accordingly, a relatively high level of 26S proteasome activity has been detected in mature spermatozoa from mice, suggesting a role of the proteasome in normal sperm physiology [77]. In human spermatozoa, the proteasome is found to be concentrated in the neck region where the centrioles are located, suggesting that the proteasome might be involved in centrosome reduction, an important step in spermatid maturation [78]. Two ubiquitin C-terminal hydrolase enzymes, UCH-L1 and UCH-L3 are strongly expressed during spermatogenesis. They can reciprocally modulate apoptosis of germ cells, which is thought to be important for normal spermatogenesis and sperm quality control [79]. In

addition, a growing number of E2s and E3s are found to be expressed during spermatogenesis.

1.5.2.2 Ubiquitin-dependent mitochondrial inheritance and sperm quality control

Humans as well as other mammals inherit mitochondria from the mother only. A mechanism for strict maternal inheritance of mitochondria and mitochondrial DNA has been suggested by the observation of ubiquitination of sperm mitochondria during spermatogenesis, in the male reproductive tract and inside the oocyte cytoplasm [80]. The initial ligation of ubiquitin molecules to sperm mitochondrial membrane proteins, such as high molecular weight isoforms of prohibitin, occurs during spermatogenesis [81]. Most ubiquitin-tagged mitochondria are lost to the discarded residual body, the others are destroyed in the oocyte cytoplasm after insemination in mammals. The degradation of sperm mitochondria in the cytoplasm of the fertilized oocyte can be blocked by the proteasome inhibitors lactacystin and MG132 [82, 83]. These data suggest the participation of the ubiquitin-proteasome proteolytic system in control of mammalian mitochondrial inheritance. Although lysosomal degradation may also contribute to sperm mitochondrial degradation in the cytoplasm of oocyte, its function is probably not crucial [84]. Learning more about the mechanism of mitochondrial ubiquitination may help us better understand inherited mitochondrial diseases.

During the maturation and storage of spermatozoa in the epididymis, defective sperm are eliminated. Ubiquitin is secreted by the epididymal epithelium and binds to the surface of defective sperm. Most of the ubiquitinated sperm are phagocytosed by the epididymal epithelial cells, a portion escapes and can be found in the ejaculate. This finding suggests a possible mechanism for sperm quality control and a new diagnostic method for male factor infertility [85].

1.5.2.3 The E1, E2 and E3 enzymes in spermatogenesis

The murine Y-chromosomal gene *Ubely* (previously known as Sby), a ubiquitin E1 homologous gene, is expressed only in the testis [86]. It is ~90% identical to its X-linked homolog Ube1x, which is expressed ubiquitously [4]. The *Ube1y* gene is mapped to a region of the murine Y chromosome that is required for normal spermatogonial proliferation, and plays a role in initiation of spermatogenesis in mouse [87]. However, the Ubely gene has been lost from the Y chromosome during evolution of the primate lineage and is therefore absent from the human Y chromosome [88, 89]. The physiological significance of a second E1 for murine spermatogenesis is still unclear. Recently, a novel human E1, Uba6/UBE1L2 was identified [5]. The protein sequence of Uba6/UBE1L2 shows a 40% identity to UBE1 and also contains an ATP-binding domain and an active site cysteine conserved among E1 family proteins. Uba6/UBE1L2 can activate ubiquitin in vitro and in vivo. In vitro, it can transfer the activated ubiquitin to UbcH5b, and this activated ubiquitin can be used for ubiquitination of p53 and MDM2 and autoubiquitination of E6-AP. In tissue culture cells, Human Uba6 and UBE1 have distinct preferences for E2 charging. Uba6 is required for charging a previously uncharacterized Uba6-specific E2 (Use1), whereas Ube1 is required for charging the cellcycle E2s Cdc34A and Cdc34B [4]. Expression of UBE1L2 in the testis is about 5-fold higher than in other organs, suggesting a testis specific regulation of ubiquitin activation. nUBE1L, a splice variant of UBE1L2, was also found to be predominantly expressed in adult human testis [90].

Certain ubiquitin-conjugating (E2) enzymes show increased or exclusive expression in testes of rat, mouse and human. The primary function of the mature testis is spermatogenesis. During spermatogenesis, most cellular proteins need to be degraded to form mature sperm cell. Although the molecular mechanism of this process is not clearly known, the identification of E2s with high expression level in the testis suggests that these enzymes play an important role in the loss of protein during spermatogenesis.

Mouse *HR6B* gene, encoding an E2 enzyme, is a mammalian autosomal homolog of the Saccharomyces cerevisiae gene *UBC2*. UBC2 in yeast is a ubiquitin conjugating enzyme and required for a variety of cellular functions such as sporulation, DNA repair and mutagenesis [91]. Another homolog of Rad6 found in mouse and human is the X-chromosomal *HR6A*. *HR6A* and *HR6B* are expressed in many tissues, with the highest mRNA levels in brain, heart and testis. In most tissues, the amounts of HR6A and HR6B proteins are similar, but the protein level of HR6B is relatively high in elongating spermatids of mouse [92]. Homozygous inactivation of the *HR6B* gene results in male, but not female, infertility, without any other prominent phenotype [93, 94]. The HR6B knockout mouse was the first mammalian knockout model of any of the enzymes involved in the ubiquitin pathway. Its male-infertility phenotype points to a critical role

for the ubiquitin system in spermatogenesis. Defective spermatogenesis in the *HR6B* knock-out mice becomes pronounced during the post-meiotic condensation of chromatin in the spermatids, which requires replacement of histones by protamines. Both UBC2 and its mammalian homologue can ubiquitinate histones in vitro. However, in the knockout mice, no overt defect in the overall pattern of histone ubiquitination has been found [95]. So the exact substrates targeted by HR6B in the testis remain unclear.

Rat E2_{17Kb} is very similar to another Drosophila E2 enzyme UbcD1, whose mutation leads to male sterility [96]. Rat E2_{17Kb} is a 16.7 kDa protein with basic PI and it is an ortholog of yeast UBC4 with which it shares 83% amino acid identity. E2_{17Kb} supports ubiquitination to testis proteins more rapidly in vitro and produces larger conjugates than E2_{14Kb}, an E2 that supports ubiquitination and protein degradation in reticulocyte extracts. Northern blotting from different tissues indicates that E2_{17Kb} is expressed in a broad spectrum of tissues but at particularly high levels in the testis. E2_{17Kb} is the first mammalian E2 cloned with high homology to *S. cerevisiae* UBC4/UBC5, which are required for degradation of short-lived and abnormal proteins, and perform most of the ongoing ubiquitination of proteins in the yeast cell. The ability of E2_{17Kb} to actively conjugate ubiquitin to endogenous proteins, especially histone H2A, and its high expression in the testis suggest that E2_{17Kb} may play a role in the proteolysis seen during spermatogenesis [97, 98].

Isoform 8A [99], also known as UBC4-testis, is an isoform of rat E2_{17Kb}, but encoded by another gene that is expressed exclusively in post-meiotic germ cells, in round and

elongating spermatids. It was isolated by screening a testis cDNA library and its amino acid sequence is very similar to other isoforms of E2_{17Kb}, with more than 90% identity. Northern blot analysis indicated its unique expression in the testis. 2D gel electrophoresis confirmed the expression of the protein. Unlike other mammalian homologs of *S. cerevisiae* UBC4/UBC5, it possesses an acidic PI. Moreover, UBC4-testis is developmentally regulated in the testis. Analyses of RNA samples from various stages of postnatal life showed that UBC4-testis expression was not detectable until day 25 of life. Based on the highly specialized, developmentally regulated expression and the distinct biochemical properties of UBC4-testis, I speculated that it may target a specific subset of proteins for conjugation and degradation at a particular stage of spermatogenesis [99].

In order to study the function of UBC4-testis, the UBC4-testis knockout mouse was generated in Dr. Wing's laboratory. We found that this gene is not essential for mouse spermatogenesis. In my project, I will test whether its function is required in spermatogenesis under stress conditions. To do this, I will examine the potential phenotypes in testis of UBC4-testis knockout mice that are exposed to heat stress introduced by experimental cryptorchidism.

Many E3 enzymes are expressed within the testis. Inactivation of some E3s leads to impaired spermatogenesis. The mammalian Siah genes encode highly conserved and widely expressed proteins with an N-terminal RING domain. To date, three functional murine Siah genes have been found: Siah1a, Siah1b and Siah2. Siah1a and Siah1b proteins differ at only six amino acids; Siah2 protein is almost identical to the Siah1

protein except for a divergent and extended region N-terminal to the RING domain. There are only two human Siah family genes, encoding SIAH1 and SIAH2 which are highly similar to murine Siah1a and Siah2 proteins respectively. To date, no variant human SIAH1 cDNAs corresponding to murine Siah1b have been identified [100-103]. Siah proteins facilitate the ubiquitination and degradation of diverse proteins including α-tubulin, Bag-1 and DCC [104-106]. They also interact with UbcH5 and UbcH9. The most profound defects in Siah1a knockout mice are postnatal growth retardation and male infertility. The sterility of Siah1a-/- mice results from interrupted spermatogenesis. In the cross-section of the seminiferous tubule from adult Siah1a-/- mice, intertubular regions, Sertoli cells, spermatogonia and spermatocytes in prophase I of meiosis appeared normal, however, post-meiotic round and elongating spermatids are completely absent or severely depleted. Defects included apoptosis of metaphase and anaphase cells and bi or multinucleated cells, indicating failure to complete chromosome segregation and meiotic division. Thus, Siah1a is required for male meiosis I [107].

E3^{Histone} is a 482 kDa, HECT domain containing ubiquitin protein ligase, which can conjugate ubiquitin to histones H1, H2A, H2B, H3 and H4 in vitro. This enzyme is the major UBC4-1-dependent histone-ubiquitinating E3 [108]. It has been previously demonstrated that the activation of ubiquitin conjugation during spermatogenesis is dependent on the UBC4 pathway; therefore, E3^{Histone} is possibly responsible for chromosome condensation during spermatid maturation [97].

The HERC family is defined as a group of proteins that contain both HECT and RCC1 (regulator of chromosome condensation -1) - like domains in their amino acid sequences. Six HERC genes have been identified from the human genome. They endcode two types of polypeptides: HERC1 and 2 are gigantic proteins (more than 500 kDa), HERC 3 to 6 are small proteins that possess little more than the HECT and RCC-1 domains. HERC proteins may be ubiquitin ligases, as at least HERC 1, 3 and 5 have been shown to form thiolester bonds with ubiquitin. However, no ubiquitination substrates have been reported for any of these proteins. Other evidence suggests that some HERC family members play important roles in intracellular membrane trafficking. Interestingly, most HERC proteins or their mRNAs are highly expressed in testis, suggesting specialized functions of HERC proteins in spermatogenesis [109]. This has been proven for HERC2, which is essential for mouse spermatogenesis. Mutations in mouse HERC2 lead to sperm acrosome defects and therefore male sterility [110, 111].

EDD is the mammalian ortholog of the *Drosophila melanogaster* hyperplastic disc gene (*Hyd*), which is critical for cell proliferation and differentiation in flies by regulating hedgehog and decapentaplegic signaling [112, 113]. EDD is a highly conserved, large, predominantly nuclear protein (around 300 kDa) that contains a number of putative protein-protein interaction domains, such as the PABC (C terminus of poly (A)-binding protein), UBA (ubiquitin associated) domain and the UBR box, suggesting multiple functions. For example, EDD functions as a UBC E3 ubiquitin protein ligase via its conserved c-terminal HECT domain. Interestingly, temperature-sensitive point-mutations of EDD cause imaginal disc hyperplasia or male and female infertility [114, 115]. Rat

EDD, also known as Rat100, is expressed abundantly in germ cells and is highly expressed in spermatocytes, moderately in round and slightly in elongating spermatids. It is induced during postnatal development of the rat testis, peaking at day 25. A number of unidentified testis proteins can be ubiquitinated by Rat EDD [116]. The above properties suggest that activity of Rat EDD may be important in male germ cell development.

Identification of substrates of an enzyme is critical for understanding its function. Therefore, in order to study the function of rat EDD in spermatogenesis, I will try to identify the substrates of this E3 ligase in testis. We had previously produced a polyclonal antibody against this protein. In my project, I will try to identify its substrates by coimmunoprecipitation from testis lysates followed by mass spectrometry.

1.5.2.4 Deubiquitinating enzymes in spermatogenesis

Although functions of DUBs in spermatogenesis have not been extensively studied, certain data indicate that some DUBs are essential for spermatogenesis. CYLD is a DUB and a tumor suppressor that is mutated in cylindromatosis, a predisposition towards tumors of skin appendages [117]. CYLD can physically interact with and inhibit the ubiquitination of receptor-interacting protein 1 (RIP1), a ubiquitin-dependent NF-κB activator. Loss of CYLD in testicular cells results in accumulation of ubiquitinated RIP1, causing chronic activation of NF-κB and therefore aberrant expression of antiapoptotic factors, Bcl-2 or Bcl-XL. This attenuates an early wave of germ cell apoptosis that is thought to function in keeping a proper balance between germ cells and supporting

Sertoli cells. Deregulation of this early phase of apoptosis caused by loss of CYLD results in aberrant germ cell differentiation during the late stages and impaired spermatogenesis. Thus, CYLD is an essential DUB in the regulation of spermatogenesis and male fertility.

USP42 is a DUB first identified from mouse embryonic stem cells [118]. It is expressed in many tissues, with strong expression in the testis. In the embryo, USP42 is expressed strongly at day E10.5, which is the stage of gonad development in mouse. During testis development, expression of USP42 rises from 2 weeks after birth, persists until the round spermatid stage and rapidly decreases in condensing spermatids. The regulated pattern of expression of USP42 suggests a role of this DUB in mouse germ cell development and spermatogenesis. Another USP enzyme, USP2 was also reported to have testis specific expression with induction in late elongating spermatids [119].

Expression of another DUB, mUBPy was found throughout spermatogenesis, but increased in the postmeiotic phase [120]. It has a diffuse distribution in the cytoplasm of spermatocytes, with localization predominantly in patches around the nuclear envelope in round spermatids and compartmentalization around the acrosomal vesicle and centrosomal region in elongating spermatids. MSJ-1, a male germ cell-specific chaperone protein that can interact with mUBPy *in vitro*, has a similar distribution pattern in late-differentiating spermatids and spermatozoa. Distribution of proteasome partially

overlaps that of both mUPBy and MSJ-1 in late-differentiating spermatids and spermatozoa. These findings suggest possible MSJ-1/mUBPy/proteasome interactions during spermiogenesis and possibly fertilization.

Two UCH enzymes, UCH-L1 and UCH-L3 play important roles in spermatogenesis [79]. These two UCH isoenzymes have 52% amino acid identity and share significant structural similarity. UCH-L1 is restrictively expressed in the neural system and testis, whereas UCH-L3 is expressed in all tissues. In the testis, UCH-L1 is mainly expressed in spermatogonia and Sertoli cells, whereas UCH-L3 is expressed in spermatocytes and spermatids. The different expression patterns of these two isoenzymes suggest that they have different functions during spermatogenesis [121]. UCH-L1 and UCH-L3 are reciprocal modulators of germ cell apoptosis. In cryptorchid testes, the UCH-L1 mutant mice have increased expression of both antiapoptotic proteins Bcl-2 and Bcl-xL and prosurvival proteins pCREB and are relatively resistant to cryptorchid injury, whereas UCH-L3 knockout mice have slightly increased expression of mainly apoptotic proteins p53, Bax and Caspase-3 and show profound apoptosis-mediated germ cell loss [122]. In addition, overexpression of UCH-L1 induces massive apoptosis during spermatogenesis [123]. During spermatogenesis, apoptosis controls germ cell numbers and eliminates defective germ cells to facilitate testicular homeostasis. UHC-L1 is essential for the early apoptotic wave of germinal cells and for sperm quality control during spermatogenesis [124].

1.6 Muscle wasting and the ubiquitin system

Skeletal muscle is the most abundant tissue in the human body; it constitutes about 50% of total body weight. As a major site of metabolic activity, it directly converts chemical energy into mechanical energy and heat. It is also the largest reservoir of protein of the human body, providing amino acids as a source of energy in starvation. Muscle mass reflects a balance between protein anabolism and catabolism in the muscle tissue. Muscle wasting, which is loss of muscle mass, can be caused by many pathological conditions, such as starvation, cancer, sepsis, diabetes, denervation and immobilization. In these catabolic conditions, muscle wasting can result from increased protein breakdown, particularly breakdown of myofibrillar proteins.

1.6.1 Structure of skeletal muscle [125]

Skeletal muscle is made up of bundles (fasciculi) of muscle fibers, each fiber constituting a multi-nucleated syncytial cell 10-80 microns in diameter, and several to many centimeters long. Muscle fibers are formed in development by the fusion of uninucleate muscle precursor cells called myoblasts. The myoblast nuclei persist in the differentiated muscle fiber without further replication, for the life of the muscle fibre. Generally, each muscle fiber spans the entire length of the muscle and terminates at both ends in tendons.

The plasma membrane of an individual muscle fiber is termed the sarcolemma, which encloses the intracellular contents called sarcoplasm. Within the sarcoplasm are several hundred to several thousand myofibrils (1-2 microns in diameter), arranged in parallel. Myofibrils are serially – repeated linear arrays of the fundamental contractile unit, the sarcomere. The sarcomere is 2-3 microns in length and consists of parallel interdigitating protein filaments, termed myofilaments, some of which attach to a disk-like protein structure, termed the Z disk, which demarcates the ends of the sarcomere. The distribution of myofilaments gives different optical properties to various parts of the sarcomere so that with appropriate illumination, dark (A-bands) and light (I-bands) regions can be seen. In vertebrate skeletal muscle the sarcomeres of the numerous myofibrils are all in register across the width of the cell, which generates the characteristic striated appearance in the microscope.

1.6.2 The Ubiquitin-Proteasome System and Skeletal Muscle Wasting

Muscle wasting refers to a decrease in the size of skeletal muscle, which occurs in a variety of settings including disuse (i.e. immobilization, denervation etc.), starvation and many pathological states (cachexia, AIDS, sepsis, renal and liver diseases, diabetes, burns etc.). The maintenance of muscle mass is controlled by the normal balance between protein synthesis and protein degradation. During muscle wasting, loss of muscle protein occurs primarily through depressed synthesis and enhanced degradation pathways. Recent studies have shown that ubiquitin-proteasome dependent proteolysis is mainly responsible for the breakdown of muscle protein [126-128].

1.6.2.1 The activation of the ubiquitin pathway

Much evidence indicates that ubiquitin-proteasome dependent proteolysis plays an important role in muscle wasting. Increased skeletal muscle mRNA levels of ubiquitin have been reported in many catabolic states in both rodents and humans [129-131]. The elevated ubiquitin mRNA levels reflect increased transcription in muscle [132]. The expression of ubiquitin is also increased in skeletal muscle upon fasting, and the increased expression reverts rapidly to fed levels upon refeeding in parallel with the changes in the rates of proteolysis [133, 134]. Furthermore, starvation and denervation can cause an increase of 50-250% in levels of ubiquitin conjugated proteins in rat muscles [135]. Like rates of proteolysis, the amount of ubiquitin-protein conjugates and the fraction of ubiquitin conjugated to proteins increase progressively during food deprivation and returns to normal within one day of refeeding. Thus the changes in the pools of ubiquitin-conjugated proteins coincide with and may account for the alterations in overall proteolysis in skeletal muscle.

Although the ubiquitin system appears activated under conditions of muscle wasting, the exact sites of activation of this proteolytic pathway are still being uncovered. The mRNA level of E1 is low in skeletal muscle and has not been found to be increased in diabetic rats [136, 137]. It is a common essential enzyme in all processes dependent on ubiquitination. E1 is also a highly active enzyme and such highly active enzymes are usually not regulated or rate limiting. To date, regulation of E1 in mammalian skeletal

muscle has not been reported. Thus, the more likely sites of regulation would be mediated by E2 and E3.

There are possibly up to 40 mammalian E2s. However, only a small number of them are elevated in several, but not all conditions of muscle wasting. For instance, an isoform of yeast UBC4/5, UBC4-1 (human UBCH5B) is reported to be induced at the mRNA level in muscle of glucocorticoid treated rats [138]. Moreover, increased mRNA levels of UBC2/HR6B/E2_{14k} are seen in many forms of muscle wasting [134, 137, 139-141]. However, analysis of skeletal muscle protein degradation in mice lacking the HR6B/E2_{14k} gene has shown that these mice have similar muscle size, protein content and rates of proteolysis as those of the wild type mice [142]. This could be explained by the fact that in the null HR6B/E2_{14k} mice, levels of HR6A (highly similar to HR6B) are high enough to support conjugation by major E3s in the skeletal muscle. The possibility of the complementary role of HR6A is difficult to critically test because HR6A/HR6B double mutants are not viable [143]. Taken together, these findings demonstrate that regulation of ubiquitination can occur at the level of ubiquitin conjugating enzymes.

E3s form by far the largest family of ubiquitination enzymes. Among hundreds of members, E3 α /Ubr1, a RING-H2 E3 ligase recognizing substrates for the N-end rule pathway, is the first E3 identified to be up-regulated in muscle wasting induced by sepsis, diabetes and fasting [137, 144, 145]. An increase in mRNA levels of E3 α /Ubr1 has been observed in muscle in various catabolic models [137]. Furthermore, specific inhibitors of E3 α /Ubr1 suppress the increased ubiquitin conjugation in atrophying muscles from

tumor-bearing and septic rats [127]. However, the E3 α /Ubr1 knockout mice are actually 15-20% smaller in body weight which is at least partially due to a reduced mass in skeletal muscle and adipose tissues [146]. Thus, the physiological function of E3 α /Ubr1 in muscle protein degradation remains unclear.

Differential expression screening studies identified two genes whose expression increase dramatically in multiple models of skeletal muscle wasting: Muscle Ring Finger1 (MuRF1) and Muscle Atrophy F-box (MAFbx/Atrogin-1). MuRF1 and MAFbx/Atrogin-1 are muscle specific E3s. Expressions of MuRF1 and MAFbx are up-regulated in at least 13 distinct models of skeletal muscle wasting including denervation, immobilization, sepsis, glucocorticoid treatment. [147-149]. Therefore, they are thought to be involved in myofibrillar protein degradation. The MuRF1 gene encodes a protein containing three domains: a RING-finger domain, which has ubiquitin ligase activity, a B-box and a coiled-coil domain [36, 150]. Cardiac Troponin I and titin have recently been shown to be substrates of MuRF-1, suggesting that MuRF-1 may play a role in contractile apparatus degradation or titin turnover [151, 152]. MAFbx/Atrogin-1 consists of an F-box which is found in the substrate recognition subunit of the SCF (Skp1, Cullin, F-box) family. Recently, MyoD (a transcriptional factor in myoblast) and calcineurin (a phosphatase in cardiac myocytes) have been identified as substrates of MAFbx, suggesting that it functions in myotube differentiation and cardiac hypertrophy [153, 154]. MyoD controls myoblast function and differentiation, and is necessary to maintain the differentiated phenotype of adult fast skeletal muscle fibres. MAFbx targets MyoD for degradation in several models of skeletal muscle atrophy. In cultured myotubes undergoing atrophy,

MAFbx expression increases, leading to a cytoplasmic-nuclear shuttling of MAFbx and a selective suppression of MyoD. Overexpression of a mutant MyoDK133R, which lacks MAFbx-mediated ubiquitination, prevents atrophy of mouse primary myotubes and skeletal muscle fibres in vivo. Thus the suppression of MyoD by MAFbx seems to be a major event leading to skeletal muscle wasting [155].

The MuRF1 knockout and MAFbx knockout mice are both phenotypically normal. But, upon denervation, much less muscle mass is lost in either MuRF1-/- or MAFbx-/- mice in comparison to littermates, which indicates that these ubiquitin ligases play an important role in skeletal muscle wasting [148].

1.6.2.2 Activation of the deubiquitinating machinery

Skeletal muscle also contains a large number of DUBs, which are very active in soluble muscle extracts and responsible for removing ubiquitin from proteins. Ubiquitin aldehyde, an inhibitor of many DUBs, can increase the levels of ubiquitinated proteins in various tissue extracts including skeletal muscle in vitro [156]. Thus, down-regulation of DUBs may result in enhanced ubiquitination of proteins and activation of proteolysis, but no such downregulation has been observed to date.

However, some DUBs have been shown to be upregulated in wasting conditions. For instance, increased expression in USP-14 (ubiquitin-specific protease 14), a proteasome associated DUB, has been found in gene array studies of four different muscle wasting

conditions — fasting, diabetes, uremia and tumor [157]. Furthermore, in Dr. Wing's laboratory, another DUB, USP19 was also found to be over-expressed at the mRNA level in muscle wasting conditions of fasting, diabetes, cancer and glucocorticoid treatment [158]. Although the levels of expression of USP19 are not strictly parallel to the rates of ubiquitin-dependent proteolysis, it is inversely proportional to muscle mass.

The increased rather than the originally expected decreased expression suggests that these DUBs are functioning in a matter other than in negative regulation of overall protein degradation in muscle wasting. It is possible that the up-regulation of these enzymes help to recycle free ubiquitin and in this way support ubiquitination and protein degradation more efficiently in skeletal muscle wasting. The up-regulated expression of USP14 may also serve to increase efficiency of the proteasome. It is also possible that they may deubiquitinate and thereby stabilize specific proteins that are required for muscle wasting.

1.6.2.3 The regulation of the proteasome

The 26S proteasome is associated with myofibrils in mature skeletal muscle [159]. The demonstration that proteasome inhibitors (lactacystin, MG132) suppress the enhanced rates of overall proteolysis measured in muscles isolated from wasting conditions also provided support for a major role of the proteasome in the breakdown of muscle proteins [160-162].

Increased proteasome-dependent rates of muscle proteolysis have been reported to correlate with elevated mRNA levels of some subunits of the 20S core proteasome. For example, the increased expression of a rat 20S proteasome subunit C9 was seen in wasting arising from the unweighted soleus muscle, an increase in transcription of the C3 20S proteasome subunit mRNA was observed in acidosis, and enhanced transcription of C3, C5 and C9 were seen in insulinopenic rats [132, 163, 164].

Some subunits of the 19S complex are also up-regulated in muscle wasting; this up-regulation clearly depends on the given catabolic state [165]. The selective increased expression of some 20S or 19S proteasome subunits suggests that these subunits may be rate-limiting in assembly of the mature complex. In muscle, a variety of regulators has been found to affect the expression of subgroups of proteasome subunits. For example, TNF increases subunit C8 expression in muscle of tumor-bearing rats, and dexamethasone can induce subunit C3 expression in L6 muscle cells [166, 167].

1.6.2.4 The regulation of the ubiquitin proteasome system in muscle wasting

Many physiological factors that are involved in the regulation of overall muscle protein degradation also regulate the ubiquitin system in skeletal muscle. Various hormones, cytokines (TNF- α and interleukin-6 etc.) and myostatin [168] up-regulate the UPS, whereas insulin or IGF-1 inhibit the UPS.

- (1) Glucocorticoid hormones, which promote catabolism, can increase skeletal muscle mRNAs of Ub, E2_{14k}, and subunits of the proteasome [169, 170]. It is also required for the increased mRNA levels of Ub and proteasome subunits in muscle of rats subjected to fasting, acidosis or sepsis [171-173]. The mechanism of the glucocorticoid stimulated polyubiquitin gene transcription might involve a novel MEK and Sp1 dependent pathway [174].
- (2) On the other hand, the glucocorticoid stimulated expression can be blunted by administration of insulin-like growth factor-1 (IGF-1) through the PI3-kinase and Akt pathway. Insulin deficiency also results in increased expression of Ub, E2_{14k}, MAFbx/Atrogin-1, UBR1, USP14 and USP19 [157, 158, 164, 175, 176].
- (3) The NF- κ B transcription factor family mediates the activation of the UPS in various muscle catabolic states. NF- κ B can be activated by stimulating the phosphorylation of its inhibitor I κ B α . Mice with activated NF- κ B due to overexpression of activated I κ B kinase beta in skeletal muscle have increased expression of MuRF1 and severe muscle wasting, but normal expression of Ub, E2_{14k} and MAFbx/Atrogin-1 [177].
- (4) In addition, cytokines play important roles in mediating the catabolic response to sepsis and cancer cachexia. TNF- α can stimulate production of Ub, ubiquitinated proteins and E2_{20k} [178-180]. Proteolysis-inducing factor (PIF), isolated from a cachexia-inducing murine tumor (MAC 16), can stimulate transcription of Ub, E2_{14k} and the C9 subunit of the proteasome in mice [181, 182]. Myostatin is a transforming growth factor-beta (TGF-

beta) super-family member. Inactivation of the myostatin gene can cause an increase in both the size and the number of myofibers in cattle and mice [183, 184]. It has been found that myostatin can negatively regulate muscle growth and development by upregulating the ubiquitin associated genes atrogin-1, MuRF-1, and E2_{14k} [168].

In conclusion, based on the above discussion, the ubiquitin proteasome system plays an important role in skeletal muscle wasting. Despite the extensive studies of E2s and E3s, the importance of DUBs in skeletal muscle wasting has not drawn significant attention. In my project, I will study the function and mechanism of a DUB, USP19 in skeletal muscle growth and atrophy.

In this thesis, I will explore the function of several enzymes of the ubiquitin proteasome system in spermatogenesis and muscle wasting, which are both involved with bulk protein degadation. My objectives are:

- 1. To determine the function of E2 UBC4-testis in testis under stress conditions.
- 2. To identify substrates of E3 EDD/Rat100.
- 3. To determine the function of DUB USP19 in myofibrillar protein expression and modulation of the catabolic effects of TNF-α/IFN-γ or dexamethasone in muscle cells.

Chapter 2

Function of the E2 enzyme UBC4-testis in mammalian

spermatogenesis

The Saccharomyces cerevisiae E2s are 17 kDa UBC4/5 enzymes that are essential for degradation of short-lived and abnormal proteins. To date, at least six mammalian homologues of yeast UBC4/5 have been described in the literature; they are human UBCH5A [185, 186], UBCH5B, UBCH5C [187], UBCH6 [188] and rodent UBC4-1 [98], UBC4-testis [99]. Among these isoforms, UBC4-1 and UBC4-testis, previously named isoforms 2E and 8A respectively, were identified in Dr. Wing's laboratory and are highly expressed and induced during spermatogenesis [98, 99]. UBC4-testis is so named because of its restrictive expression in the testis. Expression of UBC4-testis is absent in early life, but is induced during sexual maturation. UBC4-testis mRNA is expressed mainly in round spermatids, but its protein is found not only in round spermatids but persists also in elongated spermatids. UBC4-testis is highly similar to S. cerevisiae UBC4/5, with 91-93% amino acid identity. However, the different amino acids in UBC4testis confer a unique acidic pI (approximately 5.4), in contrast to the basic pI of the other UBC4 isoforms. This difference in sequence between UBC4-testis and other rat isoforms also conferred differences in biochemical functions. For instance, in in vitro ubiquitination assays, UBC4-testis was less effective than the ubiquitous isoform UBC4-1 in conjugating ubiquitin to certain fractions of a testis protein extract. Thus, the specific

expression and induction in the testis and the distinct biochemical characteristics of UBC4-testis suggest a unique role in spermatogenesis [99].

In order to explore the *in vivo* function of UBC4-testis, mice bearing inactivation of this gene were produced [189]. Homozygous (-/-) mice showed normal body growth, fertility as well as testis morphology. In young mice, testes during the first wave of spermatogenesis showed a developmental delay, being approximately 10% smaller in weight at 40 and 45 days of age but became normal at 65 days of age. In adult mice, the testis weight and morphology became normal. No obvious biochemical abnormalities (overall protein content, levels of ubiquitinated proteins, and ubiquitin-conjugating activity) were detected in homozygous (-/-) mice. The quantity and function of the sperm as determined in in vitro fertilization assays and in motility analyses were also normal.

To maintain efficient spermatogenesis in most mammals, testes must descend shortly after birth into the scrotum, where the temperature is approximately 5 °C lower than the body core temperature. Failure of the testes to descend into the scrotum results in cryptorchidism, a common cause of sterility. Thus, experimental cryptorchidism is extensively used as a model of stress of the testis. Exposure of the testis to the higher body core temperature can affect all the main cell types in the testis, including germ, Leydig, and Sertoli cells. However, the earliest cellular changes mainly involve early pachytene spermatocytes and early spermatids. In the high temperature environment, these cells are progressively depleted by apoptosis, which accounts for the decrease in the testicular mass [190, 191]. To determine whether the germ cells lacking UBC4-testis

might be more sensitive to stress, I exposed testes from wild-type and knockout mice to heat stress by experimental cryptorchidism [189].

2.1 Materials and methods

Protocols for animal experiments were approved by the Animal Care Committee, McGill University. The UBC4-testis heterozygous (-/+) mice were produced in Dr. Wing's laboratory (Fig. 4A). These heterozygotes were backcrossed over seven generations on a BALB/c background before they were mated to obtain homozygous knockout (-/-) and wild-type (+/+) littermates [189]. There were totally 120 mice of approximately 100 days old used in this experiment. Homogenous (-/-) inactivation of the UBC4-testis gene was confirmed by Southern Blotting and PCR analysis of tail genomic DNA (Fig. 4B). Wild type (+/+) mice from the same litter were used as negative controls. Anaesthesia was induced with 1µl/g body weight *i.m.* injection of Ketamine HCl (100 mg/ml), Xylazine maleate (10 mg/ml) and Acepromazine (20 mg/ml). A median abdominal incision was made through the skin and the abdominal muscle. After both testes were identified, the right testis was raised into the abdominal cavity and sutured via its perigonadal fat pad to the ipsilateral lowest rib (cryptorchid testes), the left one was mock manipulated and then returned to the scrotum to serve as a control (scrotal testes).

The mice were sacrificed 2, 4, 6, 8, and 10 days after the surgery. If a testis was necrotic or descended into scrotum due to a loosened suture, this sample was excluded from the analysis. Otherwise, the testes were isolated quickly, weighed and then fixed by

immersion in Bouin's solution. After dehydration with progressively increasing concentrations of ethanol, the testes were sectioned (4 μ m) and stained with haematoxylin-eosin staining.

2.2 Results

Although a developmental delay of the testis was identified in the UBC4-testis knockout mice between 40 and 45 days of age, no obvious defects of the testis were detected in adult knockout mice under normal conditions. Therefore, we asked whether a stress to the testis - experimental cryptorchidism - can induce a defect in the testis of knockout mice.

After surgery, the mice were sacrificed at different time points, and the weight and morphology of the testes were analyzed. The ratio of the cryptorchid testis and the scrotal testis weight were plotted in Figure 5. During the early stage of experimental cryptorchidism, the cryptorchid testes gained weight relative to the scrotal testis, which was likely due to the acute inflammatory edema induced by the heat stress or cell death. The weight of the cryptorchid testes peaked at the 4th day after the surgery and then gradually diminished. This decrease is likely due to the depletion, predominantly by apoptosis, of seminiferous epithelial cells in the heat-stressed testes. The evolution of the weights of the testes of both the knockout and the wild type mice followed similar changes. No significant difference was noted between the knockout and wild type mice.

The testes were subjected to histological analysis. (1) Under normal conditions, the seminiferous tubules in the testes of the UBC4-testis knockout mice were round in shape

in cross section and showed normal spermatogenesis (Fig. 6A, B). The seminiferous tubules in the cryptorchid testes had a similar shape in cross section but the diameter showed progressive reduction with increasing duration of cryptorchidism. (2) On the 2nd day of cryptorchidism, a reduction of diameter was only seen in some seminiferous tubules. Depletion of germ cells was not significant. Some spermatozoa with relatively normal morphology still appeared in the lumen of the seminiferous tubules (Fig. 6C, D). (3) In the 6-day cryptorchid testes, spermatogenesis was clearly disturbed; disorganization and damage in the seminiferous tubules were evident. There were only 2-3 layers of seminiferous epithelial cells with some degree of degeneration. Most of these cells appeared to be degenerating spermatocytes. Vacuoles started to appear within the seminiferous epithelium. A few morphological abnormal spermatozoa and detached round seminiferous epithelial cells remained in the lumen. The diameter of the tubules was more reduced. However, due to the loss of seminiferous epithelial cells, the tubules' lumen was widened (Fig. 6E, F). (4) Ten days after cryptorchidism, the seminiferous tubules were totally devoid of spermatozoa, but some round detached epithelial cells were still seen in the lumen. The seminiferous epithelium contained merely a single layer of severely degenerated cells as well as numerous vacuoles. Spermatocyte-like cells were rarely seen. The tubule diameter was further reduced, with the lumen more widened (Fig. 6G, H). Histological analysis showed similar degrees of germ cell degeneration in both the knockout and the wild type mice. In addition, seminiferous tubules of the same stage were compared in cryptorchid testes of the wild type and the knockout mice at time points when enough germ cells remained to allow staging. No significant differences were seen.

2.3 Discussion

Because of the specific expression of UBC4-testis in spermatids, we hypothesized that it played an important role in spermatogenesis and that homozygous inactivation of this gene would severely interfere with spermatogenesis. To our surprise, adult knockout mice were fertile and showed normal testis weights, spermatid number, protein content, rate of ubiquitination and quantity and quality of sperm. Even when subjected to the heat stress of experimental cryptorchidism, the profile of germ cell degeneration was not significantly different from that of wild type mice. However, a subtle delay in postnatal development during the first wave of spermatogenesis had been found in knockout mice. The testes of the UBC4-testis knockout mice were approximately 10% lower in weight during 40 to 45 days of age and became normal after 65 days [189].

The above results indicate that UBC4-testis can facilitate testis growth in young mice, but it is not essential for spermatogenesis. It appears to promote the evolution of the first wave of spermatogenesis beginning at 25 days of age, which is implicated by its induction in round spermatids during this period of time. In adult mice, UBC4-testis is expressed predominantly in round spermatids, but persists into elongating spermatids [99]. However, despite careful examination, we found no evidence of disturbance at any stage of spermatogenesis in UBC4-testis knockout mice. Indeed, these mice were fertile and produced normal sperm as measured by motility assays, indicating that UBC4-testis is not essential for spermatogenesis.

The delay in testis development may occur because UBC4-testis binds a specific cognate E3 that recognizes specific substrates during the first wave of spermatogenesis. Alternatively, some other highly similar isoforms of UBC4, such as UBC4-1, coexist in testis and also increase in expression during elongation of round spermatids [97]; the mass action of these other increasing isoforms may eventually complement the loss of UBC4-testis, explaining the catch up to the normal testis weight towards 65 days. UBC4-testis may still have some other functions in spermatogenesis, but in UBC4-testis knockout mice, these functions might be complemented by the other abundant isoforms. We cannot exclude at this time that it is required for response to stresses other than the heat stress of cryptorchidism. Identification of bona fide UBC4-testis specific E3 and substrates will help us understand the specific functions of UBC4-testis in spermatogenesis.

In conclusion, the delay in postnatal development during the first wave of spermatogenesis in UBC4-testis knockout mice reveal a function of UBC4-testis in facilitation of testis maturation in young mice. In adult mice, it does not have an essential function in either spermatogenesis or in the response of testis to heat stress. This result suggests that different isoforms of UBC4 may serve redundant complementary functions in testis; however, at the specific stage of testis development (postnatal days 25-30), they may play distinct roles to meet more complex functional requirements. This result is included in a publication characterizing the UBC4-testis knockout mice [189].

Chapter 3

Identification of substrates for EDD/Rat100, a 300 kDa ubiquitin protein ligase

Our previous work indicated that UBC4 isoforms are markedly induced during spermatogenesis [98, 99]. Since E2s must interact with E3s to mediate ubiquitination, it is important to identify UBC4 dependent E3s involved in mammalian spermatogenesis. Rat100 was previously identified as a 100 kDa HECT domain E3 that was highly expressed in the rat testis [192, 193]. In Dr. Wing's laboratory, it has been observed that Rat100 can accept ubiquitin from several UBC4 isoforms, including UBC4-1 and UBC4-testis [194]. The expression of Rat100 is induced during postnatal development of the rat testis, peaking at day 25. It is highly expressed in spermatocytes, moderately in round spermatids and slightly in elongating spermatids. These data suggest a function of Rat100 in mammalian spermatogenesis, which is supported by the essential function of hyperplastic discs (HYD), a Drosophila ortholog of Rat100, in Drosophila spermatogenesis [113].

The HYD gene was initially cloned by investigating temperature-sensitive mutants that caused imaginal disc overgrowth in larvae at restrictive temperatures [113, 195]. Some mutations of the HYD gene result in imaginal disc hyperplasia and adult sterility due to germ cell defects, while the null HYD phenotype is lethality in the pupal or larval stages [113, 196]. The human homologue of HYD, also called EDD (E3 isolated by Differential

Display), is an approximately 300 kDa HECT-domain ubiquitin ligase, which can be transcriptionally induced by progestin in human breast cancer cells [112]. Aberrant expression or mutation of EDD has been identified from a variety of cancers, including those of breast, ovary, liver and squamous cell [197, 198]. Recently, it has been reported that EDD can act as a putative colorectal tumor suppressor by interacting with and upregulating the expression level of the APC (adenomatous polyposis coli) tumor supressor. EDD and APC can interact with each other both in vivo and in vitro. They are colocalized in the perinuclear region of the cytoplasm of HEK293T or Hela cells. Overexpression of EDD increased the protein expression level of APC, resulting in inhibition of beta-catnenin and therefore the downstream Wnt signaling. Conversely, siRNA mediated depletion of EDD decreased APC at the protein level without altering its mRNA level, causing enhanced protein expression of beta-catenin. The mechanism by which EDD stabilizes APC remains to be determined [199]. EDD can also interact with the DNA damage checkpoint kinase CHK2 and is necessary for the efficient activation by phosphorylation of CHK2 in response to DNA damage [200]. EDD-depleted cells have decreased CHK2 activation and therefore defective checkpoint activation, leading to radio-resistant DNA synthesis, premature entry into mitosis, accumulation of polyploid cells, and cell death via mitotic catastrophe [201]. In addition, expression of EDD is upregulated in ultraviolet-irradiated normal HaCaT human keratinocyte cells [202]. These data indicate that EDD can function as a mediator in DNA damage signal transduction and in the maintainance of genomic stability.

EDD has an essential role in embryonic development. While EDD +/- mice have normal development and fertility, no viable EDD -/- embryos have been observed beyond E10.5, with delayed growth and development evident from E8.5 onward. In EDD -/- embryos, failed yolk sac and allantoic vascular development, along with defective chorioallantoic fusion, compromise fetal-maternal circulation, leading to a general failure of embryonic cell proliferation and widespread apoptosis [115].

Although several proteins, such as APC, CHK2, anti-proliferative protein Tob2, importinα5, progesterone receptor, and calcium- and integrin-binding protein have been found to interact with EDD, to date, only Topoisomerase II\(\beta\) binding protein (TopBP1) and Katanin p60 have been identified as bona fide substrates of EDD [30, 114, 203, 204]. (1) TopBP1 colocalizes with BRCA1 at stalled replication forks and functions as a DNA damage checkpoint protein and cell cycle regulator [205]. Human HYD can bind and ubiquitinate TopBP1, which is degraded by the proteasome. In vitro, human UbcH4, UbcH5B, and UbcH5C can all transfer ubiquitin molecules to human HYD, leading to the ubiquitination of TopBP1. The HYD-TopBP1 relationship further supports functions of EDD/HYD in DNA damage response. (2) In addition, EDD can form a complex with DYRK2 (Dual-specificity tyrosine (Y) - phosphorylation regulated kinase 2), DDB1 (DNA-damage binding protein 1) and VPRBP (Vpr HIV-1 binding protein). DYRK2 functions as a molecular assembler required for the specific recruitment of EDD to DDB1-VPRBP, thus forming a novel E3 ligase complex, the DYRK2-EDVP complex. In this complex, VPRBP, a WD40 domain containing protein, is the substrate binding receptor subunit, and EDD is the catalytic subunit. Katanin p60, a microtubule APTase is

a substrate of the DYRK2-EDVP E3 ligase complex. DYRK2 mediated phosphorylation of Katanin p60 is required for its polyubiquitination by EDD. Since Katanin is responsible for severing microtubules at the mitotic spindles when disassembly of microtubules is required to segregate sister chromatids during anaphase, the DYRK2-EDVP E3 ligase complex can regulate mitotic progression by modulating Katanin protein levels. Overexpression of EDD has been reported in cancers [197, 198]. The aberrant mitosis and altered cell cycle progression via the hyperactivation of the DYRK2-EDVP E3 ligase complex might contribute to the oncogenic property of EDD.

Because of the high molecular weight, it is difficult to study the overall structure of EDD. However, some domains have been identified from EDD. They include the HECT, UBA, PABC and UBR domains. The HECT domain is located in the C terminus of EDD and its characteristics have been discussed in chapter one. The long N terminal extension is thought to be responsible for substrate binding and subcellular localization. EDD contains an N-terminal ubiquitin-associated (UBA) domain, which is present in a variety of proteins involved in ubiquitin-mediated processes. The EDD UBA domain has similar affinities in binding with polyubiquitin chains or monoubiquitin, suggesting that EDD can bind to monoubiquitinated proteins [206]. The PABC domain is a peptide-binding domain that is found in both poly(A)-binding protein (PABP) and the N terminus of EDD. PABP is a highly conserved protein and is one of the eukaryotic translation initiation factors (eIFs). It contains four RNA recognition motifs (RRMs) in its N terminal domain, and a proline-rich C-terminal domain (PABC) responsible for several protein-protein interactions. The PABC domain of PABP can recruit various regulatory

proteins and translation factors to poly(A) mRNAs. PABP can stimulate translation by promoting mRNA circularization through simultaneous interactions with eIF4G and the 3' poly(A) tail through the same RRMs [207, 208]. Activity of PABP is regulated by two PABP-interacting proteins (Paips), Paip1, a translational stimulator, and Paip2, a translational inhibitor. Paip1 and Paip2 share two conserved PABP-interacting motifs (PAMs): PAM1, which binds strongly to the RRM region of PABP, and PAM2, which binds to the PABC domain [209]. The PABC domain of EDD can bind PAM2 with structural features and binding affinity that are similar to the PAM2 domain of PABP [30]. Thus EDD might paly a role in regulation of translation, and proteins that contain the PAM2 motif are potential substrates of EDD. Finally, the UBR box is identified from a unique E3 class that recognizes N-degrons or structurally related molecules, via the ~70-residue zinc finger-like UBR box motif, for ubiquitin dependent proteolysis. In the N-end rule pathway, a group of proteins bearing degradation signals, termed N-degrons, whose determinants include destablizing N-terminal residues, are selectively degraded in the ubiquitin-proteasome system. E3 ligases that recognize N-degrons are called Nrecognins. EDD can bind to destablizing N-terminal residues through the UBR box in the N terminus of EDD. This identifies EDD as a N-recognin E3 ligase [210]. The in vivo Nend rule pathway substrates of EDD remain to be determined.

Rat100 was originally identified as a 100 kDa protein-encoding cDNA, whose transcription was upregulated during testicular maturation [193]. The *in vitro* translated 100 kDa protein shows the activity of a HECT domain E3 ligase [192, 194]. It shares 96% identity with the C terminal 889 amino acids of EDD. A subsequently identified

error in the published translation start site in the Rat100 cDNA might be responsible for the large discrepancy in the predicted size of the human EDD and Rat100 proteins, pointing to the likelihood that a larger gene product of Rat100 exists [112]. In Dr. Wing's laboratory, it has been found that the Rat100 cDNA is highly homologous to the cDNA EDD and that the apparent molecular weight of Rat100 in Western blotting with a Rat100 specific polyclonal antibody appeared to be approximately 300 kDa rather than the previously identified 100 kDa [112]. This raised the question as to whether the 100 kDa protein was the true rat gene product. In this project, carried out before the availability of full length expression libraries and whole genome sequences, I answered this question by analyzing the GenBank mouse expressed sequence tag (EST) database. In the following data, Rat100 was finally identified as a true rodent homologue of EDD, and therefore we refer to it as EDD/Rat100. Moreover, in order to expand our limited understanding of the functions of this E3 ligase, I also tried to identify some of its substrates.

3.1 Materials and methods

3.1.1 Identification of N-terminal Rat100 sequences similar to human EDD by RT-PCR and DNA sequencing.

The amino acid sequence of human EDD that was upstream from the C-terminal HECT domain was used as the query sequence in Blast searches (tBlastn) of the GenBank mouse expressed sequence tag (EST) database that was available in 2002. The obtained EST sequences were aligned according to the human EDD sequence. Alignment revealed

areas with ambiguous sequences. In order to clarify the controversial bases in the overlapping EST sequences, nine pairs of PCR primers were synthesized based on the surrounding consistent EST sequences. To ensure the best sequencing results, the predicted PCR products were designed to be 350-500 bps. Mouse testis cDNA was used as templates to amplify these sequences by PCR using the Taq polymerase. PCR products were ligated into the pGEM-T plasmid (Stratagene) and then transformed into DH5 α . The plasmids were purified on Miniprep columns (Qiagen) and sent for automatic bidirectional DNA sequencing with the T7 and SP6 sequencing oligos at the McGill University and Genome Quebec Innovation Centre. Finally, the sequencing results were aligned with the other sequences to produce a full encoding sequence. The amino acid sequence was predicted using the EMBOSS online analysis tools.

3.1.2 Antibodies and Western blotting

The anti-EDD/Rat100 rabbit antiserum was produced as previously described [116]. A nonconserved Rat100 peptide (amino acids 33-401) was used to raise the antiserum. To increase the specificity of this antiserum, I affinity purified it with a column that was coupled with a maltose binding protein (MBP)-tagged fragment of Rat100 (amino acids 219-401). The 2 ml column was first washed with 20 ml of 10 mM Tris (pH 7.5). Two ml of antiserum were diluted in 20 ml of 10 mM Tris (pH 7.5) and then passed through the affinity column 5 times. The column was subsequently washed with 40 ml of 10 mM Tris (pH 7.5), followed by 40 ml of 10 mM Tris (pH 7.5), 0.5 M NaCl. Antibody was eluted with 20 ml of 100 mM Glycine (pH 2.5) and collected in 2 ml of 1M Tris (pH 8.0) to

neutralize the pH to 6-8. The pH of the column was neutralized by washing with 10 ml of 10 mM Tris (pH 8.8). Finally, the column was washed with 10 ml of 10 mM Tris (pH 7.5) and 0.02% sodium azide. The column was saved in the final washing buffer at 4°C for repeat use. The antibody concentration was determined by the Bradford method using the Bio-Rad Protein Assay Kit. The purified antibody was saved at 4°C until use for Western blotting or immunoprecipitation.

The following antibodies were also used: rabbit polyclonal anti-ATP-citrate lyase antibody (supplied by Dr. Ingeborg Hers, University of Bristol, UK.), rabbit anti-Miwi antiserum (supplied by Dr. Haifan Lin, Duke University, US), rabbit anti-Eps15 antibody (supplied by Dr. Ted Fon, McGill University), rabbit polyclonal anti-Paip2 antibody and anti-PABP antibody (supplied by Dr. Nahum Sonenberg, McGill University), anti-CRMP-2/TOAD-64 monoclonal antibody (C4G) (supplied by Dr. Y. Ihara, Tokyo University, Japan), rabbit polyclonal anti-Cbl (C-15) antibody, rabbit polyclonal anti-NF-kB p65 (C-20) antibody and mouse monoclonal anti-GFP (B-2) antibody (Santa Cruz Biotechnology, Inc.), rabbit anti-ubiquitin antibody, mouse monoclonal anti-FLAG M2 (F3165) antibody and rabbit polyclonal anti-FLAG (F7425) antibody (Sigma).

After SDS-polyacrylamide gel electrophoresis (SDS-PAGE), proteins were transferred onto Polyvinylidene fluoride (PVDF) or nitrocellulose membranes (Amersham) by electrotransfer at 4°C overnight. The membrane was then prehybridized for 1 hour at room temperature with the TTNS buffer (25 mM Tris·HCl (pH 7.5), 0.9% NaCl, and 0.1% Tween 20) containing 5% milk. After prehybridization, the membrane was briefly

washed and incubated in TTNS buffer containing 3% bovine serum albumin (BSA) and the primary antibody (diluted according to its protocol) at room temperature for 3 hours or at 4°C overnight. The membrane was rinsed with the TTNS buffer three times and then incubated in the TTNS buffer containing 5% milk and the secondary antibody coupled to horseradish peroxidase diluted at 1:5000-1:10000 at room temperature for 1 hour. After the final rinses, chemiluminescent detection was performed with the enhanced chemiluminescence kit (ECL-plus, Amersham).

3.1.3 Immunoprecipitation of Rat100 and in vitro ubiquitination assay

E1, E2, GST and GST-Paip2 were prepared as previously described [98, 211]. EDD/Rat100 (E3) was isolated from 24 mg of testis lysate of a 40-day-old Sprague-Dawley rat by immunoprecipitation with 81 μg of immunoaffinity purified anti-EDD antibody [116] bound to 560 μl (50% slurry) of Protein A Sepharose beads. The pellet was washed twice with cold 20 mM Tris-HCl (pH 7.5), 50 mM NaCl, 1 mM MgCl₂, 1 mM DTT, 0.5% Nonidet P-40 and protease inhibitor cocktail (Roche), followed by two washes with 50 mM Tris-HCl (pH 7.5), 1 mM DTT. The ubiquitination reaction contained 50 mM Tris-HCl (pH 7.5), 2.5 mM MgCl₂, 0.5 mM DTT, E1 (125 nM), E2 (UBC4-1, 500 nM), purified GST protein (4.5 μM) or GST-Paip2 (4.5 μM), AMP-PNP (5'-adenylylimidodiphosphate lithium, 2 mM), ubiquitin aldehyde (5 μM) and as E3, 14% of the pellet containing immunoprecipitated EDD. Following pre-incubation at 37°C for 5 minutes, His-ubiquitin (5 μM) was added to start the reaction. AMP-PNP can be used by ubiquitin activating enzyme (which cleaves ATP to AMP and PPi) to support

ubiquitin conjugation, but not by the proteasome which cleaves ATP to ADP and Pi [212]. We routinely use AMP-PNP in conjugation reactions to prevent degradation of ubiquitinated protein products by any contaminating proteasome in our reagents. Ubiquitin aldehyde is an inhibitor of many deubiquitinating enzymes [213] and can therefore prevent the loss of ubiquitinated proteins by such contaminating enzymes. Ubiquitin aldehyde was synthesized as described [214]. UBC4 family isoforms were used because they have been previously shown to be the most effective E2s in supporting EDD mediated ubiquitination when a group of conjugating enzymes was tested [203]. The reaction (120 µl) was incubated at 37 °C for 55 minutes with gentle agitation every 10 minutes. Following centrifugation at 1000 rpm for 1 min to isolate the beads, the supernatant from each reaction was mixed with 30 µl (50% slurry) of glutathione agarose beads (Amersham Bioscience) in 1 ml RIPA buffer (150 mM NaCl, 1.0% NP-40, 0.5% Sodium deoxycholate, 0.1% SDS, 50 mM Tris-HCl (pH 8.0)) at room temperature for 2 hours to isolate the products. The pellets were washed four times with 1ml RIPA buffer, then resuspended in 3x Laemmli sample buffer containing 10% 2-mercaptoethanol, boiled for 10 minutes, and processed for Western blot analysis with anti-GST, anti-Paip2, or anti-ubiquitin antibodies as indicated.

3.1.4 Small RNA interference of EDD in HEK293 cells.

Six siRNA duplexes for EDD were designed as 21-mers with 3'-dTdT overhangs [215]. The siRNAs were purchased from Dharmacon. Two siRNA duplexes that produced the best depletion of EDD were used in this experiment. The sequences are: #295, 5'-

AATTGTGCAACGTAGCAGAGT-3'; #297, 5'-AATGGGGATTGCTCGTCCAAC-3'.

A non-specific siRNA control duplex VII (57% GC content) was used as a negative control (Dharmacon).

HEK293 cells were grown in Dulbecco's modified Eagle's medium (DMEM-high glucose, Gibco) supplemented with 10% fetal bovine serum (Gibco) and penicillin/streptomycin solution (Gibco) in 5% CO₂. The cells were seeded in 6-well plates and were grown to 40-50% confluence before transfection. SiRNA oligonucleotides were transfected at a final concentration of 100 nM, using Lipofectamine and the Plus reagent (Invitrogen) according to the manufacturer's protocol. Forty eight hours after transfection, cells were harvested in the denaturing lysis buffer (50 mM Tris pH 7.5 and 2% Sodium dodecyl sulphate (SDS)). Cell lysates were passed through 30-gauge needles for 5 times to shear the DNA. Protein concentrations of the cell lysates were determined with a detergent-compatible Micro BCA Protein Assay Kit (Pierce). For SDS-PAGE, the same amount of protein lysate (100 µg) from each sample was loaded onto a polyacrylamide gel. EDD, actin and other proteins were detected by Western blotting, using the ECL-plus kit (Amersham) as mentioned before. The chemiluminescent signal from each protein band was quantified using a Bio-Rad model 3000 VersaDoc Gel Imaging System and the Quantity One software. The amount of βactin was used as a loading control to normalize the quantity of other proteins from the same sample.

3.1.5 Immunoprecipitation of EDD/Rat100 and identification of co-purified proteins by mass spectrometry

The antibody was cross linked to Protein-A beads with dimethyl pimelimidate dihydrochloride (DMP). Immunoaffinity purified anti-Rat100 antibody (500 µg) was incubated with 600 µl 50% slurry of Protein A sepharose beads (Amersham Biosciences) with gentle agitation at 4°C overnight. The beads were then washed twice with 2 ml of freshly made 0.15 M Sodium Borate (pH 9.0). The beads were resuspended in 3 ml of the same buffer and crosslinked with 0.0233 g DMP at room temperature for 45 minutes. The crosslinking was then quenched by washing the beads once with 3 ml of 0.2 M ethanolamine (pH 8.0) followed by incubation of the beads in 3 ml of the same buffer at room temperature for 2 hours. Finally, the beads were washed with 20 mM Tris (pH 7.5) supplemented with 0.02% sodium azide and saved at 4°C before using. To test the efficiency of crosslinking, a small amount of the crosslinked beads were treated with 3x Laemmli sample buffer containing 10% 2-mercaptoethanol, boiled for 10 minutes, and analyzed with SDS-PAGE and silver staining. Only less than 5% of the antibody heavy chain could be eluted from the beads, indicating good crosslinking efficiency. Normal rabbit IgG was crosslinked in the same way, and was used in the immunoprecipitation as a negative control.

The rat testis lysate was produced as previously described. The expression of Rat100 is subject to developmental regulation and peaks between 25 to 40 days after birth [116]. Therefore, testes of 30-day rats were used to produce the lysate. Briefly, testes of

Sprague-Dawley rats were suspended in 5 ml/g of cold 50 mM Tris-HCl (pH 7.5), 0.25 M Sucrose, 1 mM DTT, 1 mM EDTA and protease inhibitor cocktail (Roche). The testes were sliced and homogenized with a Potter Elvehjem (Wheaton Science Products, Millville, NJ) tissue grinder. The homogenates were subjected to centrifugation at 10,000 g for 10 minutes. The supernatant was then centrifuged at 100,000 g for 1 hour. The final supernatant was divided into aliquots and frozen at -80°C. The protein concentration was determined by the Bradford method using the Bio-Rad Protein Assay Kit.

For immunoprecipitation, 4.5 ml of 50% Protein A sepharose was noncovalently bound with 1.5 mg normal rabbit IgG for use in preclearing. Freshly made rat testis lysate 30 mg was diluted to approximately 2 mg/ml with the IP buffer (20 mM Tris (pH 7.5), 50 mM NaCl, 5 mM N-ethylmaleimide (NEM, to inactivate EDD and to increase the possibility of substrate trapping), 0.5% Nonidet P-40 and protease inhibitor cocktail) and incubated with the beads coupled to normal rabbit IgG at 4°C for 1 hour. The precleared rat testis lysate was divided into 3 aliquots for the subsequent immunoprecipitation. One aliquot was incubated with 75 µg of DMP crosslinked anti-Rat100 antibody. The second aliquot was incubated with 75 µg of DMP crosslinked normal rabbit IgG as a negative control. As another negative control, the same amount of DMP crosslinked anti-Rat100 antibody was first incubated at a 1:2 molar ratio with the Rat100 peptide (amino acids 219-401), which was used to immunoaffinity purify the anti-Rat100 antibody, to saturate the antigen binding sites on the antibody [116]. The preabsorbed antibody was then washed with the IP buffer and incubated with the third aliquot of the precleared rat testis lysate. All of the aliquots were incubated with gentle agitation at 4°C for 1 hour. Then the beads

were collected by centrifugation and washed four times with the IP buffer. The pellets were resuspended individually with 100 µl of 3x Laemmli sample buffer containing 10% 2- mercaptoethanol, boiled for 10 minutes and loaded onto a 7.5-15% gradient polyacrylamide gel. Following SDS-PAGE, the gel was stained with the Invitrogen Colloidal Blue Staining Kit. Gel slices containing distinct protein bands specifically found in the first aliquot from specific immunoprecipitation of EDD/Rat100 but not in the two controls were sent for analysis by mass spectrometry in the McGill University and Genome Quebec Innovation Centre.

3.1.6 Plasmids and transfections.

Mammalian expression plasmid for FLAG-tagged EDD, pcDNA3-FLAG-EDD, was previously described [114] (supplied by Dr. Nahum Sonenberg, McGill University). Green fluorescent protein (GFP) tagged CRMP-2 (CRMP-2-GFP) plasmid was previously described [216] (supplied by Dr. Peter McPherson, McGill University).

HEK293 cells were cultured as described above. The cells were seeded in 10 cm diameter dishes and were grown to 40-50% confluence before transfection. FLAG-EDD plasmid or CRMP-2-GFP plasmid (1.5 μ g) was transfected in each dish, using Lipofectamine and the Plus reagent (Invitrogen) following the manufacturer's protocol. Forty-eight hours after transfection or at ~95% confluence, the cells were washed with cold PBS and harvested by scraping in 1 ml/10⁷ cells of cold 10 mM Tris-HCl (pH 8.0), 0.3 M Sucrose, 10 mM NaCl, 3 mM MgCl, 0.5% NP-40 and protease inhibitor cocktail (Roche).

Then, the cells were lysed by incubation on ice for 20 minutes with gentle agitation every 5 minutes. The lysates were subjected to centrifugation at 10,000 g for 10 minutes. Supernatants were carefully recovered and used for subsequent immunoprecipitation assays or saved at -80°C in small aliquots. The protein concentration of cell lysates was determined with the Bio-Rad Protein Assay Kit.

3.2 Results

3.2.1 The Rat100 cDNA encodes a 300 kDa protein

After identification of the first HECT domain E3, E6-AP, Huibregtse *et al.* used BLAST programs to search the NCBI data base for similar proteins. By this means, they discovered cDNAs for several HECT domain proteins, such as Rat100 (rat) and Rsp5 (yeast). In vitro transcription/translation of the Rat100 cDNA produced a 100 kDa protein that can form a ubiquitin-thiol ester through the cysteine residue in its HECT domain, confirming that Rat100 belongs to the HECT domain E3 family [16]. Northern blot revealed a 9.5-Kb mRNA of this protein suggesting a 6-Kb 5' noncoding region [193]. Subsequently, Callaghan *et al.* identified EDD, a human HECT domain protein with its C terminal amino acids 96% identical to Rat100. They also found a sequence error in the published translation start site of the Rat100 cDNA. Correction of this error would result in a longer continuous open reading frame and therefore a larger gene product [112]. However, they could not identify a DNA sequence containing Rat100 that encoded a 300 kDa protein and were unable to detect a 300 kDa protein by immunoblot analysis of any

rat tissues. Therefore, the real structure of the product of the Rat100 gene was still unclear

In Dr. Wing's laboratory, a rabbit polyclonal antibody was raised against a fragment of the 100 kDa Rat100 protein that is N terminal to the conserved HECT domain. This antibody successful recognized a 300 kDa protein band in Western blotting of rat testis lysates. A BLAST search in the mouse EST database also revealed many overlapping cDNA sequences that are highly similar to the 5' region of the human EDD cDNA (Fig. 7A). This suggests that Rat100 might be a much larger protein [116]. However, because of the relatively high frequency of sequencing errors in the EST database, it was difficult to determine the mouse EDD cDNA by directly using the EST sequences. In my project, I have corrected the sequencing errors in these EST sequences by PCR and DNA sequencing. By analyzing the overlapping EST sequences, I identified 9 regions containing controversial bases that resulted in sequence changes. (Degenerate codons encoding the same amino acids were not considered controversial.) These controversial bases were corrected according to the sequencing results. Thus, the validity of the EST sequences has been significantly improved.

In the EST BLAST search results, two regions of EDD had no apparent homologous mouse EST, producing two gaps amongst the overlapping EST sequences. To explore whether these sequences were present in the mouse orthologue, primers were derived from the adjacent ESTs and used in PCRs with mouse testis cDNA as template. DNA fragments were amplified and when sequenced predicted protein sequences that were 97

and 98% similar to the EDD sequence. The 5' end of the mouse cDNA was also sequenced by using the 5' RACE method [116]. Finally, I aligned all of these sequences together into an 8394 bp continuous open reading frame. The predicted mouse EDD/Rat100 amino acid sequence was 96% identical and 97% similar to human EDD (Fig. 7B). The theoretical molecular weight of mouse EDD is 309 kDa, which is consistent with the apparent molecular weight of rat EDD in our Western blotting results. Therefore, although we have not yet cloned a full length mouse EDD cDNA, our results of EST BLAST searches and Western blotting have sufficiently confirmed that Rat100 is indeed a much larger protein, which is highly homologous to human EDD, and therefore we refer to it as EDD/Rat100.

3.2.2 EDD/Rat100 can ubiquitinate the PABP-interacting protein 2 (Paip2)

For the so far identified HECT domain E3s, the substrate recognition domains all localize in the region N terminal to the HECT domain. Analysis of the predicted amino acid sequence of EDD/Rat100 revealed a PABC domain N terminal to the conserved HECT domain. As discussed in the introduction of this chapter, PABP can interact with Paips through the PABC domain. Therefore, we determined whether EDD/Rat100 can also directly interact with Paips through the PABC domain. If so, Paips might be substrates of EDD/Rat100 and be ubiquitinated by it.

To answer this question, we tested whether EDD/Rat100 directly catalyzes the ubiquitination of Paip2 in an *in vitro* ubiquitination system. Immunopurified

EDD/Rat100 was incubated with either bacterially expressed recombinant GST-Paip2 or GST, and other required ubiquitination components (including E1, and E2). The products were isolated using glutathione agarose beads, resolved by SDS-PAGE and then probed with anti-GST, anti-Paip2 or anti-ubiquitin antibodies (Fig. 8). In the presence of EDD/Rat100, GST-Paip2 underwent polyubiquitination (lane 6 and 7), but GST was not affected (lanes 9 and 10), indicating specificity for Paip2. Probing with the anti-ubiquitin antibody confirmed that these higher molecular weight conjugates of GST-Paip2 contained ubiquitin (lane 7). The anti-ubiquitin antibody detected even higher molecular weight conjugates. These conjugates likely contained multiple ubiquitins per moiety of GST-Paip2 and were therefore readily detected with the anti-ubiquitin antibody but not detected with the anti-Paip2 antibody (lane 6). In lane 3, a small amount of GST-Paip2 migrated slightly slower. This may represent monoubiquitinated GST-Paip2 due to the activity of E2 acting alone, as in some replicates of this experiment, a faint band can be detected in that position when probed with the anti-ubiquitin antibody. But polyubiquitination of GST-Paip2 can only be catalyzed by EDD/Rat100 (lanes 6 and 7). In vitro, EDD/Rat100 cannot catalyze ubiquitination of Paip1 (data not shown). These results indicate that EDD/Rat100 is an E3 ubiquitin ligase that has specificity for Paip2.

Subsequently, I asked whether EDD/Rat100 can ubiquitinate Paip2 in vivo. I first tested whether Paip2 can be coimmunoprecipitated by EDD/Rat100. In this experiment, EDD/Rat100 was immunoprecipitated by the anti-Rat100 antibody, and the coimmunoprecipitated proteins were analyzed by Western blotting with the anti-Paip2 antibody. Paip2 was not found to be coimmunoprecipitated by EDD/Rat100 in lysates of

either the rat testis or the HEK293 cell. Furthermore, I tested whether a reduction in the EDD/Rat100 protein level affects Paip2 in HEK293 cells. Polyubiquitinated proteins are usually targeted for proteasome proteolysis. My hypothesis was that if EDD/Rat100 can polyubiquitinate Paip2 in vivo, the reduction of EDD/Rat100 should decrease the polyubiquitination of Paip2 and therefore stabilize Paip2. I successfully knocked down EDD/Rat100 in HEK293 cells by RNA interference (RNAi), but the protein level of Paip2 was not significantly changed. Thus in the present study, it was unclear whether Paip2 is a true substrate of EDD/Rat100 in vivo.

3.2.3 Identification of putative substrates/interacting proteins of EDD/Rat100 by coimmunoprecipitation and mass spectrometry

In addition to Paip2, I also searched for other substrates of EDD/Rat100. I screened for substrates of EDD/Rat100 from proteins that can directly interact with EDD/Rat100 in vivo by using immunoprecipitation and mass spectrometry.

3.2.3.1 Isolation of potential substrates of EDD/Rat100 by coimmunoprecipitation

Since EDD/Rat100 is highly expressed in the rat testis, rat testis lysates were used to identify substrates of EDD/Rat100. In the present study, I immunoprecipitated EDD/Rat100 from rat testis lysates, resolved the copurified proteins by SDS-PAGE and excised the protein bands for identification by mass spectrometry analysis. Three steps were taken to optimize the immunoprecipitation. (1) The antibodies were covalently

crosslinked to Protein A sepharose with DMP to prevent the antibody from being coeluted with EDD/Rat100 and its associated proteins upon incubation of the beads with Laemmli sample buffer. Elution of the large amount of antibody present on the beads would obscure many other proteins when the eluates were analyzed by SDS-PAGE. (2) Enzyme catalyzed reactions usually are rapid. Although carrying immunoprecipitation experiment at 4°C may lower the enzyme's activity, we could not exclude the possibility that, during the long process of the experiment, some substrates that were bound to EDD/Rat100 at the beginning of immunoprecipitation may have become ubiquitinated. Products generally have much lower affinity with the enzyme and so may be released quickly after catalysis, causing the loss of the coimmunoprecipitated proteins at the end of immunoprecipitation. Therefore, to prevent the loss of substrates, the immunoprecipitation buffer was supplemented with NEM, which can permanently inactivate EDD/Rat100 by covalently modifying its active site cysteine in the HECT The inactivated EDD/Rat100 can still interact with substrates but cannot domain. catalyze ubiquitination, causing the substrates to be trapped with it. (3) To minimize the nonspecificity of immunoprecipitation, a control immunoprecipitation was carried out in which the antibody was preabsorbed with the antigen peptide that was used to affinity purify the antibody. This maneuver helped us successfully eliminate several nonspecific binding proteins in this experiment. As shown in Figure 9 Lane 3, the antigen peptide efficiently blocked the immunoprecipitation of the endogenous EDD/Rat100. Visible protein bands other than the antibody and the antigen peptide in this lane were considered to be nonspecifically bound to the anti-EDD/Rat100 antibody and therefore were excluded from the subsequent mass spectrometry analysis. In conclusion, after these three

optimizing steps mentioned above, the efficiency and specificity of the coimmunoprecipitation were significantly improved.

3.2.3.2 Identification of potential substrates by mass spectrometry

After immunoprecipitation, pellets were resolved on a gradient acrylamide gel by SDS-PAGE (Fig. 9A). Meanwhile, a small fraction (1% v/v) of the supernatants and the pellets were analyzed by Western blotting, which confirmed the efficiency of the immunoprecipitation of EDD/Rat100 (Fig. 9B). Nineteen Protein bands that only appeared in lane 2 were excised and sent for analysis by tandem mass spectrometry. Results are summarized in Table 2. The experimental fragmentation results from mass spectrometry were further analyzed by Mascot search in the mammalian primary protein sequence database. EDD/Rat100 was identified from the highest molecular weight band.

3.2.3.3 Confirmation of the results of mass spectrometry by Western blotting

We searched for available antibodies against the proteins that were identified by mass spectrometry. By using antibodies obtained from our collaborators, I confirmed that ATP-citrate lyase (ACL), CBL, Miwi, Collapsin response mediator protein-2 (CRMP-2), NF-κB and Eps-15 can be coimmunoprecipitated by anti-EDD/Rat100 antibody from rat testis lysates. Although PABP and ERCC4 (XPF) were also identified along with the above proteins by mass spectrometry, I was not able to confirm that they can be coimmunoprecipitated by EDD/Rat100 from rat testis lysates by Western blotting (Fig.

10). In the mass spectrometry results, we also found many ribosomal proteins and heat shock proteins. Ribosomal proteins are abundant and high molecular complex and therefore are likely contaminants that bound nonspecifically to the Sepharose beads during immunoprecipitation. Heat shock proteins are chaperone proteins that can bind with various nascent proteins to facilitate their proper folding. It is possible that these two types of proteins are nonspecifically pulled down in the immunoprecipitation, and therefore they were excluded from our preferential candidates for subsequent analysis.

In order to confirm that ACL, CBL, Miwi, CRMP-2, NF-κB and Eps-15 can interact with EDD/Rat100 in vivo, I immunoprecipitated these proteins from rat testis lysates and analyzed pellets by Western blotting for the presence of EDD/Rat100. All 6 proteins were immunoprecipitated by their own specific antibodies, but EDD/Rat100 was only coimmunoprecipitated by anti-CBL, anti-ACL and anti-Miwi antibodies (Fig. 11). These results indicate that CBL, ACL and Miwi can interact with EDD/Rat100 in vivo. Since the other three proteins, CRMP-2, NF-κB and Eps-15 did not coimmunoprecipitate EDD/Rat100 in this assay, they were possibly nonspecifically bound to the anti-Rat100 antibody during the immunoprecipitation for mass spectrometry. Nevertheless, it is possible that they bind EDD/Rat100 through a surface that is overlapping with an epitope recognized by their antibodies. In this situation, the epitope of the EDD/Rat100 bound proteins would be hidden by EDD/Rat100, resulting in lack of immunoprecipitation by their antibodies. Although the free proteins are still recognized and immunoprecipitated by their antibodies, they do not copurify EDD/Rat100. Another possible explanation is that the protein is much more abundant than EDD/Rat100, so that only a small fraction of the protein is associated with EDD/Rat100. Because of the relatively complete immunoprecipitation of EDD/Rat100, its associating proteins can easily be coimmunoprecipitated. However, abundant proteins are difficult to immunoprecipitate completely. Under this condition, even though a tiny amount of EDD/Rat100 can be coimmunoprecipitated by the protein, it is too low to be detected by Western blotting. In conclusion, based on the current data, we cannot exclude a possible *in vivo* association of EDD/Rat100 with CRMP-2, NF-κB and Eps-15.

3.2.3.4 Screening for substrates of EDD/Rat100 by RNAi in HEK293 cells

In order to distinguish substrates of EDD/Rat100 from interacting proteins, I depleted EDD/Rat100 in HEK293 cells by RNAi and measured levels of its interacting proteins by Western blotting. Based on the previous publication about polyubiquitination of DNA topoisomerase II-binding protein by EDD/Rat100, we hypothesize that EDD/Rat100 can also polyubiquitinate its substrates for proteasomal degradation in HEK293 cells as well as in testis. If so, a substrate of EDD/Rat100 should be stabilized when EDD/Rat100 is depleted. Since HEK293 cells express EDD/Rat100 and most of the candidate proteins, except for the germ cell specific protein Miwi, I did RNAi in this cell line. Two siRNA oligo duplexes, #297 and #295, were used to lower the protein level of EDD/Rat100 to less than 50% percent (Fig. 12). Although the protein levels of ACL, CBL, NF-κB and Eps-15 did not change significantly in comparison with negative controls, the protein level of CRMP-2 increased by ~50% upon silencing of EDD/Rat100.

Next, I tested by immunoprecipitation whether CRMP-2 can interact with EDD/Rat100 in HEK293 cells. Although CRMP-2 can be copurified by anti-EDD/Rat100 antibodies from HEK293 cell lysates, it did not copurify with EDD/Rat100 from the same lysates, indicating that CRMP might be bound nonspecifically to the anti-Rat100 antibody during immunoprecipitation (Fig. 13A). In order to answer this question, I coexpressed FLAG tagged EDD and GFP tagged CRMP-2 in HEK293 cells. Immunoprecipitation of FLAG-EDD with the anti-FLAG antibody did not copurify CRMP-2-GFP or endogenous CRMP-2. Similarly, immunoprecipitation of CRMP-2-GFP with the anti-GFP antibody did not copurify FLAG-EDD (Fig. 13B). Thus, copurification of CRMP-2 from immunoprecipitation of EDD/Rat100 was possibly due to crossreaction of CRMP-2 with the anti-Rat100 antibody. To confirm this hypothesis, I depleted EDD/Rat100 from rat testis lysates by immunoprecipitation with the anti-Rat100 antibody. After four sequential rounds of immunoprecipitations, most EDD/Rat100 had been removed from the lysates, and only trace amounts of EDD/Rat100 could be detected by Western blotting from the pellet; however, a significanct amount of CRMP-2 was still identified from the pellet. Similar results were obtained using HEK293 cell lysates (Fig. 13C). Therefore, we concluded that CRMP-2 can crossreact with the anti-Rat100 antibody and it does not interact with EDD/Rat100 in vivo.

Interestingly, the immunoprecipitate of anti-CRMP-2 antibody was analyzed by Western blotting with anti-CRMP-2 antibody, which revealed several high-molecular-weight bands above CRMP-2. Meanwhile, the immunoprecipitate was analyzed by Western blotting with anti-ubiquitin antibody, revealing a smear of high-molecular-weight

ubiquitin conjugates (Fig. 13A). These results indicate that CRMP-2 might be subjected to ubiquitination in HEK293 and Hela cells. Taken together, CRMP-2 is not a *bona fide* substrate of EDD/Rat100. However, since it is stabilized by depletion of EDD/Rat100, it might be indirectly regulated by EDD/Rat100 and be subjected to ubiquitination.

3.3 Discussion

In this project, I have clarified confusion regarding the structure of Rat100 by searching the EST database. I also identified Paip2 as a substrate of EDD/Rat100 by demonstrating that EDD/Rat100 can ubiquitinate Paip2 in vitro. Finally, I identified many proteins by mass spectrometry that were coimmunoprecipitated by anti-EDD/Rat100 antibody.

In my present study, although EDD/Rat100 can ubiquitinate Paip2 *in vitro*, RNAi mediated depletion of EDD/Rat100 did not significantly change the protein level of Paip2 in HEK293 cells. Interestingly, our collaborators from Dr. Nahum Sonenberg's laboratory found that PABP depletion by RNAi caused co-depletion of Paip2 protein without affecting Paip2 mRNA levels. Upon PABP knockdown, Paip2 interacted with EDD/Rat100, which led to Paip2 ubiquitination. The simultaneous knockdown of PABP and EDD/Rat100 expression by RNAi led to an increase in Paip2 protein stability, supporting a role for EDD/Rat100 in Paip2 degradation in vivo [29]. Our model is that PABP and EDD/Rat100 compete for the PAM2 motif of Paip2 through their PABC domains. Under normal conditions, the abundant PABP may sequester Paip2 from ubiquitination by EDD/Rat100. In PABP-depleted cells, the PAM2 of Paip2 is free to

interact with EDD/Rat100, which leads to Paip2 ubiquitination and degradation through the proteasome. The physiological significance of these results is that a decrease in the PABP level leads to the ubiquitination and proteasomal degradation of Paip2, and that, as a negative regulator of PABP, this decrease of Paip2 level may restore the activity of PABP. Thus, homeostasis of PABP activity is maintained. On the other hand, overexpression of EDD/Rat100 may cause a decrease in the level of Paip2 and therefore increase the PABP activity in translation, which could contribute to oncogenic transformation. This is consistent with the suspected oncogenic function of EDD in previous publications, in which breast ductal carcinoma is associated with overexpression of EDD [197, 198]. Thus, by combining the *in vitro* and *in vivo* results, we came to the conclusion that the turnover of Paip2 in the cell is mediated by EDD/Rat100 but is regulated by PABP. This result is included in a publication about the Paip2 mediated homeostasis of PABP [29].

Another PABP interacting protein Paip1 was also tested in our study. Paip1 can interact with PABP: the PAM2 of Paip1 interacts with PABC, and the PAM1 interacts with the RRMs 1 and 2 of PABP [217]. And the in vitro interaction of the PABC domain of EDD/Rat100 and Paip1 has been published [218]. However, Paip1 is neither ubiquitinated by EDD/Rat100 in vitro nor degraded in PABP-knockdown cells in our study (data not shown). This result was unexpected because the PAM2 motif of Paip1 is similar to that of Paip2 and would be predicted to bind to EDD/Rat100. We hypothesize that the PAM2 motif might not be sufficient for degradation of Paip1 or that an additional

yet unknown factor might be required for specific ubiquitination of Paip1. Alternatively, Paip1 may be stabilized by interacting with other proteins.

The mass spectrometry results revealed many potential substrates of EDD/Rat100 in rat testis. Western blotting confirmed that ACL, CBL, Miwi, CRMP-2, NF-κB and Eps-15 can be coimmunoprecipitated by EDD/Rat100 from rat testis lysates (Fig. 10). Furthermore, in HEK293 cells, silencing of EDD led to elevation of the CRMP-2 protein level, suggesting that CRMP-2 might be a potential substrate of EDD/Rat100 for proteasomal degradation (Fig. 12).

CRMP-2 is a phosphoprotein that is mainly involved in neurite outgrowth and axonal guidance [219]. It regulates axonal growth by interacting with tubulin-heterodimers to promote microtubule assembly [216]. Although CRMP-2 was originally characterized as a neuron specific protein, in our study, I have identified CRMP-2 by mass spectrometry from rat testis. I also detected a 65 kDa protein band in Western blotting with an anti-CRMP-2 monoclonal antibody (C4G [220]) from rat testis lysates and HEK293 cell lysates (Fig. 10, 12). In addition, a 65 kDa protein can be immunoprecipitated with this antibody from rat testis lysates and HEK293 lysates (Fig. 11 and 13 A). These data for the first time demonstrated the expression of CRMP-2 in both rat testis and HEK293 cells.

Although silencing of EDD/Rat100 in HEK293 cells resulted in increased levels of CRMP-2, we concluded that it was not a direct substrate for the following reasons: (a) EDD/Rat100 cannot stably interact with CRMP-2 (Fig. 13A and B), and (b) the anti-Rat100 antibody can crossreact with CRMP-2 in immunoprecitation (Fig. 13 C). Indeed, this antibody may also crossreact with CRMP-2 in immunoblotting. In our prevous results of Western blotting with the anti-Rat100 antibody from rat testis lysates, in addition to a 300 kDa band of EDD/Rat100, two low molecular weight bands, one 60~70 kDa and one ~32 kDa, could be seen in the film. The 60~70 kDa band was possibly CRMP-2 (data not shown).

The increase in protein level of CRMP-2 upon silencing of EDD/Rat100 suggests that EDD/Rat100 is an indirect regulator of CRMP-2. Recenlty, it has been reported that an EDD containing E3 ligase complex (DYRK2-EDVP) can polyubiquitinate microtubule ATPase Katanin p60 through a substrate binding subunit VPRBP [204]. In our future studies, it would be interesting to test whether CRMP-2 can interact directly with VPRBP. If so, CRMP-2 might be another substrate of this DYRK2-EDVP E3 ligase complex. Though overexpression of CRMP-2 leads to cell death [221], it is still unknown whether depletion of this protein would prevent cell death or even cause oncogenic transformation. This is an interesting question because overexpression of EDD has been found in several types of tumors, and if depletion of CRMP-2 can induce oncogenesis, it would be consistent with the oncogenic function of EDD in breast ductal carcinoma as previously published [197, 198]. In addition, we found that the anti-CRMP-2 antibody precipitated

some high-molecular-weight ubiquitin conjugates from HEK293 and Hela cell lysates, suggesting that CRMP-2 might be subjected to ubiquitination in these cells (Fig. 13A). However, these ubiquitin conjugates may not necessarily be ubiquitinated CRMP-2 because in the non-denaturing immunoprecipitation, some ubiquitinated CRMP-2 associating proteins, such as tubulin, can be coimmunoprecipitated. Unfortunately, our available anti-CRMP-2 antibody (C4G) was not effective under denaturing conditions, and therefore we were not able to determine whether these ubiquitin conjugates were indeed polyubiquitinated forms of CRMP-2.

To date, I have elaborately studied six proteins that were copurified from immunoprecipitation of EDD/Rat100. None of them was confirmed to be a substrate of EDD/Rat100. Immunoprecipitation of NF-κB and Eps-15 could not copurify EDD/Rat100 and their protein levels were not significantly changed upon silencing of EDD/Rat100. CBL and ACL could copurify EDD/Rat100 in immunoprecipitation; however, their protein levels were not changed upon silencing of EDD/Rat100. The reciprocal copurification of EDD/Rat100 and Miwi suggested Miwi as an EDD/Rat100 interacting protein. Unfortunately, it is exclusively expressed in testis, and therefore we could not test the effect of silencing of EDD/Rat100 on Miwi in cultured cell lines. This problem is expected to be solved by using the EDD/Rat100 knockout mice in the future. Thus, Miwi remains a potential substrate of EDD/Rat100.

Several reasons may have caused difficulties in identifying substrates of EDD/Rat100 in the present study. First, in addition to TopBP1, EDD/Rat100 might have other nuclear protein substrates [203]. However, our rat testis lysate was produced by homogenization with a Potter Elvehjem tissue grinder, which releases proteins mainly from cytosol rather than the nucleus. For instance, a nuclear protein Histone cannot be detected by Western blotting from the rat testis lysates produced with this method (data not shown). Thus, nuclear substrates of EDD/Rat100 would probably not be identified using our approach. Second, normal rabbit IgG is not an ideal antibody for the negative control. A much better negative control for our immunoprecipitation study would be immunoprecipitation with the same anti-Rat100 antibody from the EDD/Rat100-/- rat testis lysate. Unfortunately, this is so far impossible due to the lethal effect of inactivation of the EDD/Rat100 gene. Third, although the specificity of our rabbit anti-Rat100 polyclonal antibody was improved with immunopurification, it still crossreacted with many proteins. A monoclonal antibody would be potentially more specific in immunoprecipitating EDD/Rat100. However, none of the currently available monoclonal anti-EDD/Rat100 antibodies can efficiently immunoprecipitate EDD/Rat100. Lastly, similar to the relationship among PABP, Paip2 and EDD/Rat100, other substrates of EDD/Rat100 might also be sequestered by other proteins, which prevent the substrates from associating with EDD/Rat100 in normal conditions.

Hereafter, more proteins identified by mass spectrometry will be analyzed when specific antibodies are obtained. Since only distinct protein bands were excised from the gel for

analysis by mass spectrometry, some low level EDD/Rat100 interacting proteins might not be upon Coomassie staining and therefore missed. Evaluating the whole sample by cutting the gel lane into multiple bands and analyzing them all by mass spectrometry would be a more comprehensive method for protein identification in this experiment. However, due to the above four reasons, the method currently used in our present study still has limitations in its ability to identify substrates of EDD/Rat100. Testis specific EDD/Rat100 knock out mice would be helpful in identifying substrates of EDD/Rat100, which is necessary for understanding the mechanism and function of this E3 in spermatogenesis. in vitro expression cloning has been used to successfully identify substrates of ubiquitination or sumoylation [222, 223]. Basically, a small fraction of cDNA library (100-300 individual genes) is expressed in vitro in the presence of radiolabelled amino acid. The resulting labeled proteins are subsequently incubated with whole cell extracts with or without the active E3. If the E3 can cause degradation of any of these proteins, this small pool of cDNA is futher fractionated until an individual gene is identified. Finally, substrates of EDD/Rat100 can also be identified by using other highthrough-put technologies, such as protein micrarrays and proteomics [224, 225].

Chapter 4

Function of USP19, a deubiquitinating enzyme, in skeletal

muscle

Muscle wasting and spermatid development are both characterized by extensive cellular protein degradation. In both conditions, there is activation of ubiquitin dependent proteolysis and increased levels of ubiquitinated proteins [97, 135, 226]. So far I have explored the function of genes that can modulate ubiquitination. I have studied two enzymes, UBC4-testis (E2) and EDD/Rat100 (E3), which are both involved in conjugation of ubiquitin. Deubiquitinating enzymes (DUB) may also play an important role in modulating ubiquitination. In this chapter of my thesis, I have studied the function of USP19, a DUB that was found to be induced in muscle wasting in Dr. Wing's laboratory.

Muscle wasting is a state of negative protein balance that arises from a fall in protein anabolism and/or an increase of protein catabolism. It can be caused by many pathological conditions including nutritional insufficiency, cancer, infection, glucocorticoids, immobilization and denervation. One of the most common catabolic states is cancer cachexia. Cachexia is a complex metabolic state with progressive weight loss, mainly due to loss of adipose tissue and skeletal muscle. Cancer cachexia occurs frequently in late-stage malignancy and is associated with more than 20% of cancer

deaths. Survival of cancer patients is directly related to the total weight loss as well as the rate of weight loss [227]. Therefore, understanding the mechanism of muscle wasting is very important in the holistic management of cancer patients. Although the pathophysiology of cancer cachexia remains largely unclear, several proinflammatory cytokines, including TNF-α, IFN-γ, IL-1 and IL-6, have been implicated as key mediators of cachexia in cancer patients [228]. Levels of these cytokines are raised in the serum of cancer patients, produced either by the host in an inflammatory response to the tumor or by the cancer cells themselves. These cytokines have similar activities in induction of metabolic derangements leading to cachexia. Features of cancer cachexia can be mimicked by these cytokines under experimental conditions [229].

In muscle wasting, increased protein degradation mainly results from increased activity of the ATP-dependent ubiquitin-proteasome proteolytic pathway, which is accompanied by increased levels of ubiquitinated proteins in atrophying skeletal muscle [230]. This has been extensively discussed in the introduction section. However, most of these studies have focused primarily on activation of ubiquitination as an explanation for the increase of ubiquitinated proteins in skeletal muscle. Although deubiquitinating enzymes can also modulate levels of ubiquitinated proteins, the roles of these enzymes remain largely unexplored. It has been found that expresssion of USP-14, a proteasome associated DUB, is up-regulated in four different muscle wasting conditions — fasting, diabetes, uremia and tumor [157]. In Dr. Wing's laboratory, a 150 kDa deubiquitinating enzyme USP19, which belongs to the USP family, has been found to be widely expressed in various

tissues including skeletal muscle, heart, testis and kidney [158]. Little is known about its function. It can play a role in cell proliferation by stabilizing KPC1, the catalytic subunit of an E3 for the p27^{Kip1} inhibitor of the G1-S transition of the cell cycle [231]. It has also been shown to be present on the endoplasmic reticulum and can negatively regulate endoplasmic reticulum associated degradation [232]. Previous work in Dr. Wing's laboratory has also demonstrated that levels of USP19 mRNA increase by 30-200% in rat skeletal muscle atrophy induced by cancer, dexamethasone, fasting or diabetes. During refeeding, the increased mRNA levels of USP19 in the fasted state return to normal coincident with recovery of muscle mass. Indeed, the level of USP19 mRNA was found to be inversely correlated with muscle mass in all of these catabolic conditions. However, the potential role of USP19 in muscle wasting remains unclear. In this project, I have determined whether silencing of USP19 in muscle cells can regulate myofibrillar protein expression as well as muscle protein content. I also determined whether silencing of USP19 can modulate the catabolic effects of TNF-α/IFN-γ or dexamethasone in muscle cells.

4.1 Materials and methods

4.1.1 Cell culture

Two myoblast cell lines rat L6 and mouse C2C12 have been extensively used in *in vitro* muscle research. In my experiments, I selected L6 cells because the myotubes were more reliably transfected with siRNA oligonucleotides than C2C12 cells [233]. Another

reason is that previous work indicated that L6 cells respond equally well as C2C12 cells to TNF- α stimulation [134] and better than C2C12 cells to dexamethasone stimulation [234].

For proliferation, rat L6 myoblasts were cultured at low density in growth medium-Dulbecco's modified Eagle's medium (DMEM high glucose, Gibco) supplemented with 10% fetal bovine serum (Gibco) and penicillin/streptomycin solution (Gibco), in 5% CO₂. For preparation of myotubes, L6 myoblasts were first seeded in 6-well plates (2X10⁵ cells/well) in 2 ml of growth medium on day -1. The next day (day 0), when the cells were 60% confluent, the cells were switched into 2 ml of differentiation medium -DMEM high glucose supplemented with 2% horse serum (Gibco) and penicillin/streptomycin solution. The differentiation medium was changed every 2-3 days until harvesting on day 4 or day 5.

To induce catabolism in L6 myotubes with TNF- α and IFN- γ , L6 cells were grown and differentiated as described above. On day 3, cells were treated with 10 ng/ml of TNF- α alone (diluted in PBS) or 10 ng/ml of TNF- α and 100 U/ml of IFN- γ (both diluted in PBS) or 10 μ M of DEX (diluted in ethanol) in differentiation medium for 48 hours. Cells exposed to the same concentration of PBS or ethanol diluted in differentiation medium were used as negative controls. The final concentration of ethanol in differentiation medium was 0.038%. At harvesting on day 4 or day 5, cells were rinsed with 1 ml cold PBS and lysed directly in the 6-well plates with 200 μ l/well of 50 mM Tris (pH 7.5) and 2% SDS. Lysates were harvested with rubber scrapers, transferred to 1.5 ml Eppendorf

tubes and passed through 30-gauge needles 5 times to shear the DNA. Protein concentrations of the cell lysates were determined with the detergent-compatible Micro BCA Protein Assay Kit (Pierce).

4.1.2 RNAi of USP19 in L6 myotubes

Six rat USP19 specific siRNA duplexes were designed and purchased from Dharmacon. Two siRNA duplexes producing the best depletion of USP19 were used in these studies: #1, 5'-AAAGTGCAGACTCACAAGGGT-3'; #7, 5'-AAGGGTGGTCTTCTACAGTTG-3'. A non-specific siRNA control duplex (predicted not to affect any gene) with the same GC content was used as a negative control (Dharmacon).

SiRNA transfection was done in 6-well plates. On day 3 of differentiation, L6 myotubes were transfected with the siRNA duplex (final concentration 25 nM) using Lipofectamine and OPTIMUM medium (Gibco). Briefly, the siRNA was mixed with 100 μl OPTIMUM medium (solution A). Concomitantly, 1.5 μl Lipofectamine was mixed with 100 μl OPTIMUM medium (solution B). Solutions A and B were then mixed and incubated at room temperature for 30 minutes. At the end of this period, L6 myotubes in 6-well plates were washed once with OPTIMUM medium at 37°C. Subsequently, 800 μl of OPTIMUM and the mixture of A and B were mixed together and then added into the well. The cells were incubated for 5 hours, and then 500 μl of DMEM with 6% horse serum was added into the well to give a final concentration of 2% horse serum. Incubation was continued overnight. The next morning (day 4), the medium was replaced

with fresh DMEM with 2% horse serum and antibiotics. 24 and 48 hours after transfection, cells were harvested in SDS lysis buffer as described before.

In studies involving treatment with TNF- α /IFN- γ or dexamethasone, siRNA transfection was done on day 2 of differentiation using the same transfection protocol. The following morning (day 3), TNF- α /IFN- γ or dexamethasone was added into fresh differentiation medium.

4.1.3 Antibodies and Western blotting

Rabbit anti-USP19 antibody was produced in our laboratory. A His-tagged peptide encompassing amino acids 454-699 of rat USP19 (NCBI accession AAT35219) was expressed in E. coli and used to raise this antibody. The antibody was then affinity purified using a soluble rat USP19 peptide (amino acids 454-536). The anti-myosin heavy chain antibody was purchased from Sigma (Product No. M4276). This monoclonal antibody specifically recognizes the heavy chain of the fast twitch (type II) myosin molecules. The anti-γ-tubulin and anti-myogenin antibodies were purchased from Sigma (Product No. T6557) and Santa Cruz Biotechnology, Inc. (sc-12732) respectively. Western blotting was performed as described in chapter 3.

4.2 Results

4.2.1 Regulation of USP19 during differentiation of L6 muscle cells

Since our previous work with USP19 was done in adult skeletal muscles, we first determined whether USP19 is expressed in L6 muscle cells and whether it is regulated during differentiation. When cultured in differentiation medium, L6 cells stopped proliferating within one day. Cell fusion started to be seen on day 2, and longitudinal myotubes became obvious on day 3. On day 5 or 6, the culture dish appeared mostly occupied with fused myotubes. These morphologic changes of L6 cells mimic differentiation of myoblasts *in vivo* and are consistent with previous publications [235]. USP19, detected successfully in Western blotting, was already expressed at the beginning of differentiation. It moderately increased on days 2 and 3, and then returned to its original level on days 4 and 5 (Fig. 14). The elevation of USP19 during the early stage of L6 differentiation suggests that it might be involved in regulation of differentiation.

In order to biochemically monitor the differentiation of L6 cells, protein levels of myosin heavy chain (MHC) and myogenin, two myogenic differentiation markers, were analyzed by Western blotting in cell lysates. Transcription of the muscle specific gene MHC is activated after initiation of differentiation [236, 237]. Myogenin, which is a member of the muscle regulatory factor (MRF) family and is required for initiation of differentiation, remains at a very low level until differentiation has been triggered by withdrawal of growth factors [238]. In our experiments, the amount of MHC was very low on day 0 of differentiation and accumulated progressively towards day 5. Myogenin was hardly

detectable at the beginning of differentiation but became readily detectable after 24 hours of differentiation when fusion started to appear (Fig. 14). These observations demonstrate that our model exhibited the biological characteristics of muscle differentiation in a chronologically appropriate manner.

4.2.2 Depletion of USP19 increased MHC levels in L6 myotubes

Since USP19 mRNA is inversely correlated with muscle mass in catabolic conditions, we tested whether there may be a causal link by determining the effects of depletion of USP19 on muscle protein levels in L6 myotubes. Two rat USP19 specific RNAi duplexes, #1 and #7, were used to deplete the USP19 protein level by more than 50% (Fig. 15). No significant change in the total amount of protein was detected in the USP19 depleted L6 myotubes (data not shown). Since L6 myotubes became overfused and detached from cell culture plates after 5 days of differentiation, it was very difficult to maintain cultured L6 myotubes beyond this time. Thus, whether or not depletion of USP19 can increase the overall protein content in L6 myotubes later than 48 hours of RNAi remains unknown. In addition, we tested whether expression of specific myofibrillar proteins might be modulated. Since MHC is a major myofibrillar protein, we tested it first. An increase in the level of MHC protein upon RNAi mediated depletion of USP19 was seen 24 to 48 hours after siRNA transfection (Fig. 15). These results indicate that USP19 can negatively regulate MHC expression.

4.2.3 Depletion of USP19 can blunt loss of MHC induced by TNF- α or dexamethasone in L6 myotubes

Cytokines mediate muscle wasting in many catabolic conditions in vivo. TNF- α and IFN- γ can decrease the MHC protein level in mouse C2/C12 myotubes, which mimics their muscle wasting effects in animal models [239]. Therefore, I tested whether TNF- α and INF- γ would have similar effects in L6 cells. L6 cells were induced to differentiate for 3 days and then treated with 10 ng/ml TNF- α with or without 100 U/ml INF- γ for 48 hours. TNF- α alone induced more than 50% loss of MHC in L6 myotubes. Unlike previous reports in C2C12 cells, IFN- γ did not further increase the effect of TNF- α in L6 myotubes (Fig. 16A). Therefore, in subsequent experiments, MHC catabolism in L6 myotubes was induced using only TNF- α .

Since expression of USP19 is increased in muscle atrophy induced by tumor implantation [158], and that TNF- α is one of the major cytokines that mediate tumor induced muscle catabolism [240], we hypothesized that USP19 is required by TNF- α for muscle wasting. We also tested whether TNF- α might increase expression of USP19. To test this hypothesis in vitro, I determined whether depletion of USP19 would block the catabolic effects of TNF- α (Fig. 16B). USP19 RNAi oligo nucleotides were transfected on day 2, TNF- α was added to differentiation medium on day 3, and cells were harvested on days 4

and 5. MHC and USP19 were analyzed by Western blotting. As seen before, TNF- α alone induced significant loss of MHC on day 5. Concomitantly, it also increased the level of USP19 protein on day 5, suggesting this increase may mediate loss of MHC. RNAi of USP19 alone increased the MHC level on day 5, as described earlier. Interestingly, when USP19 levels were lowered, the ability of TNF- α to lower MHC was now blocked.

Since USP19 is induced also by dexamethasone (DEX), a synthetic glucocorticoid, in muscle in rats [158], we similarly tested the effect of this hormone in this in vitro model. The ability of different concentrations of DEX to affect MHC levels was determined (Fig. 17A). DEX at concentrations greater than 10 μM were required to significantly decrease the MHC level. To test whether USP19 is required by DEX for muscle wasting, USP19 was lowered by RNAi on day 2, and the L6 myotubes then exposed to 10 μM DEX from day 3. On days 4 and 5, and MHC and USP19 were analyzed by Western blotting. DEX induced loss of MHC in L6 myotubes and caused a marginal increase (P=0.1) in the level of USP19 protein on day 5. Depletion of USP19 partially reversed DEX induced loss of MHC on day 5 (Fig. 17B).

IV. Discussion

In this chapter for the first time, we characterized expression of USP19 in L6 myotubes, showing a modest but significant increase of expression in early differentiation. In addition, we demonstrated that silencing of USP19 expression can increase expression of MHC in L6 myotubes, and this can partially reverse the TNF- α or DEX stimulated catabolism of MHC. We also demonstrated that TNF- α and possibly DEX can increase expression of USP19 in L6 myotubes.

Depletion of USP19 in L6 myotubes increased the level of MHC protein. Although myosin has been found to be ubiquitinated in muscle [241], our results do not suggest that MHC is a substrate of USP19. If so, loss of deubiquitination by depletion of USP19 should have increased ubiquitination and proteasomal degradation of MHC, which should promote the loss of the MHC protein. USP19 does not appear to facilitate degradation of muscle proteins including MHC by recycling ubiquitin and maintaining a free ubiquitin pool in myotubes, as depletion of USP19 did not produce a general effect of stabilization of total myotube protein. Further support of this is that depletion of USP19 in HEK293 cells does not alter steady state levels of ubiquitinated proteins (unpublished data). Thus, USP19 does not appear to regulate the degradation of MHC. In fact, lowering USP19 increases not only MHC protein but also MHC mRNA (unpublished data). This suggests that USP19 functions to downregulate expression of MHC in L6 myotubes by inhibiting its transcription or by stimulating degradation of its mRNA. However, the target of USP19 regulation in MHC transcription or mRNA stability is so far unclear. It might be either a transcription factor or an upstream regulator of a transcription factor of MHC.

The myogenic regulatory factor (MRF) family includes a group of muscle specific transcription factors that are master regulators of skeletal muscle development [242]. The MRF family members can functionally interact with many other transcription regulators to build a complex network, which controls muscle specific transcription [243]. For instance, the activity of MRFs can be negatively regulated by a transcriptional repressor, inhibitor of DNA binding (Id) [244]. Id, a family of helix-loop-helix factors, can bind to MRF proteins and impede their ability to bind DNA and activate transcription. Theoretically, USP19 might downregulate expression of MHC by either suppressing the activity of a MRF member or enhancing the activity of a MRF suppressor, such as Id. Since L6 cells express myogenin during the process of myogenic differentiation but do not express myoD, myogenin was first tested in response to silencing of USP19 in L6 cells [245]. Interestingly, another graduate student in Dr. Simon Wing's laboratory found that silencing of USP19 increased levels of both myogenin mRNA and protein. The mechanism by which USP19 regulates myogenin is currenlty unclear. The simplest model is that a transcriptional repressor of myogenin transcription is a substrate of USP19 and can be destabilized upon silencing of USP19. It is also possible that USP19 acts on substrate(s) upstream in the signaling pathways that modulate the synthesis of myofibrillar proteins. Identification of substrate(s) of USP19 will help answer these questions. The steady state level of mRNA is determined not only by transcription but also by the rate of mRNA degradation, which can be influenced by mRNA binding proteins or mRNases [246]. Thus, an alternative hypothesis is that USP19 can facilitate the rate of decay of mRNA in L6 myotubes. In the future, we will test whether the half life of MHC mRNA can be changed by depletion of USP19 in L6 myotubes.

Furthermore, I found that the protein level of USP19 was increased in L6 myotubes treated with TNF- α for 48 hours. This is consistent with the published in vivo data that cancer implantation or dexamethasone treatment in rats can induce transcription of USP19 [158]. Although the mRNA level of USP19 in TNF- α or dexamethasone treated L6 myotubes has not been tested in my experiments, the in vivo data in rats suggest that TNF- α or dexamethasone might also induce transcription of USP19 in L6 myotubes since mRNA levels increased in skeletal muscles of these animals [158]. Importantly, I found that depletion of USP19 can partially reverse the loss of MHC induced by TNF- α and dexamethasone in L6 myotubes. Taken together, these results suggest a model that TNF- α or dexamethasone can induce transcription of USP19, which can in turn leads to suppression of transcription of MHC.

To study further the requirement of USP19 in muscle wasting, we will construct a USP19 knockout mouse and test whether or not inactivation of USP19 expression can prevent muscle wasting induced by catabolic conditions, such as tumor implantation, glucocorticoid or insulin deficiency. This will determine whether application of USP19 inhibitors might be useful in the treatment of muscle wasting in cancer cachexia and other catabolic conditions.

Chapter 5

General discussion

In this thesis, I used different approaches to explore functions of three important enzymes of the ubiquitin system - the ubiquitin conjugating enzyme UBC4-testis (E2), the ubiquitin protein ligase EDD/Rat100 (E3) and the deubiquitinating enzyme USP19 (DUB), in mammalian spermatogenesis or muscle wasting.

In the first approach, we used gene targeting in the mouse to study the *in vivo* function of UBC4-testis, a rodent spermatid-specific E2 enzyme. We found that loss of UBC4-testis does not lead to infertility nor any abnormality in the morphology of the seminiferous epithelium in adult mice indicating that UBC4-testis is not an essential gene. Although not essential, our studies nonetheless suggested some functions for UBC4-testis as the 'knockout' mice showed a delay in testis development beginning at 25 days of age, which is the time at which induction of UBC4-testis in round spermatids normally occurs [99, 189]. I attempted to elicit further functions of UBC4-testis by determining whether the response of the testis to heat stress would be different in the knockout mice. Unfortunately, the involution of the semniferous epithelium occurred similarly in both normal and 'knockout' mice.

As discussed in chapter 2, there could be several explanations for the delay in testis development that was observed in the knockout mice. One important possibility is that UBC4-testis works with specific cognate E3(s) to catalyze ubiquitination of specific substrates and the degradation of these substates is required for normal maturation of the

testis. Closely related isoforms of another E2 family have been shown to have distinct functions. For example, mouse E2 HR6A and HR6B, homologs of yeast UBC2, are 96% identical in amino acid sequence [91] and are ubiquitously expressed in many tissues, with the highest mRNA levels in brain, heart and testis [94]. Homozygous inactivation of the HR6B gene results in male, but not female, infertility, without any other prominent phenotype [93, 94]. Defects in post-meiotic condensation of chromatin were found in the spermatids of HR6B inactivated mice. In striking contrast to the result of inactivation of HR6B in male, homozygous inactivation of HR6A causes female rather than male infertility due to arresting of development beyond the embryonic two-cell stage [143]. Although these effects may be due to higher expression of HR6B in the testis and of HR6A in the oocyte, the two E2 isoforms may interact with different E3s. In support of this latter possibility, the U-box motif containing ligase cyclophilin CYC4/hCyP-60 needs HHR6B but not HHR6A, for polyubiquitination [247], whereas a RING E3 ligase, RFPL4 (Ret Finger Protein-Like 4), interacts with HHR6A but apparently not HHR6B in a yeast two-hybrid screen [248]. Thus, highly similar isoforms of E2s probably do interact with specific E3s and thereby have specific functions, but the latter are not always readily evident from gross observations of knockout mice. It would be of interest to use molecular approaches to identify E3s that interact with UBC4-testis or its ubiquitous isoforms and determine whether there are ones that are specific for UBC4testis and expressed in the testis and that could explain the developmental delay in the knockout mice.

The second approach I used also involved using loss of function, but I did so in the context of a cultured cell model and employed RNA silencing to induce the loss of function. In that study, I characterized the function of the deubiquitinating enzyme USP19 in L6 myotubes. SiRNA mediated silencing of USP19 expression increased expression of MHC in L6 myotubes under basal conditions. In addition, depletion of USP19 could also partially reverse the loss of MHC that occurs upon stimulation of catabolism by TNF- α or DEX. I also demonstrated that TNF- α can increase expression of USP19 protein in L6 myotubes. Taken together with our published in vivo data that shows that cancer implantation (which induces expression of cytokines such as $TNF-\alpha$) or dexamethasone treatment in rats can induce expression of USP19 mRNA, these results suggest a model in which TNF-α or dexamethasone can induce transcription of USP19, which can in turn suppresses expression of MHC. In collaboration with other graduate students in Dr. Simon Wing's laboratory, we showed that the increase in MHC expression was due to an increase in expression of the myogenic regulatory factor myogenin. Thus, silencing of USP19 increases myogenin dependent transcription of MHC and therefore its synthesis. These data indicate that the ubiquitin system not only mediates protein degradation in muscle wasting, but can also modulate protein synthesis. This expands the horizons of the function of the ubiquitin system in muscle physiology. To study further the mechanism of USP19 in muscle wasting, Dr. Wing's laboratory has recently constructed a USP19 knockout mouse. Indeed data to date (unpublished) indicates that inactivation of USP19 expression does lead to less muscle wasting induced by catabolic conditions. The exact mechanism(s) of the effects of USP19 on myogenin myofibrillar expression require and protein remain unclear and will

molecular/biochemical studies to identify the substrates of USP19 in skeletal muscle. Nonetheless, our findings to date suggest that inhibition of USP19 could be a novel therapeutic approach for prevention and treatment of muscle wasting.

In vivo approaches, whether whole animal or in cultured cells as described above, are useful for defining physiological functions, but generally do not readily yield insights into the molecular mechanisms. When studying the functions of enzymes, a key functional question is the identification of substrates of these enzymes. In my second project, I attempted to identify substrates of the HECT E3 EDD/Rat100 that is highly expressed in rat testis and can accept ubiquitin from UBC4 isoforms, including UBC4-1 and UBC4-testis. My studies illustrated two methods towards identification of substrates. The first was a candidate method. Both polyA binding protein (PABP) and EDD/Rat100 share a PABC domain and this domain in PABP had previously been shown to interact with Paip2. This suggested that Paip2 might also interact with EDD/Rat100 through its PABC domain and be a substrate of this E3. Indeed, using in vitro assays, we found that Paip2 was indeed a new substrate of EDD/Rat100, demonstrating for the first time that EDD/Rat100 can ubiquitinate a modulator of translation. As discussed in chapter 3, under normal conditions, the abundant PABP sequesters Paip2 from ubiquitination by EDD/Rat100. In PABP-depleted cells, Paip2 is ubiquitinated by EDD/Rat100 and degraded by the proteasome. Degradation of Paip2, a negative regulator of PABP, therefore permits restoration of the activity of PABP and therefore maintains its homeostasis. Overexpression of EDD/Rat100 may cause a decrease in the level of Paip2 and therefore increase the PABP activity in translation, which could contribute to

oncogenic transformation. This provides a potential explanation for suspected oncogenic functions ascribed to EDD in previous publications such as the observation that breast ductal carcinoma is associated with overexpression of EDD. Our findings suggest a new mechanism of the ubiquitin system in regulation of eukaryotic translation, and EDD/Rat100 could be a potential target for treatment of breast cancer.

In the other method, we attempted to identify substrates by identifying interacting proteins [204]. I identified proteins that were present in immunoprecipitates of EDD/Rat100 from the rat testis. Six of these proteins, ACL, CBL, Miwi, CRMP-2, NF- kB and Eps-15, were elaborately studied, but none of them were confirmed to be a *bona fide* substrate of EDD/Rat100. Although the protein level of CRMP-2 was elevated upon silencing of EDD/Rat100 in HEK293 cells, it could not be confirmed to interact with EDD/Rat100 in vivo, suggesting that EDD/Rat100 might be an indirect regulator of CRMP-2. Based on the recent report of the EDD containing DYRK2-EDVP E3 ligase complex, it is possible that EDD might interact indirectly with CRMP-2 through a substrate binding protein, such as VPRBP (discussed in page 57). In our future studies, the interaction between VPRBP and CRMP-2 will be tested. As discussed in chapter 3, several reasons, such as the subcellular localization of substrates, specificity of the anti-Rat100 antibody, and lack of an optimal negative control, may have contributed to the difficulties in identifying substrates of EDD/Rat100 in the present study.

It is clear that maximal understanding of the function of a protein can be obtained by integrating the physiological functions derived from whole animal studies, cellular functions derived from studies in cell culture and the molecular functions derived from biochemical studies in vitro. Indeed, my original thesis project was to use molecular approaches to identify substrates of EDD/Rat100 and to confirm these identifications and test their cellular functions using cell culture approaches. At the same time, another member of Dr. Wing's laboratory had generated a targeting vector to create conditional knockout mice for EDD/Rat100 and indeed had obtained targeted ES cells during the course of my studies. Unfortunately, none of the targeted ES cell clones resulted in germ line transmission and thereby prevented the generation of these conditional knockout mice to complement the cellular and molecular studies.

As discussed in the introduction, the number of gene encoding enzymes in the ubiquitin system is enormous. Therefore much work remains to be done in order to truly comprehend the functions of this system. Without this knowledge, the full therapeutic potential of targeting the ubiquitin system for clinical benefit will remain undeveloped.

Contribution to new knowledge:

- 1. Function of USP19, a deubiquitinating enzyme, in skeletal muscle.
 USP19 is modestly increased in early differentiation of L6 cells. Silencing of
 USP19 expression can increase expression of MHC in L6 myotubes, and this can partially reverse the TNF-α or DEX stimulated catabolism of MHC. TNF-α can increase expression of USP19 in L6 myotubes. The ubiquitin system can modulate protein myofibrillar protein synthesis during muscle atrophy.
- 2. Identification of substrates for EDD/Rat100, a 300 KDa ubiquitin protein ligase. Rat100 is a 300 KDa HECT E3 and is a rodent homologue of human EDD and Drosophila HYD. EDD/Rat100 can catalyze polyubiquitination of Paip2 *in vitro*. In normal *in vivo* conditions, depletion of EDD/Rat100 does not affect the stability of Paip2 protein. EDD/Rat100 can modulate eukaryotic translation through maintaining homeostasis of PABP. CRMP-2 is expressed not only in neuronal tissue, but also in rat testis, Hela and HEK293 cells. CRMP-2 is subject to polyubiquitination, its expression can be indirectly suppressed by EDD/Rat100. Miwi can associate with EDD/Rat100 in rat testis. Eps15, Cbl, ACL and NF-κB can interact with EDD/Rat100.
- 3. Function of the E2 enzyme UBC4-testis in mammalian spermatogenesis.
 UBC4-testis does not have an essential function in the response of the testis to heat stress in adult mice. When subjected to the heat stress of experimental cryptorchidism, the weight of the testis and the profile of germ cell degeneration

of UBC4-testis knockout mice were not significantly different from that of wild type mice.

Contribution to manuscipts:

1. USP19-deubiquitinating enzyme regulates levels of major myofibrillar proteins in L6 muscle cells. Sundaram P, <u>Pang Z</u>, Miao M, Yu L, Wing SS. Am J Physiol Endocrinol Metab. 2009 Dec;297(6):E1283-90. Epub 2009 Sep 22.

Cell culture, development of RNAi of USP19, first demonstration of effects of RNAi of USP19 on MHC and ability of RNAi to reverse effects of dexamethasone and TNF- α , Western blotting, writing introduction and discussion of the publication. Co-first author of the publication.

Poly(A) binding protein (PABP) homeostasis is mediated by the stability of its inhibitor, Paip2. Yoshida M, Yoshida K, Kozlov G, Lim NS, De Crescenzo G, Pang Z, Berlanga JJ, Kahvejian A, Gehring K, Wing SS, Sonenberg N. EMBO J. 2006 May 3;25(9):1934-44. Epub 2006 Apr 6.

in vitro ubiquitination assay, designing of RNAi oligos for EDD/Rat100, making figure 6A, writing method, result and discussion for figure 6A.

3. Mice lacking the UBC4-testis gene have a delay in postnatal testis development but normal spermatogenesis and fertility. Bedard N, Hingamp P, Pang Z, Karaplis A, Morales C, Trasler J, Cyr D, Gagnon C, Wing SS. Mol Cell Biol. 2005 Aug;25(15):6346-54.

Experimental cryptorchidism, statistics of data, making figure 6.

Figure Legends

Figure 1. The ubiquitin proteasome system. E1: ubiquitin activating enzyme. E2: ubiquitin conjugating enzyme. E3: ubiquitin protein ligase. DUB: deubiquitinating enzyme. Ub: ubiquitin (green). Sub: substrate (violet). The proteasome protease complex is indicated as a cylindric orange colored structure. (→): catalyzation or facilitation. (—): inhibition.

Figure 2. Schematic representations of HECT E3, Ring E3 and DUB. (A) The E6AP HECT domain-E2 UbcH7 complex forms a U-shaped structure [20]. Perpendicular views of the overall structure of the complex. The E6AP HECT domain N terminal lobe, C terminal lobe, UbcH7 and ubiquitin are colored in orange, pink, blue, and green, respectively. The two active-site cysteines are colored red. The N and C terminal lobes of E6AP HECT domain are connected with a mobile hinge. The dotted line indicates the open line of sight between the active-site cysteines of E6AP and UbcH7. (B) The structure of a c-Cbl-UbcH7-Phosphorylated ZAP-70 peptide ternary complex [35]. Green color: the TKB (tyrosine kinase binding) domain. Red: the RING domain. Blue: UbcH7. Cys: the active-site cysteine of UbcH7 (red). The complex has a compact overall structure, with UbcH7, the TKB and the RING domains of c-Cbl all interacting with each other across multiple interfaces. The UbcH7 active site cysteine is located on the side of the complex opposite from where the ZAP-70 recognition peptide binds and is separated by ~60 Å from the peptide. The lysine residues of the receptor tyrosine kinases that are

ubiquitinated have not yet been identified, and the ZAP-70 peptide used in the crystallization does not contain any lysine residues. (C) Structure of the catalytic core domain of a deubquituinating enzyme HAUSP [53]. Overall structure of the 40 kDa catalytic core domain of HAUSP/USP7, which comprises Fingers (green), Palm (blue), and Thumb (gold). The active site, comprising the Cys Box and the His Box, is located in a catalytic cleft between the Palm and the Thumb. The predicted ubiquitin binding site is indicated by a black oval circle.

Figure 3. Cellular components of the seminiferous tubule (A) and stages of the spermatogenesis cycle (B). (A) The seminiferous tubules consist of a tunic of fibrous connective tissue, a well-defined basal lamina and a complex seminiferous epithelium. The epithelium consists of two types of cells: supporting cells (Sertoli cells) and germ cells that constitute the spermatogenic lineage. gonia: spermatogonia. cyte: spermatocyte. tid: round spermatid. The spermatogenic cells are stacked in 4-8 layers that occupy the space between the basal lamina and the lumen of the tubule. The spermatogonia divide several times and finally differentiate, producing spermatozoa. In this figure, the angle subtended by the acrosome extends from 95° to 120°, elongated spermatids remain within the crypts of the Sertoli cells. These are characteristics of stage VI of the cycle of seminiferous epithelium. (B) Fourteen stages (I-XIV) of rat spermatogenesis are defined based mainly on the developmental changes in the acrosomal system of round spermatids and their nuclear shape [249]. Development of round spermatids into elongated spermatids is classified into 19 steps. Steps 1-8: early round spermatids. Steps 9-14: middle stage elongating spermatids. Steps 15-19: late elongated spermatids. A: type A

spermatogonia; B: type B spermatogonia. L: leptotene spermatocytes. Z: zygotene spermatocytes. P: pachytene spermatocytes.

Figure 4. Inactivation of the mouse UBC4-testis gene. (A) Design of targeting vector for inactivation of the mouse UBC4-testis gene [189]. The UBC4-testis gene (white) is intronless. Flanking sequences (gray) were subcloned around a neomycin resistance gene (NeoR) in the pNT vector. TK: thymidylate kinase gene for positive selection. The linearized targeting vector was transferred into ES cells and homologous recombination selected for by using G418 and FIAU. X: Xbal. B: Bgl II. N: Ncol. R8 is a common PCR oligo for both NeoR and UBC4-testis gene detection. PCR oligos R8 and F4 were used for detection of the UBC4-testis gene, and oligos R8 and R3 were used for detection of the NeoR gene. (B) Genotyping of wild type (+/+), heterozygous (+/-), and homozygous (-/-) mice by PCR. PCR amplifications for the neomycin resistance gene (lower panel) and the endogenous UBC4-testis gene (upper panel) was performed using mouse genomic DNA as templates. Homozygous (-/-) mice demonstrate presence of the neomycin resistance gene but absence of the endogenous UBC4-testis gene. Heterozygous (+/-) mice demonstrate presence of both the neomycin resistance gene and the endogenous UBC4-testis gene. Wild type (+/+) mice demonstrate lack of the neomycin resistance gene but presence of the endogenous UBC4-testis gene.

Figure 5. Inactivation of UBC4-testis did not affect the rate of testicular involution in response to cryptorchidism. Wild-type (WT) or knockout (KO) mice were subjected to unilateral surgical cryptorchidism as mentioned in materials and methods. The ratios of

cryptorchid to normal testis weights were plotted against time after cryptorchid surgery in the form of means \pm standard error. The effect of experimental cryptorchidism on testicular mass was statistically analyzed by two-way ANOVA. There were no significant differences between the wild-type and knockout animals.

Figure 6. Histological analysis of cryptorchid mouse testes. The pictures show the testis from a wild type mouse (A, C, E, G) or a UBC4-testis knock out mouse (B, D, F, H) at 0 (A, B), 2 (C, D), 6 (E, F) and 10 (G, H) days after surgery. (A) the normal wild type mouse, stage VII, (B) the normal UBC4-testis knock out mouse, stage VII, (C) the wild type mouse 2 days after cryptorchidism, (D) the UBC4-testis knock out mouse 2 days after cryptorchidism, (E) the wild type mouse 6 days after cryptorchidism, (F) the UBC4-testis knock out mouse 6 days after cryptorchidism, (G) the wild type mouse 10 days after cryptorchidism, (H) the UBC4-testis knock out mouse 10 days after cryptorchidism.

Figure 7. Rat100 is homologous to human EDD. (A) A tBLASTn search with human EDD (Aa. 1-2500) in the NCBI mouse EST data base (year 2002). Single short lines: overlapping EST sequences that are similar to human EDD. The similarity degrees are indicated by different colors, which refer to mathematically derived alignment scores. The higher the score, the more similar the aligned sequences. Black: alignment scores lower than 40; blue: alignment scores 40-50; green: alignment scores 50-80; pink: alignment scores 80-200; red: alignment scores higher than 200. Double short lines: the gap regions that were amplified by PCR. Triple short lines: nine regions containing

EDD amino acid sequence. Shaded amino acids: the PABC domain. Bold and underlined amino acids: the HECT domain. The conserved active cysteine residue is marked by an asterisk below the sequence.

Figure 8. Ubiquitination of Paip2 by EDD *in vitro*. EDD, isolated by immunoprecipitation with anti-EDD antibodies from rat testis lysate, was incubated with E1, E2 (UBC4-1), His-ubiquitin, ubiquitin aldehyde, AMP-PNP and either GST-Paip2A or GST. Products were then isolated using glutathione coupled beads. Higher molecular weight ubiquitinated forms of GST-Paip2A (lane 6, asterisks) were detected by immunoblotting with anti-Paip2 antibodies. As negative controls, immunoprecipitates obtained with preimmune rabbit IgG were used in the *in vitro* ubiquitination assay (lane 3) or reactions were carried out with GST as substrate and detected with anti-GST antibodies (lanes 9,10). To confirm that the higher molecular weight bands in lane 6 contained ubiquitin, replicates of samples used in lanes 3 and 6 were analysed by immunoblotting with anti-ubiquitin antibodies (lanes 7 and 8). Bands of ubiquitinated GST-Paip2A are marked with asterisks. The positions of GST and GST-Paip2A are indicated by arrows.

Figure 9. Identification of proteins copurifying with EDD/Rat100. (A) Identification of proteins coimmunoprecipitated with EDD/Rat100. Rat testis lysates were precleared with normal rabbit IgG to remove non-specifically bound proteins. The precleared lysates were treated with 5 mM NEM to inactivate EDD/Rat100 and thereby

promote trapping of substrates before being immunoprecipitated with IgG or anti-Rat100 antibody crosslinked to Protein A-Sepharose with DMP. Following thorough washing, pellets were resolved on a 5% - 15% gradient acrylamide gel by SDS-PAGE and stained with Colloidal Blue. Lane 1, pellets of IP with control rabbit IgG. Lane 2, pellets of IP with anti-Rat100 antibody. Lane 3, pellets of IP with the anti-Rat100 antibody preabsorbed with the antigen peptide. Lane 4, the antigen peptide preabsorbed with anti-Rat100 antibody only. Lane 5, the anti-Rat100 antibody only. EDD/Rat100 was indicated in the figure. A: the antigen peptide. H: the heavy chain of antibodies. L: the light chain of antibodies. M: protein markers. In lane 2, protein bands that were excised for mass spectrometry analysis were marked with asterisks. The top asterisk indicates the band of immunoprecipitated EDD/Rat100, which was confirmed by the subsequent mass spectrometry analysis. (B) Evaluation of immunoprecipitation efficiency of **EDD/Rat100** by Western blotting. 1% of the supernatants and pellets were analyzed by Western blotting for the efficiency of immunoprecipitation of EDD/Rat100. Lane 1, EDD/Rat100 was not precipitated by normal rabbit IgG, it remained in the supernatant. Lane 2, most of the EDD/Rat100 was precipitated by the anti-Rat100 antibody. However, the immunoprecipitation efficiency was not 100%, a small amount of EDD/Rat100 was left in the supernatant. Lane 3, in comparison with the result in lane 2, most EDD/Rat100 remained in the supernatant. The EDD/Rat 100 signal in the pellet was very small, but difficult to see in the image due to the high background produced by the large amount of antigen peptide that was used to preabsorb the antibody. Lane 4, supernatant of precleared lysates before being subjected to immunoprecipitation.

Figure 10. ACL, CBL, Miwi, CRMP-2/TOAD-64, NF-κB and Eps-15 can be coimmunoprecipitated with EDD/Rat100. To confirm the mass spectrometry results, immunoprecipitation of EDD/Rat100 from rat testis lysate was repeated on a small scale. The IP was carried out with 5 μg of anti-Rat100 antibody and 1 mg of rat testis lysate. The pellets were analyzed by Western blotting. Lane 1: Input (100 μg) rat testis lysate. Lane 2: pellet of the immunoprecipitation with the anti-Rat100 antibody. Lane 3: pellet of the immunoprecipitation with the anti-Rat100 antibody preabsorbed with the antigen peptide. EDD/Rat100 was not detected in this lane. Lane 4: Control IP using rabbit IgG. Protein bands were arranged from top to bottom according to their molecular weights. Eps-15 and CRMP-2 were analyzed in a separate experiment, in which the antigen peptide competition control was not included. Asterisk represent nonspecific signals in Western blotting.

Figure 11. EDD can be coimmunoprecipitated using antibodies to CBL, ACL and Miwi. ACL, CBL, Miwi, CRMP-2, NF-κB and Eps-15 were immunoprecipitated from rat testis lysate with their specific antibodies; pellets were then analyzed for EDD/Rat100 by Western blotting. The left column: Western blotting of the input rat testis lysates. The middle column, IP (+): immunoprecipitation with specific antibodies against the above proteins. The right column, IP (-): control immunoprecipitation with rabbit IgG except for CRMP-2 where an unrelated mouse monoclonal antibody (anti-Myc) was used as the negative control. Rabbit IgG was used as the negative control for the remaining antibodies. Western blotting antibodies are indicated on the right side. Asterisks: CRMP-2. Dots: the immunoglobulin heavy chain of either anti-CRMP or anti-Myc antibodies.

Figure 12. The effects of siRNA mediated silencing of EDD/Rat100 in HEK293 cells on the levels of proteins identified as co-immunoprecipitating with EDD/Rat100. (A) The cells were transfected with control siRNA (non-specific siRNA control duplex VII with 57% GC content, Dharmacon) or the EDD specific siRNAs #297 or #295. Lysates were prepared 48 hours after transfection and analyzed by Western blotting for the protein levels of EDD, cbl, ACL, CRMP-2, NF-κB and actin. Shown are representative blots. (B) Levels of these proteins were quantified with a Bio-Rad model 3000 VersaDoc Gel Imaging System and the Quantity One software. Each sample was prepared in triplicate. Average levels of these proteins are shown in panel B. Error bars: standard error. RNAi mediated depletion of EDD was more than 50%. The CRMP-2 protein level was increased upon lowering levels of EDD.

Figure 13. Copurification of CRMP during immunoprecipitation of EDD/Rat100 was due to non-specific binding of CRMP with the anti-Rat100 antibody. (A) Endogenous CRMP can be copurified with EDD/Rat100 from HEK293 and Hela cell lysates. Information on the cell lysates and antibodies used for immunoprecipitation and Western blotting is shown in the table. (Asterisk: CRMP-2. Arrow: the immunoglobulin heavy chain of anti-CRMP-2 antibody.) Four to five protein bands higher than CRMP-2 are detected by anti-CRMP-2 antibody in lanes 2 and 5. A ladder of ubiquitinated proteins is also detected by anti-Ub antibody in these two lanes. (B) FLAG tagged EDD and GFP tagged CRMP cannot be copurified from HEK293 cell lysates. Details of transfections and immunoprecipitations are indicated in the table. Asterisk: a

non-specific band detected by the anti-Flag antibody in Western blotting. Arrowhead: FLAG tagged EDD. Hollow arrow: GFP tagged CRMP-2. (C) The anti-Rat100 antibody crossreacted with endogenous CRMP-2 or GFP tagged CRMP-2. HEK293 cells were transfected with the CRMP-2-GFP plasmid. EDD/Rat100 was depleted from the cell lysates or from rat testis lysate by serial immunoprecipitation with the anti-Rat100 antibody four times. EDD/Rat100, endogenous CRMP-2 and GFP tagged CRMP-2 in pellets and supernatants were detected by Western blotting with anti-Rat100 or anti-CRMP antibodies respectively. Lanes 1 to 4: pellets from the 1st to the 4th immunoprecipitations. Lane 0: supernatant of the preclearing with rabbit IgG (Input). Lanes 1' to 4': supernatants from the 1st to the 4th immunoprecipitations. Although a declining amount of EDD/Rat100 was immunoprecipitated, the amount of CRMP-2 in each pellet remained similar (lanes 1 to 4). Arrowhead: EDD/Rat100. Arrow: endogenous CRMP-2. Hollow arrow: GFP tagged CRMP-2.

Figure 14. Levels of myosin heavy chain, USP19 and myogenin in differentiating L6 myotubes. Upper panel: L6 myoblasts were cultured in differentiation medium for up to 5 days. Levels of myosin heavy chain (MHC), USP19, myogenin and tubulin in these cells were determined by SDS-PAGE and Western blotting of 100 μg of lysates prepared from cells at the indicated days of differentiation. The anti-myogenin antibody recognized a doublet. The lower predominant one is myogenin; the upper one is possibly a phosphorylated form of myogenin [250]. Lower panel: the Western blotting results were quantified using a Bio-Rad model 3000 VersaDoc Gel Imaging System and the Quantity One software. The amount of each protein was normalized to the quantity of

tubulin in the same lane. The normalized protein levels were plotted versus time of differentiation to show the change in relative abundance of myosin heavy chain, USP19 and myogenin during the course of L6 differentiation. Data are shown as mean \pm standard error (n=3). *: P<0.05 vs. day 0.

Figure 15. RNAi mediated depletion of USP19 in L6 myotubes can increase levels of myosin heavy chain protein. L6 cells were cultured in differentiation medium for 3 days. These L6 myotubes were then transfected with siRNA duplexes #1 or #7. NSP: non-specific siRNA control (Dharmacon). L6 myotubes were harvested on days 4 and 5, and protein levels of MHC and USP19 were analyzed by Western blotting (upper panel). The Western blotting results were quantified and normalized to the tubulin levels (lower panel). Data are shown as mean \pm SE (n=3). Statistical analyses were assessed by ANOVA. *: P<0.05 vs. NSP. #: P<0.1 vs. NSP.

Figure 16. RNAi mediated depletion of USP19 can reverse TNF- α induced loss of MHC in L6 myotubes. (A) TNF- α lowers MHC protein in L6 myotubes. L6 cells were cultured in differentiation medium for 3 days and then treated with either vehicle (CTL), TNF- α (10 ng/ml) or TNF- α and INF- γ (100 U/ml). Left panel: Levels of MHC and tubulin determined by Western blotting. Right panel: quantification of MHC normalized to the expression of γ -tubulin. Shown are means \pm SE (n=3). *: p<0.05 vs CTL (B) RNAi mediated depletion of USP19 can reverse TNF- α induced loss of MHC. Control (NSP) or USP19 specific siRNA (oligonucleotides #1) were transfected into L6 myotubes on day 2 of differentiation. On day 3, TNF- α (10 ng/ml) was added into

differentiation medium to induce loss of MHC. Cells were harvested on days 4 and 5, and MHC and USP19 levels determined by Western blotting. Data are shown in the form of mean \pm SE (n=6), the mean value of negative controls on day 4 was set to one. Similar results were obtained from two separate experiments. Statistical differences were assessed by ANOVA. *: P<0.05 vs. NSP. •: P<0.05 vs. TNF 10 ng/ml, #: P<0.1 vs. NSP.

Figure 17. RNAi mediated depletion of USP19 can partially prevent dexamethasone (DEX) induced loss of MHC in L6 myotubes. (A) DEX 10 μM can decrease MHC in L6 myotubes. From day 3 of differentiation, L6 myotubes were treated with 1 μM or 10 μM of DEX for 48 hours. Left panel: levels of MHC and tubulin determined by Western blotting. CTL: negative control. Right panel: quantification of MHC normalized to the expression of γ -tubulin in the form of mean \pm SE (n=3). (B) RNAi mediated silencing of USP19 can reverse DEX induced loss of MHC. Control (NSP) or USP19 specific siRNA (oligonucleotides #1) were transfected into L6 myotubes on day 2 of differentiation. On day 3, DEX (10 μM) was added to the medium to induce loss of MHC. Cells were harvested on days 4 and 5, and MHC and USP19 levels determined by Western blotting. Data are shown in the form of mean \pm SE (n=6), the mean value of negative controls on day 4 was set to one. Similar results were obtained from two separate experiments. Statistical differences were assessed by ANOVA. *: P<0.05 vs. NSP. •: P<0.05 vs. DEX 10 μM and P<0.05 vs. NSP. #: P=0.1 vs. NSP.

Figures and Tables:

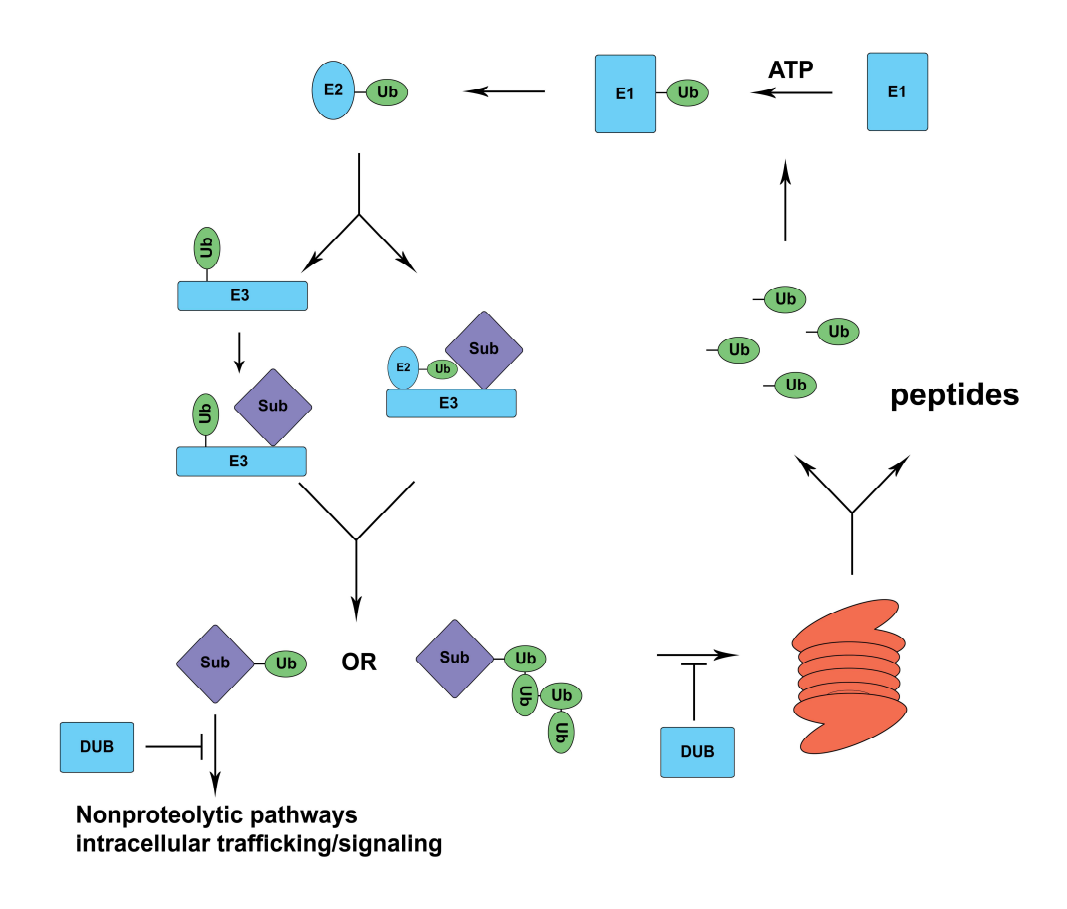
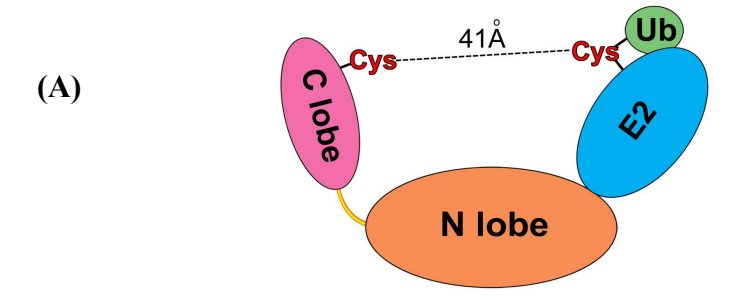
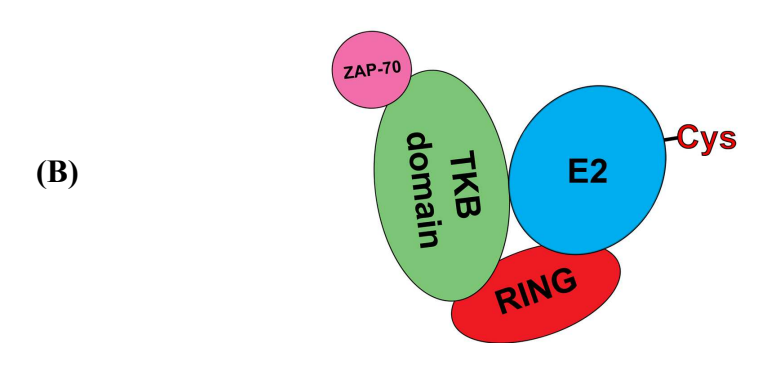


Figure 1. The ubiquitin proteasome system





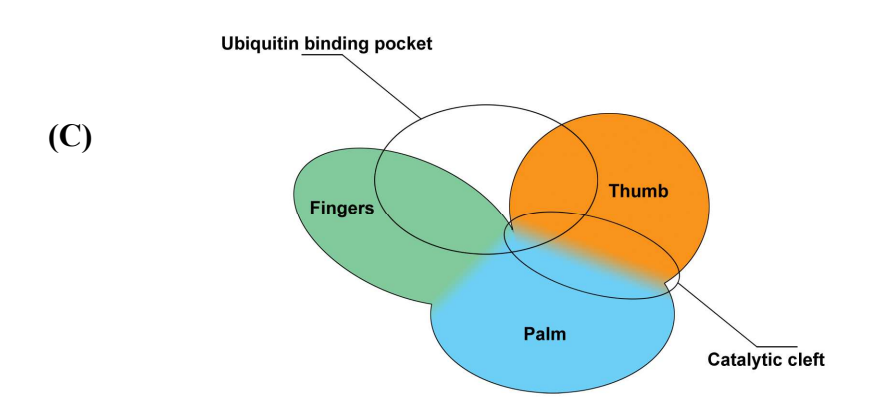
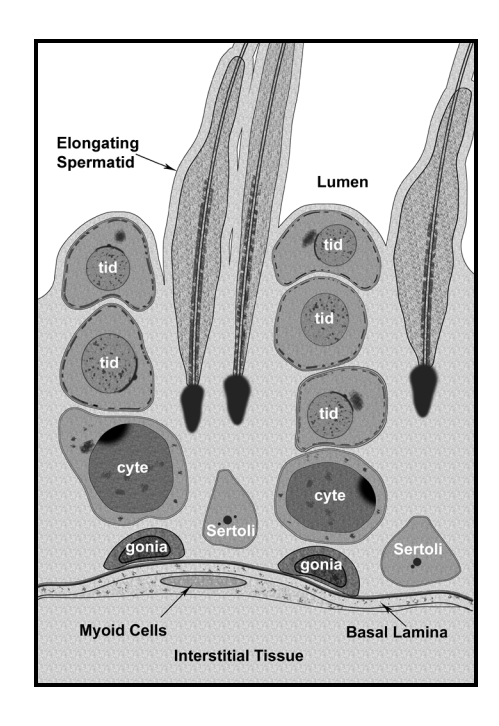


Figure 2.

(A)



Designed by Zhiyu Pang

(B)

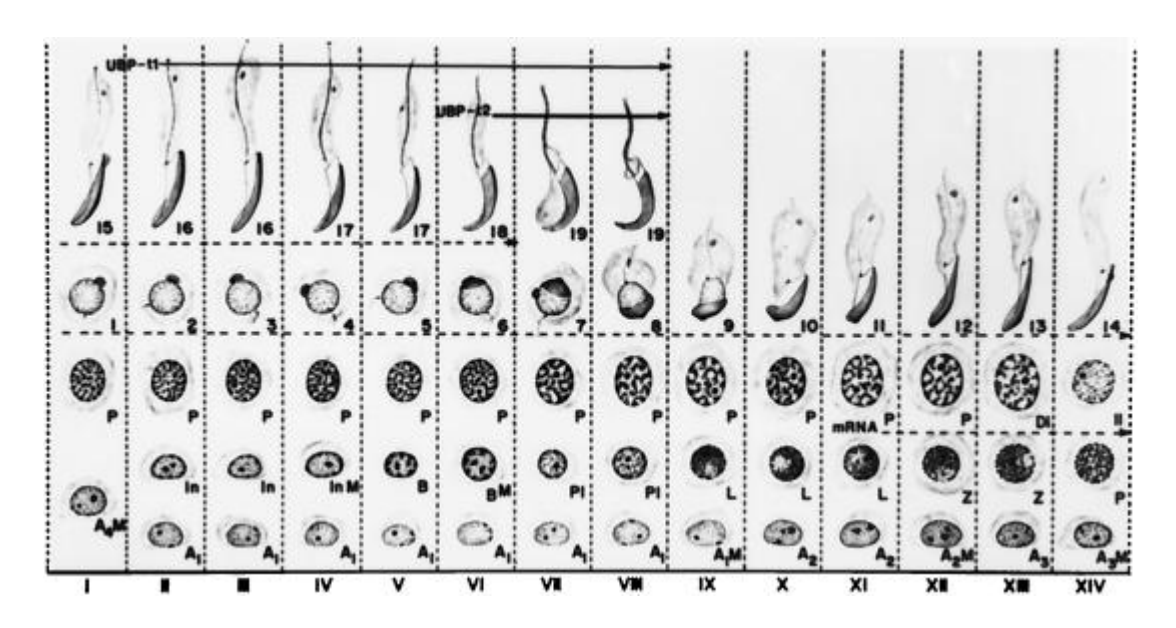
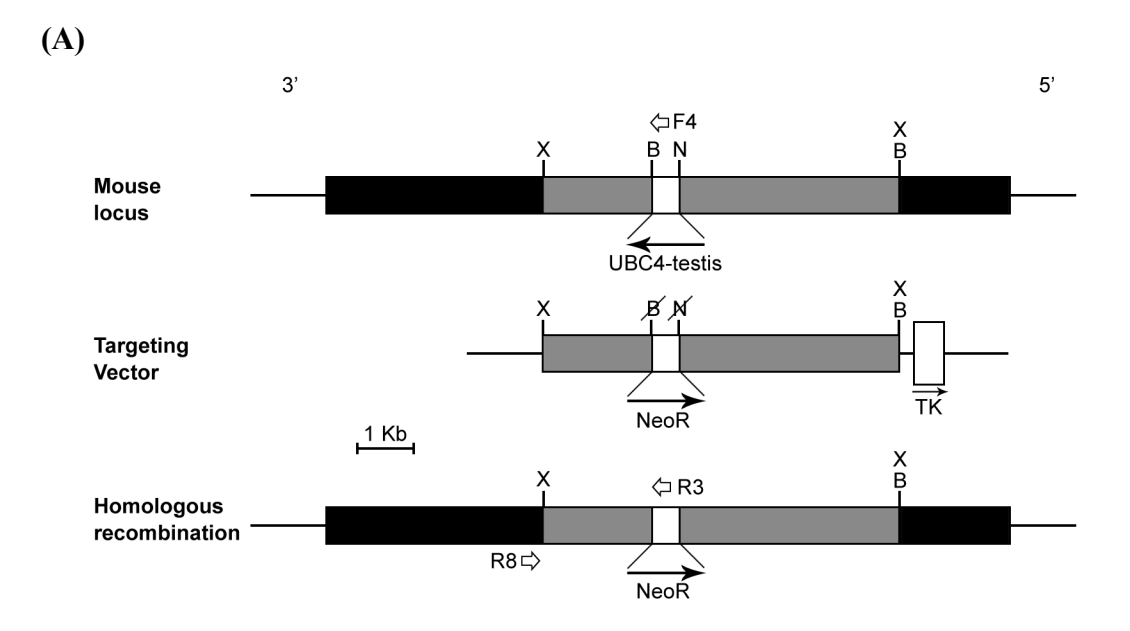


Figure 3. (Adapted from Lin's publication [251])



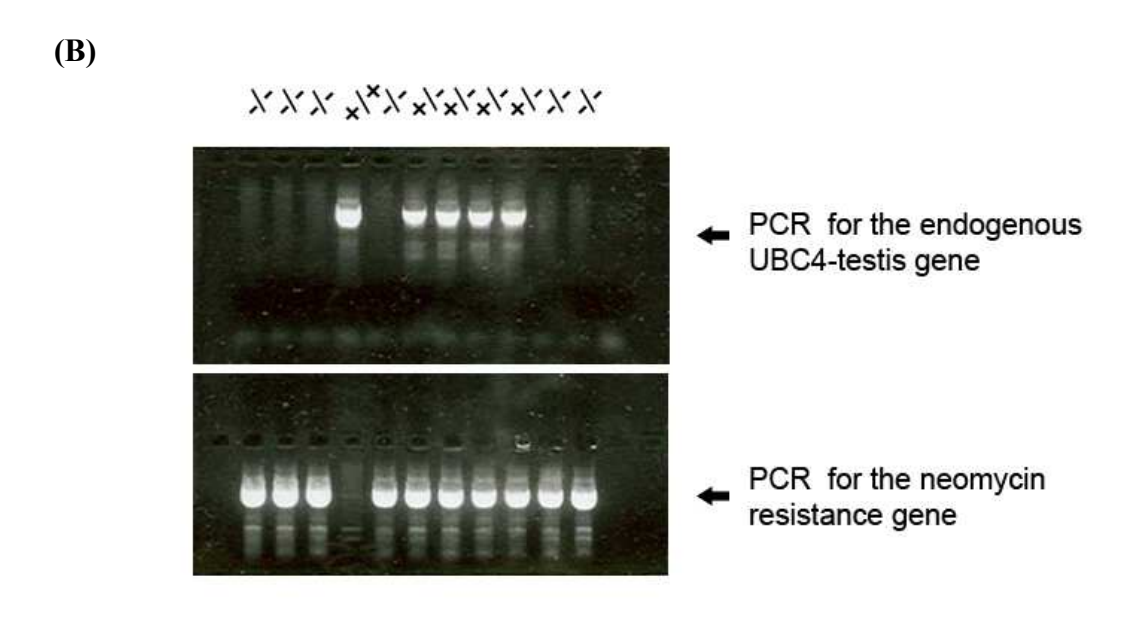
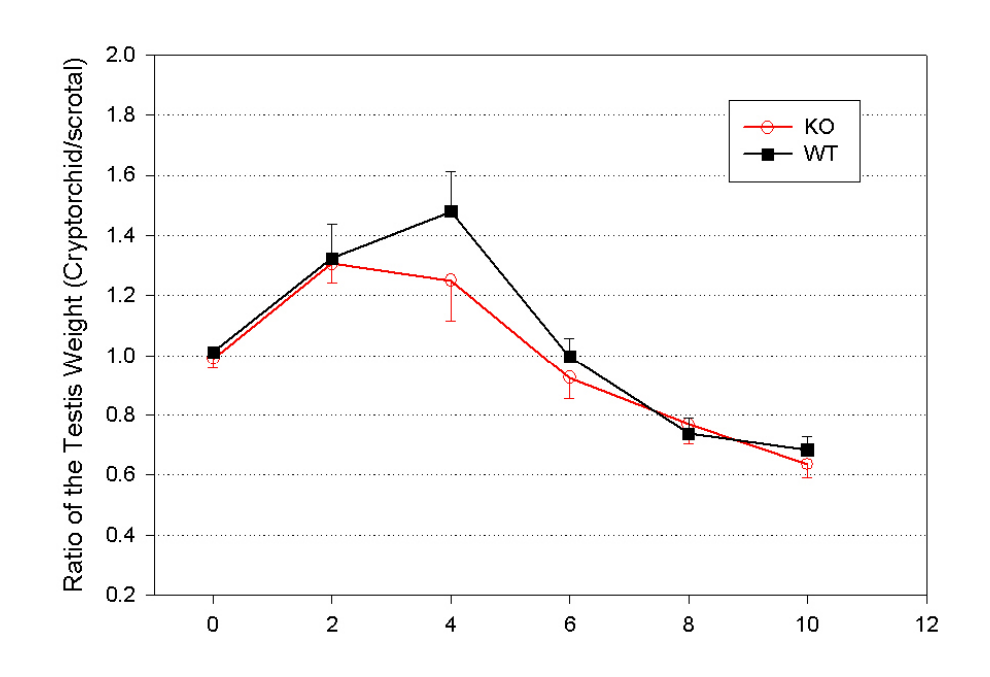


Figure 4.

Experimental Cryptorchidism



Days after Cryptorchidism Surgery

Figure 5.

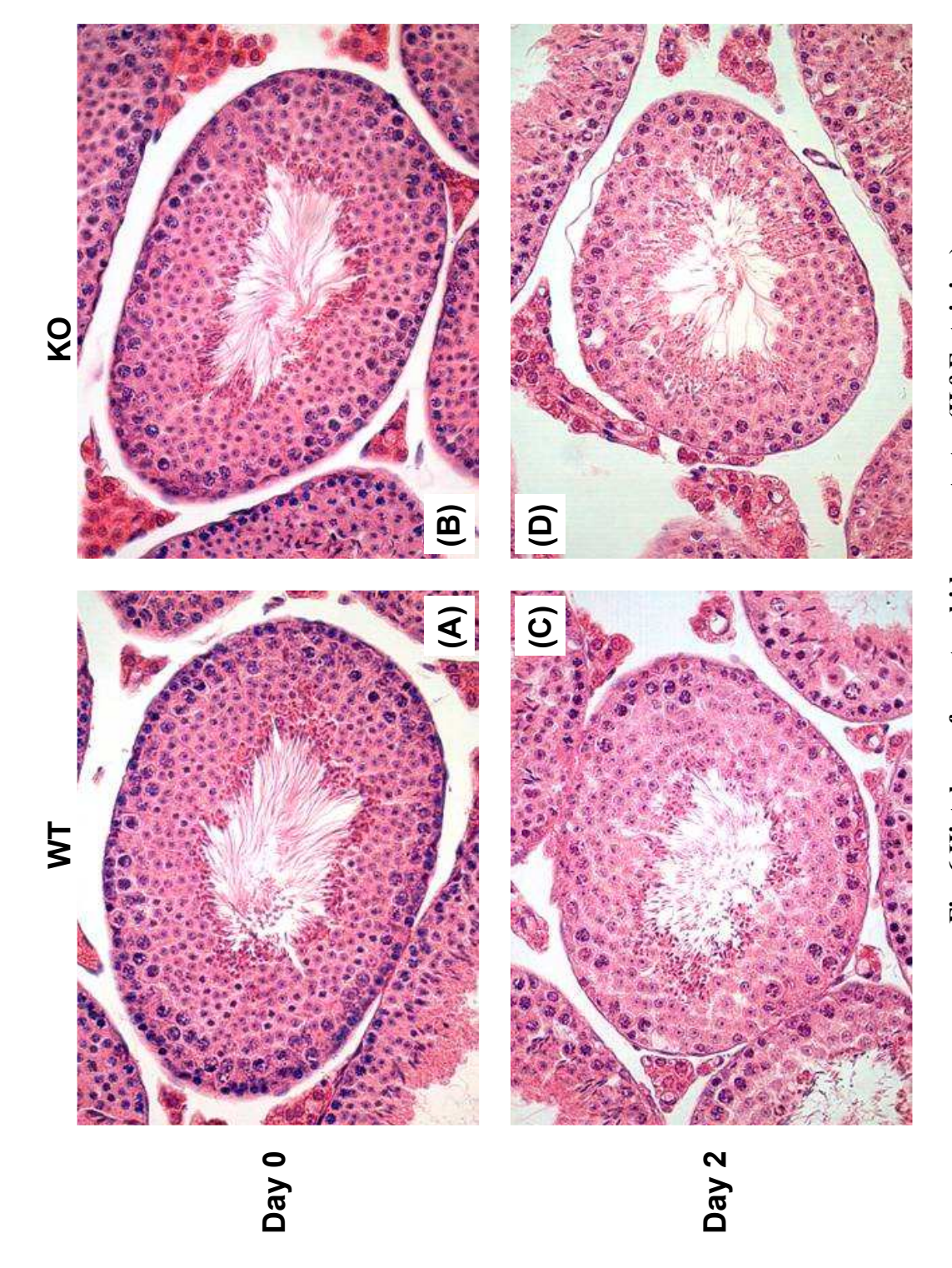


Fig. 6 Histology of cryptorchid mouse testes (H&E staining)

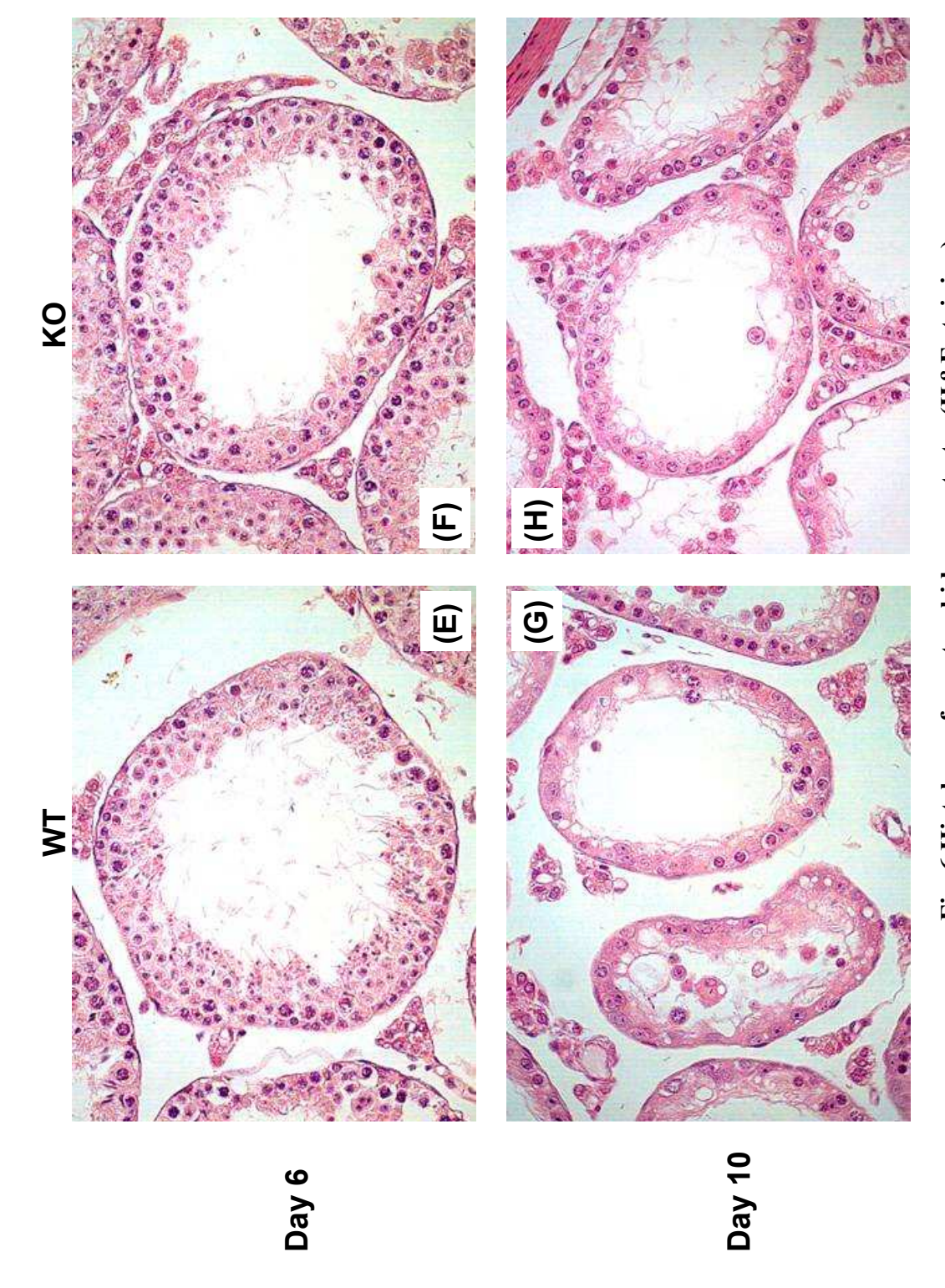


Fig. 6 Histology of cryptorchid mouse testes (H&E staining)

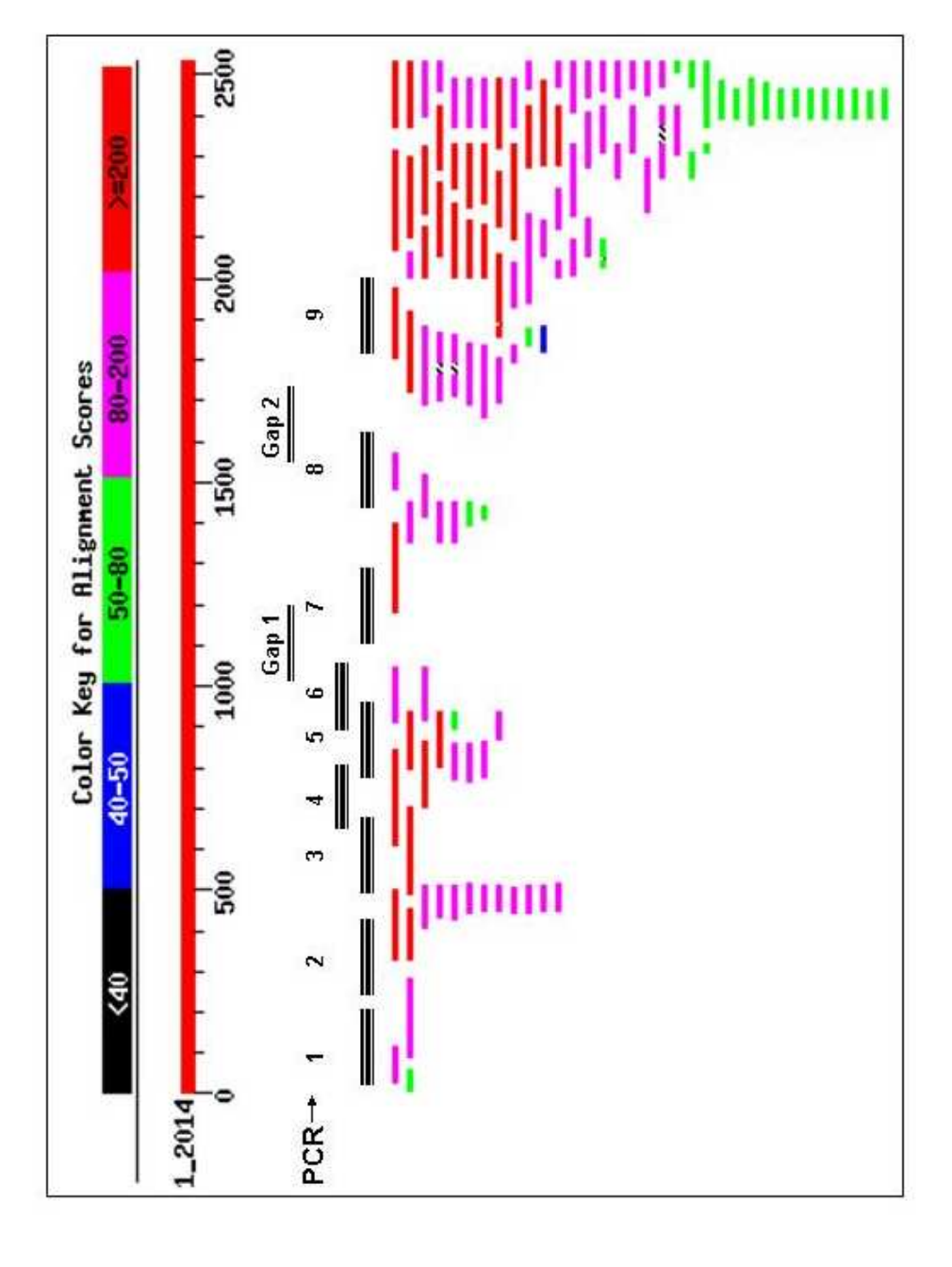


Figure 7 (A)

1 MTSIHFVVHP LPGTEDOLND RLREVSEKLN KYNLNSHPPL NVLEOATIKO CVVGPNHAAF LLEDGRICRI GFSVOPNRLE LRKPDNIDGS LLNNSSGTGR 101 TSRPGRTSDS PWFLSGSETL GRLAGNTLGS RWSSGVGGSG GGSSGRSSAG ARDSRROTRV IRTGRDRGSG LLGSOPOPVI PASVIPEELI SQAQVVLOGK 201 SRSVIIRELO RTNLDVNLAV NNLLSRDDED GDDGDDTASE SCXPGEDLMS LLDADIHLLP PSVIIDADAM LSEDISYTGY PSLRRSSLSR LGSYVVIVLP 301 LERDSELLRE RESVLRLRER RWLDGASFDN ERGSTSKEEE SNPDKKNTPV QSPVSMGEDL QWWPDKDGTK FTCIGALYYE LLAVSSKGGL YQWKWSESEP 401 YKNAQNPSLH HPRATFLGLT NEKIVFLSAN SIRATVATEN NKVATWVDET LSSVASKLEH TAQTYSELQG ERIVSLHCCA LYTCAQLENN LYWWGVVPFS 501 QRKKMLEKAR AKNKKPKSSA GISSMPNITV GTQVCLRNNP LYHAGAVAFS ISAGIPKVGV LMESVWNMND SCRFQLRSPE SLKSMEKASK TLETKPESKQ 601 EPVKTEMGPP PSPASTCSDA SSIASSASMP YKRRRSTPAP REEEKVNEEQ WPLREVVFVE DVKNVPVGKV LKVDGAYVAV KFPGTSTNTT CQNSSGPDAD 701 PSSILODORI, LRIDELOVVK TGGTPKVPDC FORTPKKLCI PEKTELLAVN VDSKGVHAVI, KTGSWVRYCI, FDLATGKAEO ENNFPTSSVA FLGODERSVA 801 IFTAGOESPI VLRDGNGTIY PMAKDCMGGI RDPDWLDLPP ISILGMGVHS LINLPPNSTI KKKAAIIIMA VEKOTLMOHI LRCDYEACRO YLVNLEOAVV 901 LEQNLQMLQT FISHRCDGNR NILHACVSVC FPTSNKETKE EEEAERSERN TFAERLSAVE AIANAISVVS SNGPGNRAGS SNSRSLRLRE MMRRSLRAAG 1001 LGRHEAGASS SDHQDPVSPP IAPPSWVPNP PSMDPDGDID FILAPAVGSL TTAATGSGQG PSTSTIPGPS TEPSVVESKD RKANAHFILK LLCDSAVLQP 1101 YLRELLSAKD ARGMTPFMSA VSGRAYPAAI TILETAQKIA KAEVSASAKE EDVFMGMVCP SGTNPDDSPL YVLCCNDTCS FTWTGAEHIN QDIFECRTCG 1201 LLESLCCCTE CARVCHKGHD CKLKRTSPTA YCDCWEKCKC KTLIAGOKSA RLDLLYRLLT ATNLVTLPNS RGEHLLLFLV OTVAROTVEH COYRPPRIRE 1301 DRNRKTASPE DSDMPDHDLE PPRFAQLALE RVLODWNALR SMIMFGSOEN KDPLSPTSRI XHLFPAEOFY LNQOSGTIRL DCFTHSLIVK CTADILLLDT 1401 LLGTLVKELQ NKYTPGRREE AIPVTMRFLR SVARVFVILS VEMASSKKKN NFIPQPIGKC KRVFQALLPY AVEELCNVAE SLIVPVRMGI ARPTAPFTLA 1501 STSIDAMOGS EELFSVEPLP PRPSSDOSSS SSOSOSSYII RNPOORRISO SOPVRGREEE ODDIVSADVE EVEVVEGVAG EEDHHDEOEE HGEENAEAEG 1601 HHDEHDEDGS DMELDLLAAA ETESDSESNH SNQDNASGRR SVVTAATAGS EAGASSVPAF FSEDDSQSND SSDSDSSSSQ SDDIEQETFM LDEPLERTIN 1701 SSHANGAAQA PRSMQWAVRN PQHQRAASTA PSSTSTPAAS SAGLIYIDPS NLRRSGTIST SAAAAAAALE ASNASSYLTS ASSLARAYSI VIRQISDLMG 1801 LIPKYNHLVY SOTPAAVKLT YODAVNLONY VEEKLIPTWN WMVSXMDXTE AOLRYGSALA SAGDPGHPNH PLHASONSAR RERMTAREEA SLRTLEGRRR 1901 ATLLSAROGM MSARGDFLNY ALSLMRSHND EHSDVLPVLD VCSLKHVAYV FOALIYWIKA MNOOTTLDTP OLERKRTREL LELGIDNEDS EHENDDDTSO 2001 SATLNDKDDD SLPAETGONH PFFRRSDSMT FLGCIPPNPF EVPLAEAIPL ADQPHLLQPN ARKEDLFGRP SQGLYSSSAG SGKCIVEVTM DRNCLEVLPT 2101 KMSYAANLKN VMNMQNRQKK EGEEQSLLAE EADSSKPGPS APDVAAQLKS SLLAEIGLTE SEGPPLTSFR PQCSFMGMVI SHDMLLGRWR LSLELFGRVF 2201 MEDVGAEPGS ILTELGGFEV KESKFRREME KLRNQOSRDL SLEVDRDRDL LIQOTMROLN NHFGRRCATT PMAVHRVKVT FKDEPGEGSG VARSFYTAIA 2301 QAFLSNEKLP NLDCIONANK GTHTSLMORL RNRGERDRER EREREMRRSS GLRAGSRRDR DRDFRROLSI DTRPFRPASE GNPSDDPDPL PAHROALGER $2401 \ \texttt{LYPRVQAMQP} \ \texttt{AFASKITGML} \ \texttt{LELSPAQLLL} \ \texttt{LLASEDSLRA} \ \texttt{RVDEAMELII} \ \texttt{AHGRENGADS} \ \texttt{ILDLGLLDSS} \ \texttt{EKVQENRKRH} \ \texttt{GSSRSVVDMD} \ \texttt{LEDTDDGDDM} \ \texttt{MORRINGADS} \ \texttt{MOR$ 2501 APLFYOPGKR GFYTPRPGKN TEARLNCFRN IGRILGLCLL ONELCPITLN RHVIKVLLGR KVNWHDFAFF DPVMYESLRO LILASOSSDA DAVFSAMDLA 2601 FAIDLCKEEG GGOVELIPNG VNIPVTPONV YEYVRKYAEH RMLVVAEQPL HAMRKGLLDV LPKNSLEDLT AEDFRLLVNG CGEVNVOMLI SFTSFNDESG 2701 ENAEKLLOFK RWFWSIVEKM SMTERODLVY FWTSSPSLPA SEEGFOPMPS ITIRPPDDOH LPTANTCISR LYVPLYSSKQ ILKOKLLLAI KTKNFGFV

Figure 7 (B)

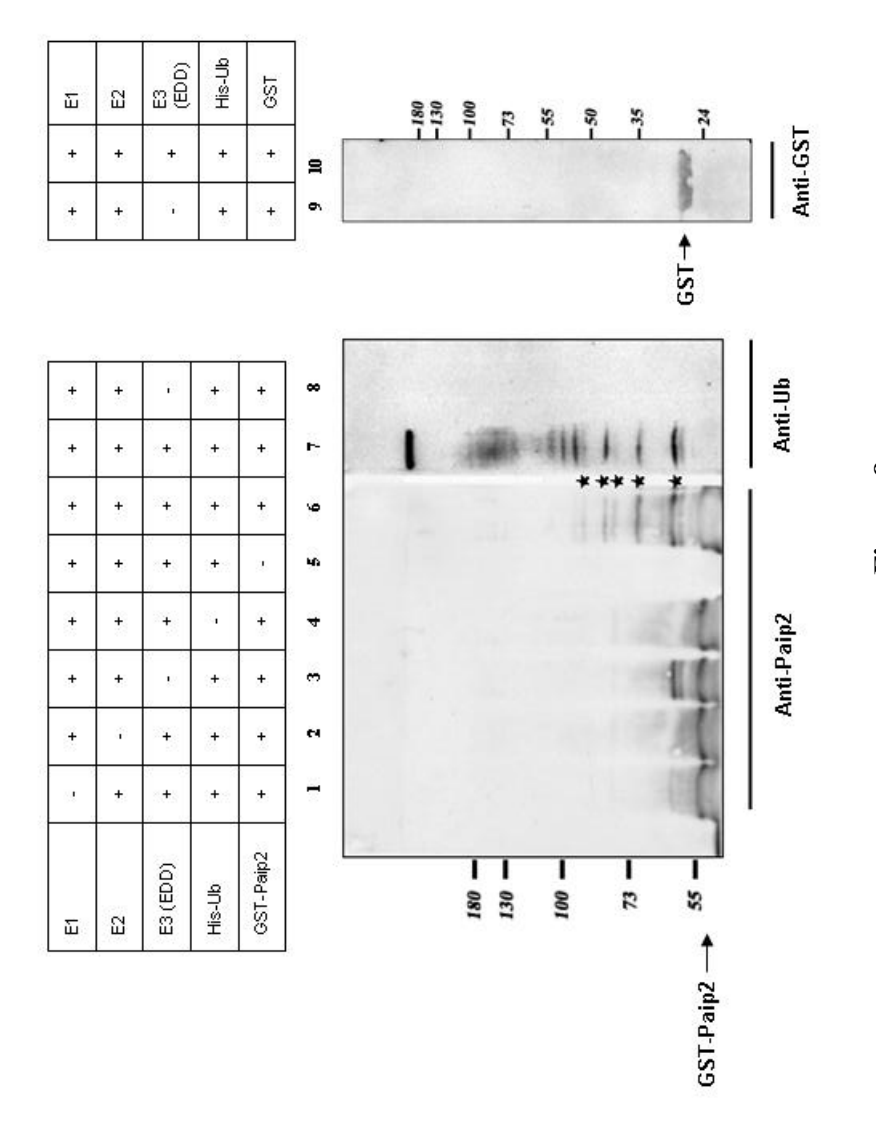


Figure 8.

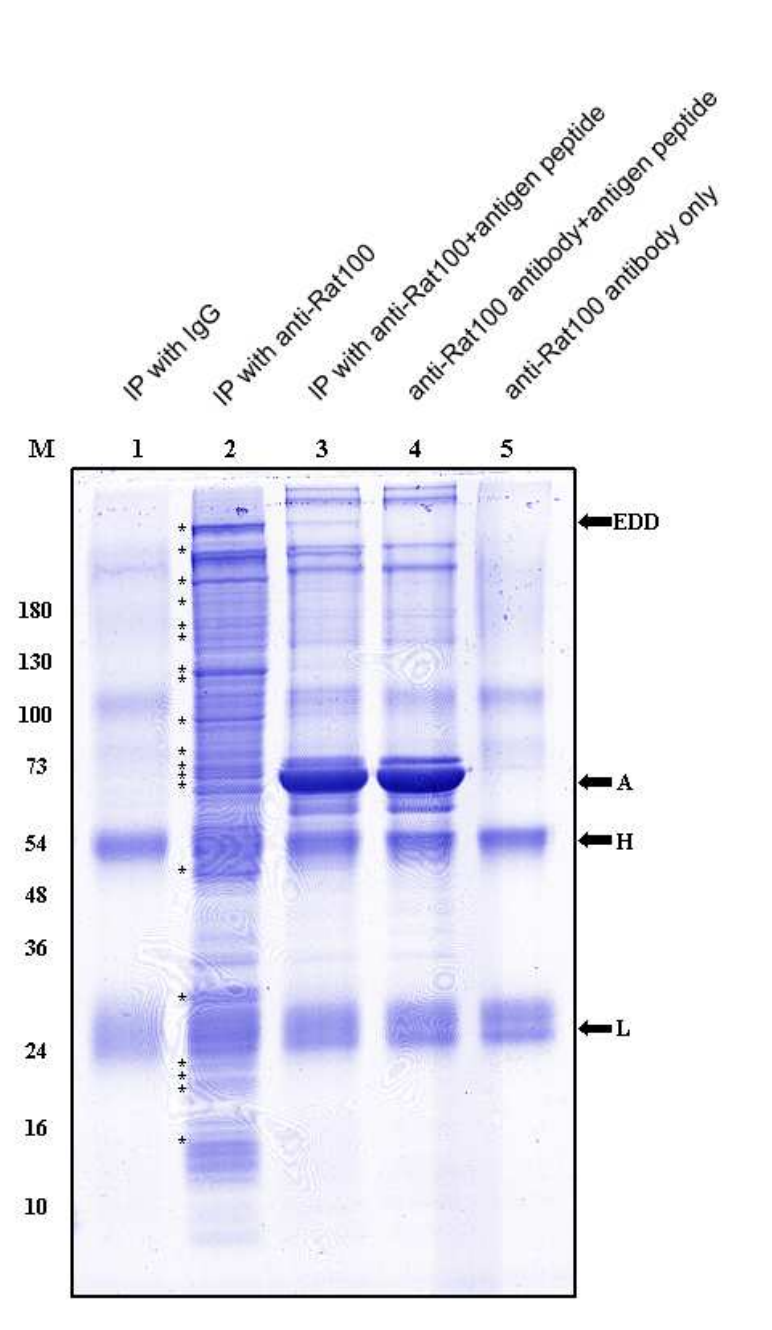


Figure 9 (A)

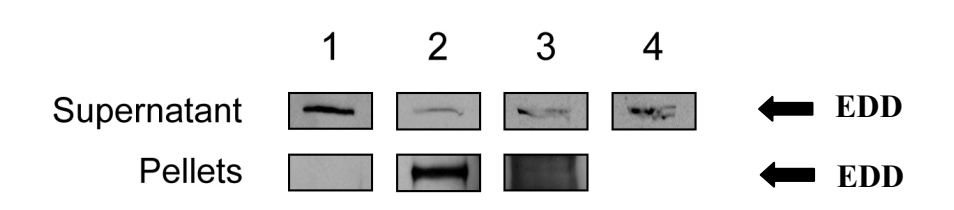


Figure 9 (B)

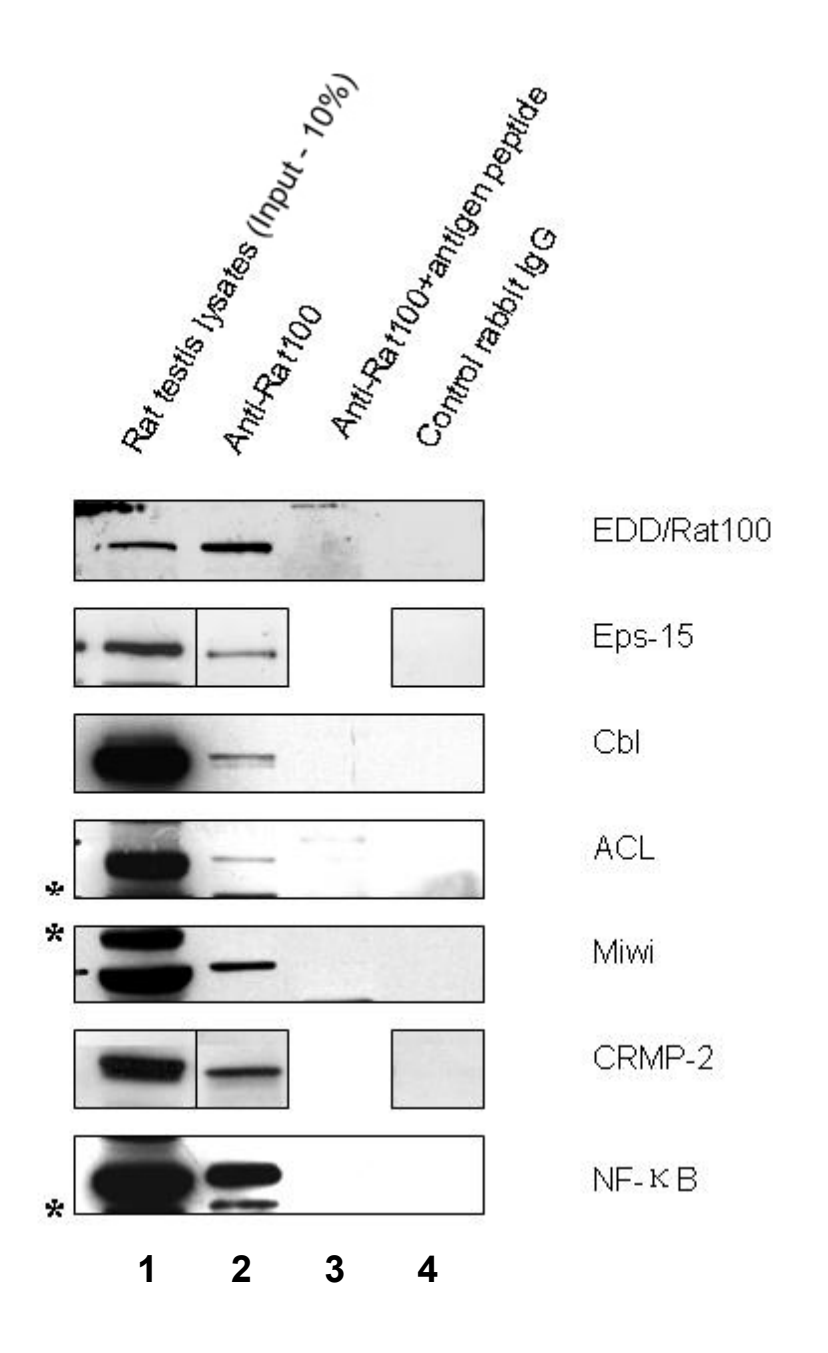


Figure 10.

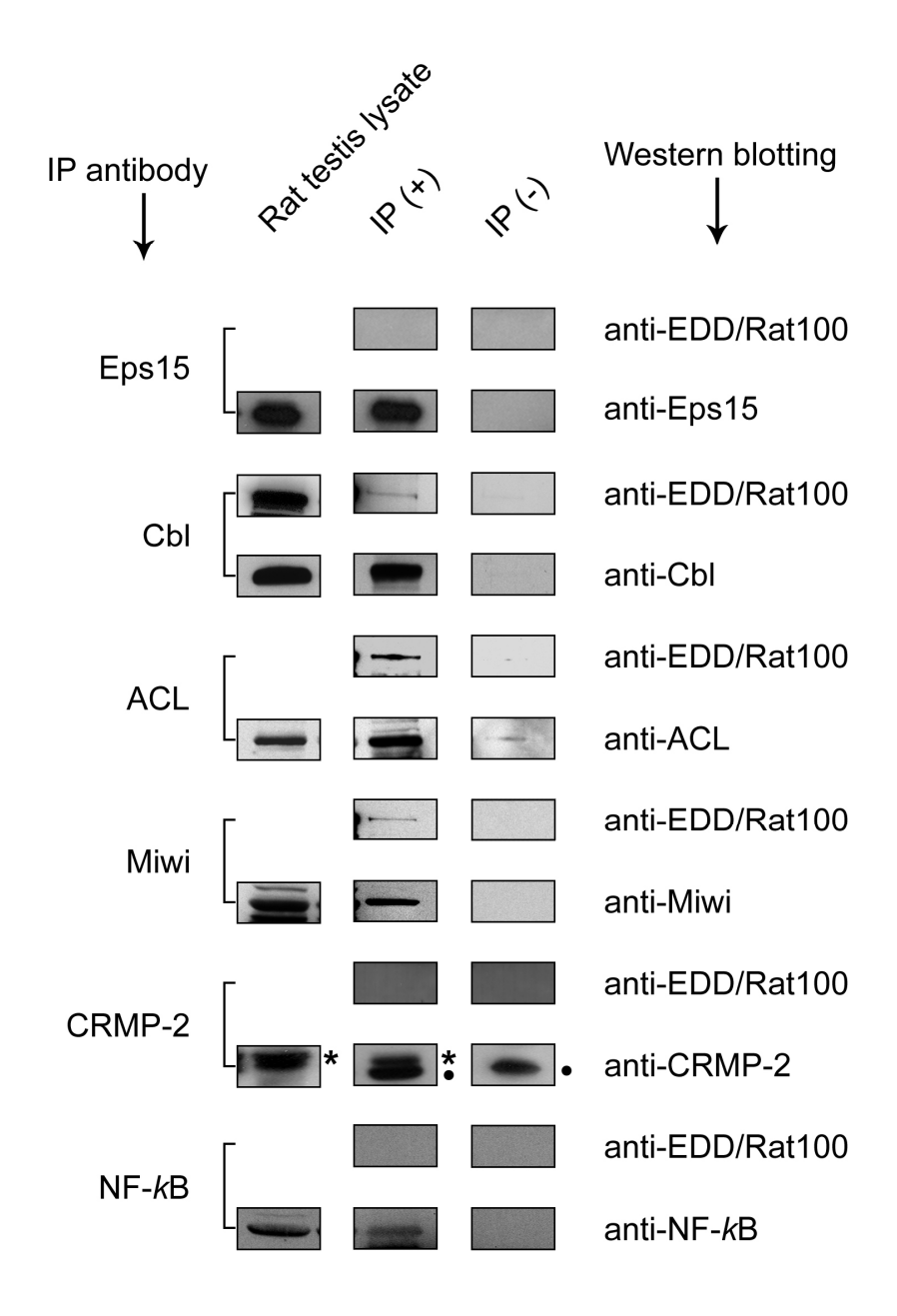


Figure 11.

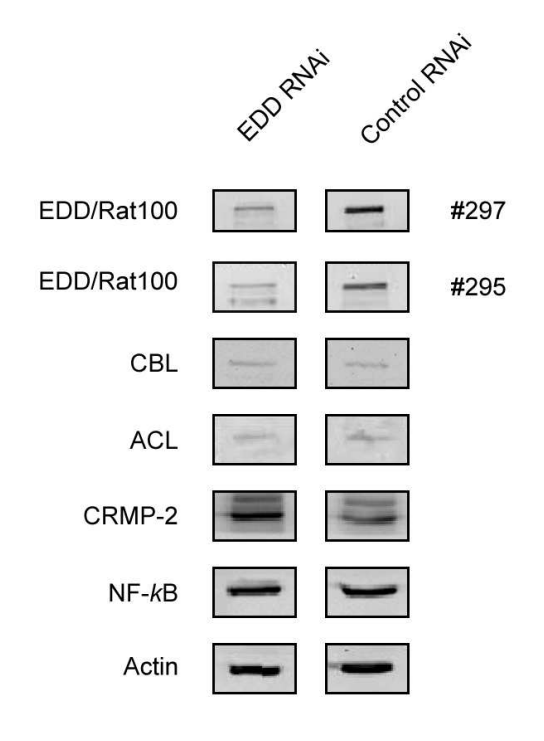


Figure 12 (A)

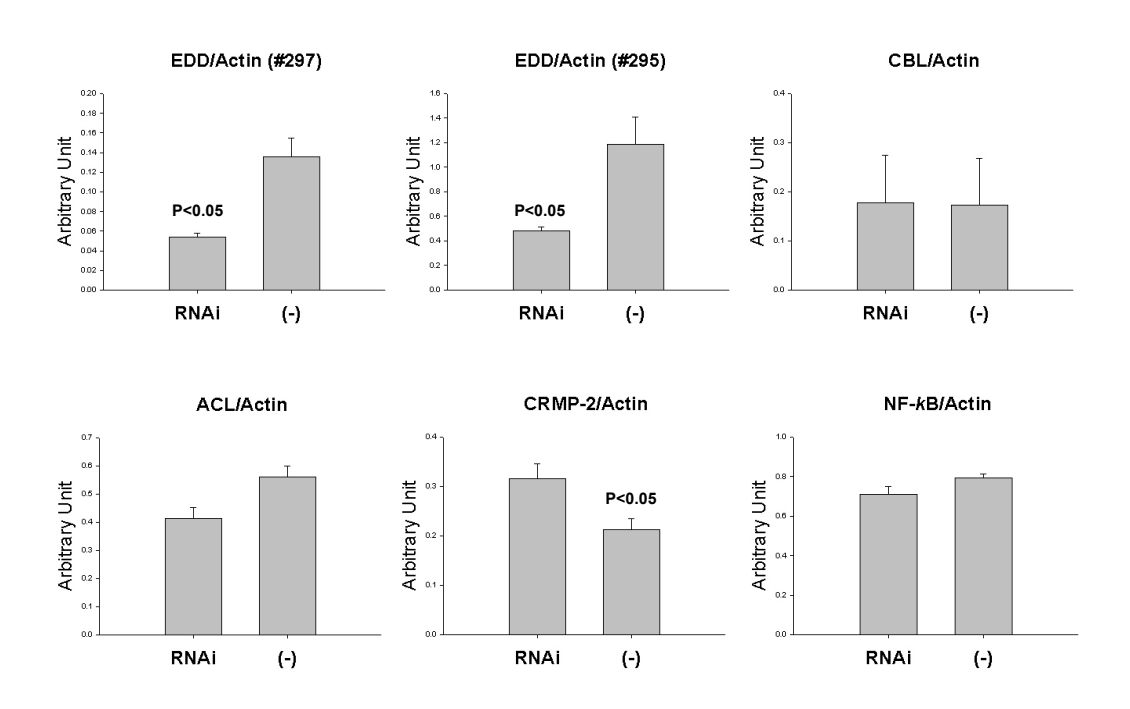


Figure 12 (B)

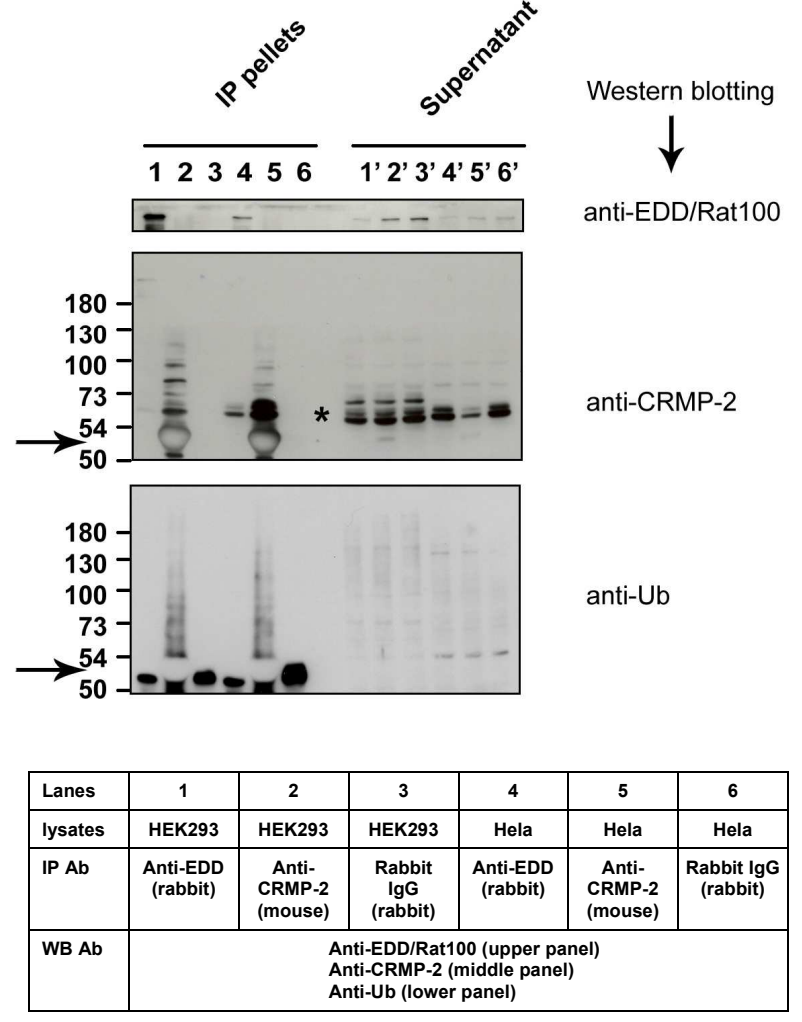


Figure 13 (A)

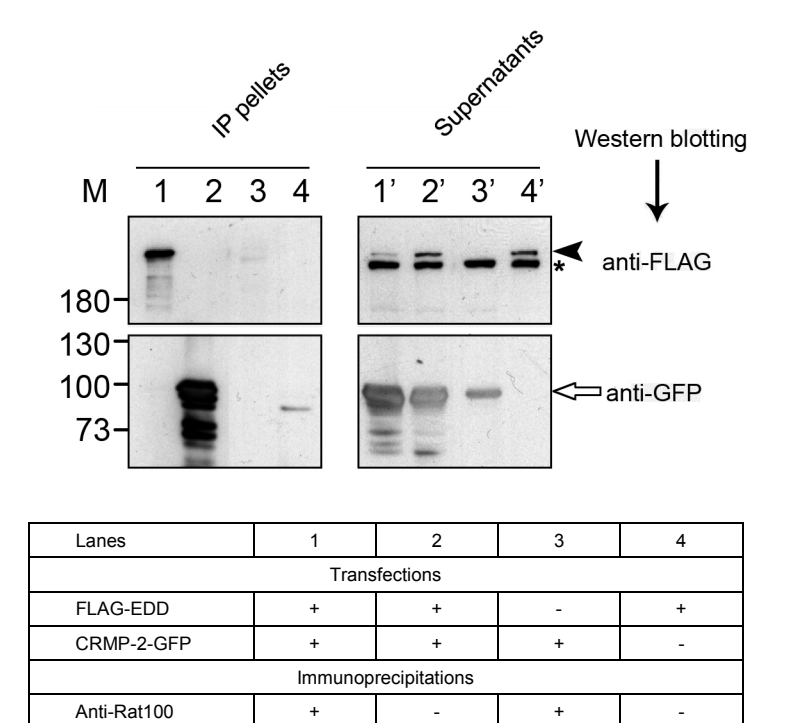


Figure 13 (B)

Anti-GFP

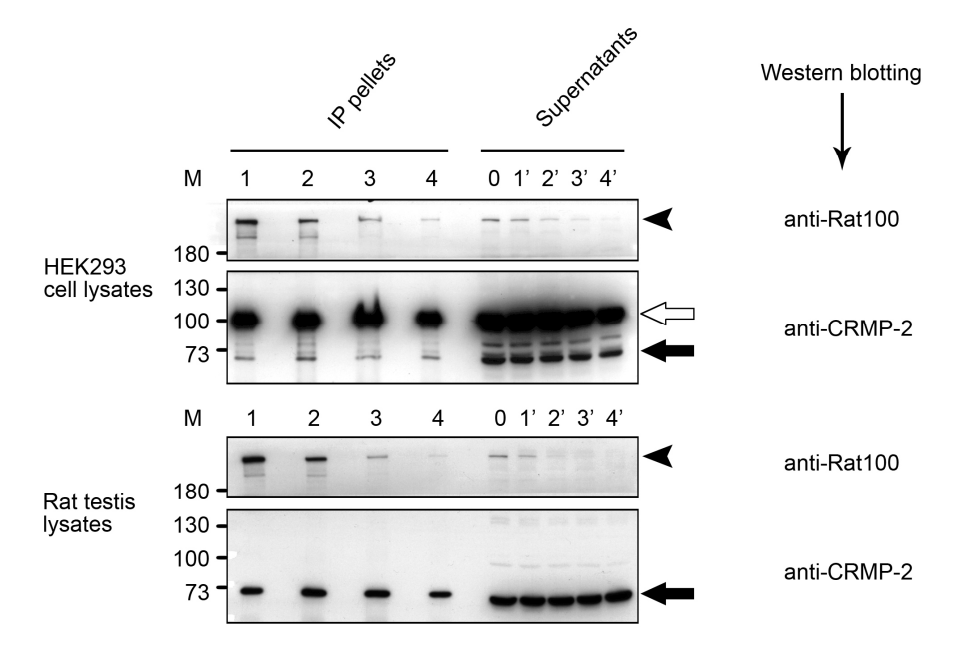
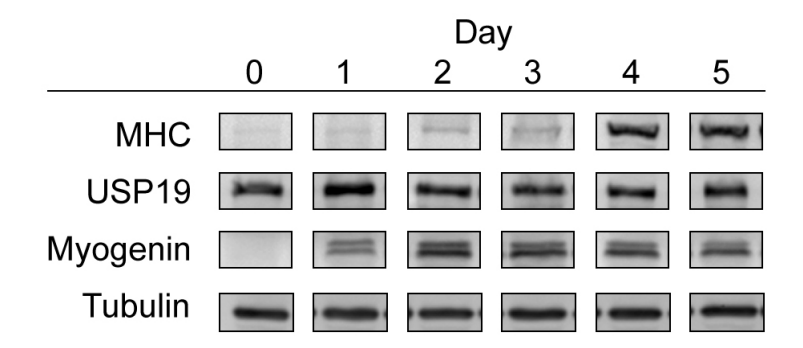
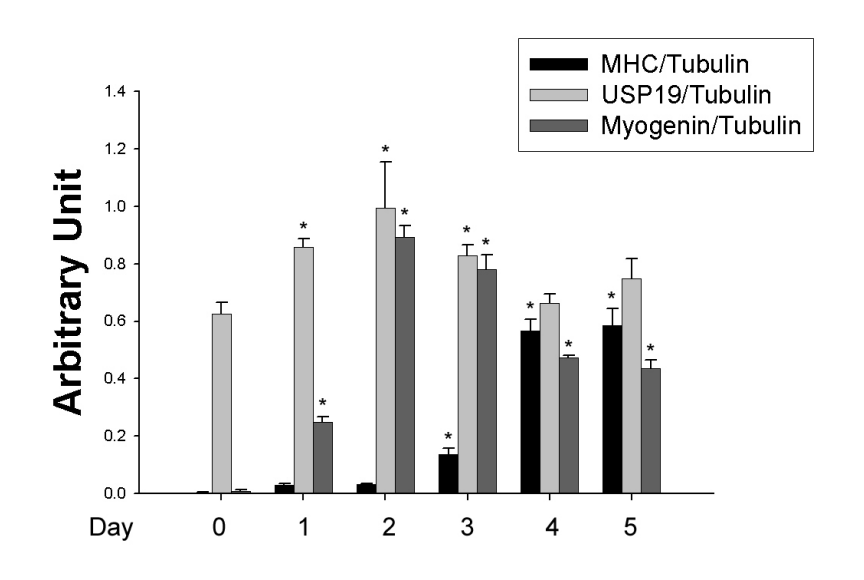


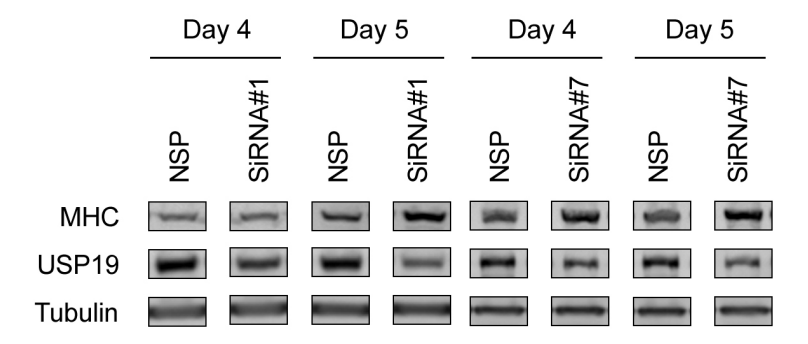
Figure 13 (C)





Day of differentiation

Figure 14



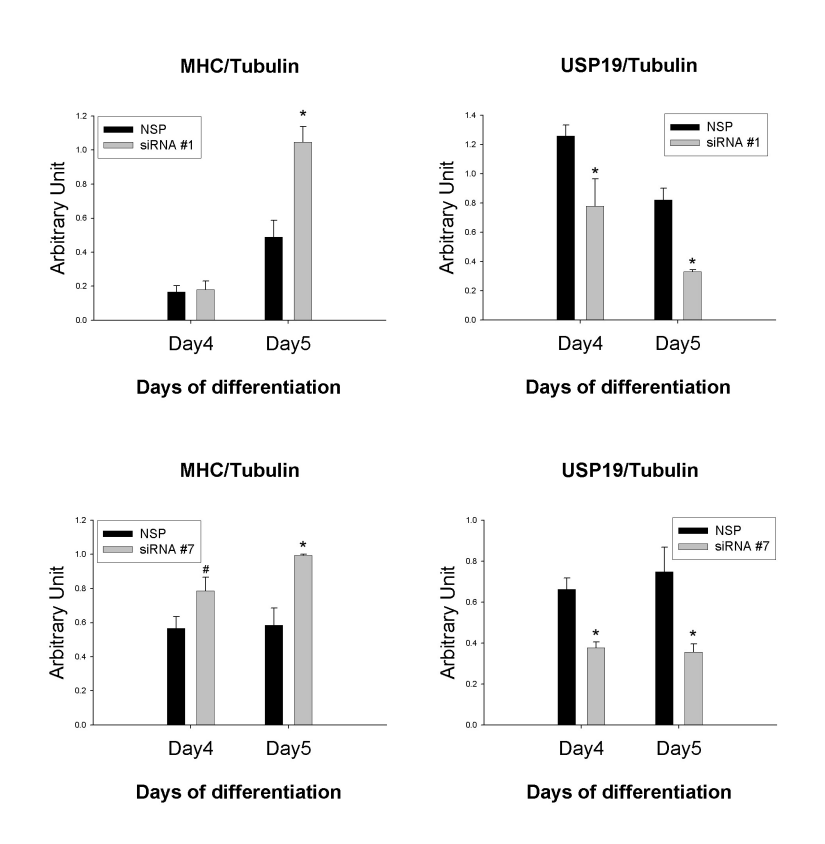


Figure 15

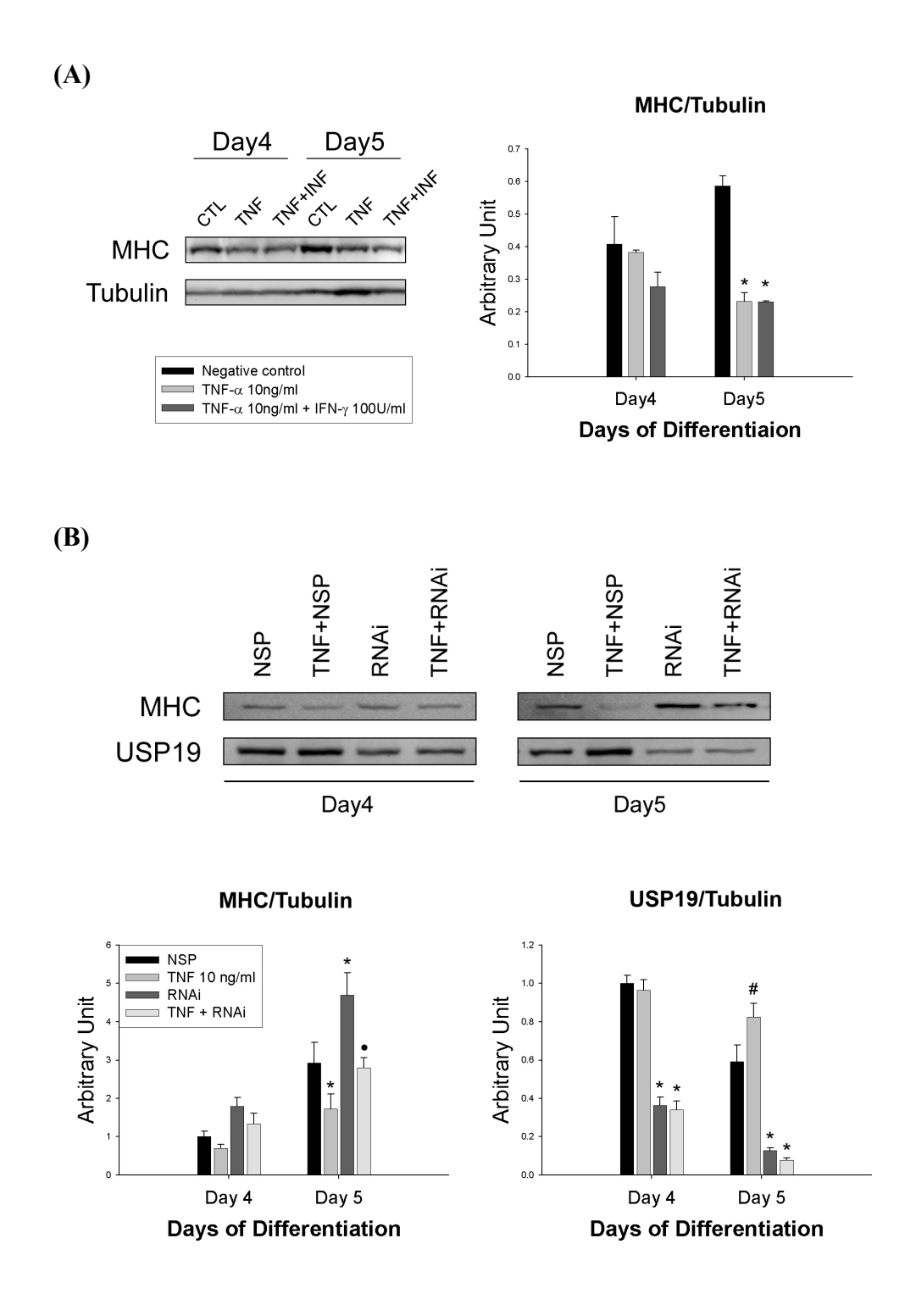


Figure 16

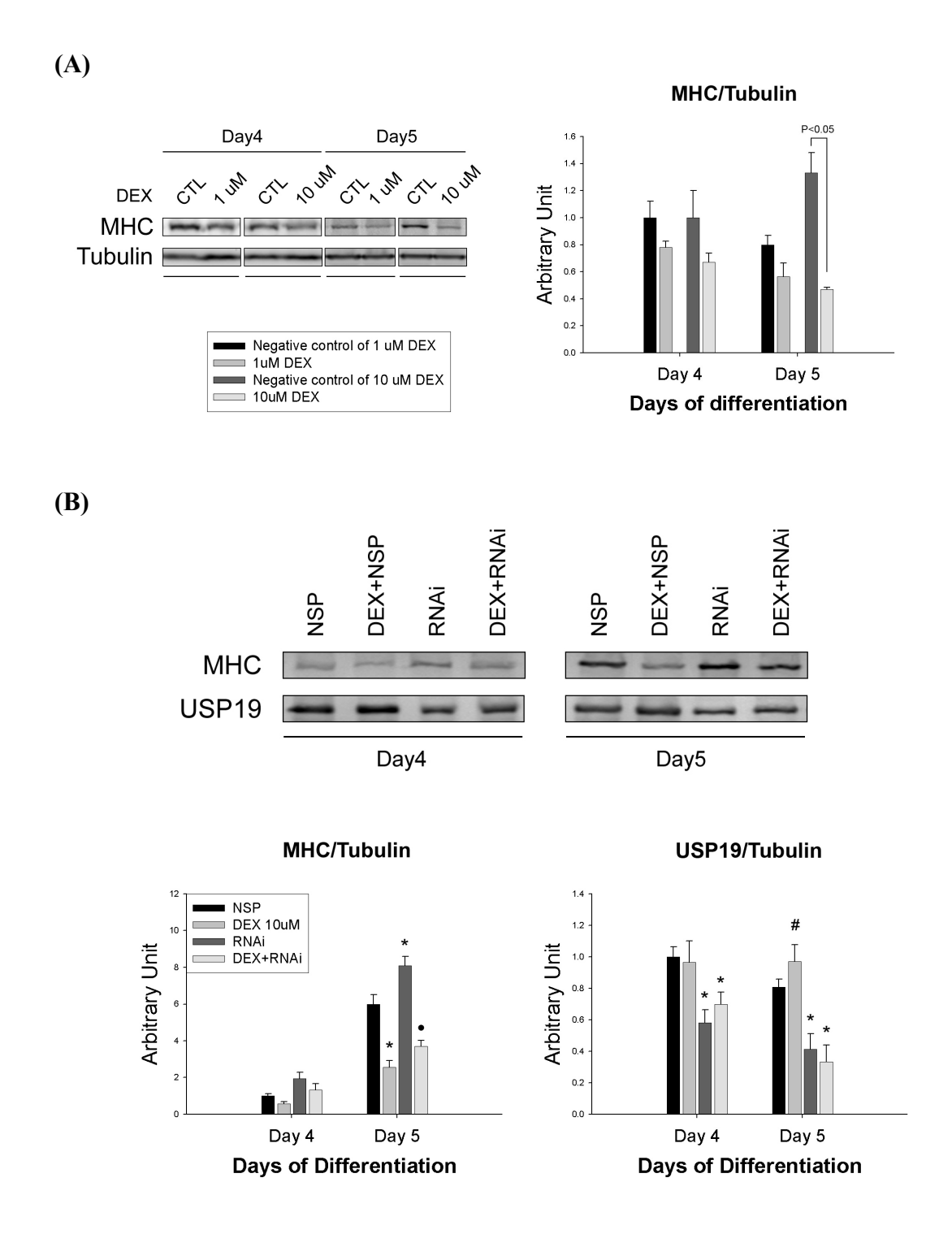


Figure 17

Table 1(A). E2 of S. cerevisiae

E2	MW(kDa)	Cognate E3	Functions	Substrates
Ubc1	24	Unknown	Degradation of selective proteins. Primary function in the early stages of growth after germination of spores. Function overlapping with UBC4/5 in cell growth and viability. Yeast carrying the ubc1/ubc4 double mutation fail to survive after undergoing sporulation and germination. [252, 253]	
		Hrd1p/Der3p (RING)	ER degradation [254]	
		Rsp5 (HECT)	Endocytosis of membrane proteins.	alpha-factor, Maltose permease and inositol permease [255]
Ubc2 (Rad6)	20	UBR1 (RING)	N-end rule proteolysis [256]	
		UBR1	Peptide import	CUP9 (a transcriptional repressor of PTR2, a gene that encodes a transmembrane peptide transporter) [257]
		UBR1	Enrichment of nuclear proteosome	Cut8 (a nuclear envelope protein) [258]
		BRE1 (RING)	Meiosis, modification of gene expression	Histone H2B [259, 260]
		Rad18 (RING)	Postreplication DNA repair	PCNA (monoubiquitination) [261]
Ubc3 (Cdc34)	34	San1 (RING)	Protein quality control	mutant nuclear proteins [262]
		SCFCDC4 (RING)	Transfer from G1 to S phase	Phosphorylated Sic1 (CDK inhibitor) [263, 264]
		SCF Grr1	S phase entry	Phosphorylated G1 cyclin Cln1 [265]
		SCFMet30	Regulation of transcription by proteolysis-independent ubiquitination	Transcriptional regulator Met4 [266, 267]
Ubc4	16		(Ubc4 and Ubc5 are 92% identical)	
& Ubc5		Unknown	Sporulation and stress resistance [252, 253]	
		Unknown	Degradation of short lived and abnormal proteins	Matα2 (a short lived transcriptional repressor) [268-270]
		Rsp5	Endocytosis of membrane proteins.	Ste3 (alpha receptor) [271], Ste6 (alpha factor transporter) [272], Gal2 (Galactose transporter) [273], Zrt1 (Zinc transporter) [274]
		Unknown (E3-Cam)	Mediation of Ca ion signals	Calmodulin [275]
Ubc6 (Doa2)	28		(UBC6 is a C terminal anchored membrane protein, it works in association with soluable UBC7.)	
		Doa10/Ssm4 (RING)	Degradation of MAT alpha 2 through the Deg1 degradation signal	Mat alpha 2 [32]
		Unknown	Regulation of protein translocation in ER.	Mutant Sec61 (a key component of the protein translocation apparatus of the ER membrane) [11, 276]
Ubc7	28		ER degradation, in association with either UBC6 or Cue1 (factor for coupling ubiquitin conjugation for ER degradation) [277]	
		Unknown	Regulation of sterol biosynthesis	HMG2p (an isoform of yeast HMG reductase) [278]
		Hrd1p/Der3p (RING)	ER degradation of malfolded proteins [32, 279]	
Ubc8	25		Unessential for yeast [280]	
		Unknown	Glucose induced proteolysis	Fructose-1,6-bisphosphatase (FBPase), a key gluconeogenetic enzyme [281].
Ubc9 (SUMO E2)	18			
Ubc10 (Pas2)	21	PEX10 (RING) [282]	Peroxisomal matrix protein import [283]	
Ubc11	17	Unknown	Unessential for yeast. Function unknown (high similarity to vertebrate E2-C/UBCx) [284]	
			Enhancement of stress tolerance in yeast when overexpressed [285].	
Ubc12 (NEDD8 E2)	21			
			DNA repair in association with Mms2 (Uev), synthesis of Lysine 63 linked	PCNA (polyubiquitination)

Table 1(B). E2 of mammalian cells

E2	MW(kDa)	Cognate E3	Functions	Substrates
HR6A	17		Homolog of yeast UBC2/Rad6. N-end rule proteolysis. DNA repair, essential for early embryonic development in mice [143].	
HR6B	17		Homolog of yeast UBC2/Rad6. N-end rule proteolysis. DNA repair in male meiosis spermatogenesis [93, 288].	
		Ubr1	Neuronal differentiation [289].	
UbcH2	20		Homolog of yeast UBC8. The UbcH2 gene is located on chromosome 7 and shows a complex expression pattern with at least five different mRNAs. Capable of conjugating ubiquiltin to histones [290].	
UbcH5A	17	E6-AP	homolog of yeast UBC4/5, mouse UBE2D1, function in the E6/E6-AP-induced ubiquitination of p53 [186,188].	
		NEDD4L	Regulate the epithelial sodium channel (ENaC) [291].	pathogenesis of a hereditary form of hypertension
		MuRF1	Muscle Turnover	MyoD, cardiac troponin [148, 151]
		Mdm2	p53 polyubiquitination [292]	
		CHIP	proper folding of proteins [293]	Hsc70
UbcH5B	17	β-ТгСР	Homolog of yeast UBC4, mouse UBE2D2. signal-induced ubiquitination of IkB α [294].	
		SNURF(RNF4)	Transcriptional regulation and growth inhibition [295].	
		CNOT4	Repression of RNA polymerase II transcription [296, 297].	
		Mdm2	p53 ubiquitination and degradation [298].	
UbcH5C	17	APC11/APC2	Homolog of yeast UBC4, mouse UBE2D3. regulation of the onset of sister- chromatid separation and mitotic exit [299].	
		BRCA1- BARD1	DNA repair [300].	
Ubc4-1	17		Rodent homolog of yeast UBC4, expressed ubiquitiously. It can interact with some E3s, such as E6Ap or Rat EDD, to support ubiquitination of Histone H2A in vitro [194]. It is upregulated in muscle wasting [138].	
Ubc4 testis	17		Rodent homolog of yeast UBC4, expressed restrictively in testis. It plays a role in early maturation of the testis [189].	
UbcH6	17	RING105	Homolog of yeast UBC4/5, mouse UBE2E1. Regulate tumor suppressor candidate TSSC5 in mammalian cells [301].	
		RNF20/40	Monoubiquitination of human histone H2B and stimulation of HOX gene expression [302].	
UbcH7	17	NEDD4	ubiquitin-conjugating enzyme E2L3 (UBE2L3), homologue of mouse Ube2l3, play a role in cell growth and differentiation [303].	
		E6-AP [304]	Regulation of P53 in association with E6 of HPV in HPV infected cells.	
		Parkin	suppresses unfolded protein stress-induced cell death and contributes to protection from neurotoxicity induced by unfolded protein stresses [305].	
UbcH8	22	NKLAM	Homolog of mouse UBE2L6, highly similar in primary structure to UbcH7 [306]. UbcH8 interacts with NKLAM in vivo, which is involved in the cytolytic function of NK cells and CTLs [307].	
		Parkin	Control protein CDCrel-Ilevels via ubiquitination, which may be related to the cause of familial autosomal recessive Parkinson's disease [308].	CDCrel-1
UbcH10	20	APC	Homolog of yeast UBC11, mouse UBE2C, influence mitotic progression, developmental regulation and cell cycle control [309]. Mutant UbcH10 inhibits the destruction of both cyclin A and B, arrests cells in M phase, and inhibits the onset of anaphase, presumably by blocking sister chromatid separation [310].	HOXC10, cyclin A and B.
UBE2N	17	TRAF6	Ubiquitin-conjugating enzyme E2N (UBC13 homolog, yeast), regulation of signal transduction in the NF-kappa B pathway [311].	
		CHIP	Degradation of misfolded proteins [312].	
UBE2R1 (E2- CDC34)	35	p45(SKP2)-CUL-1- p19(SKP1)	Homolog of yeast Ubc3, mouse Cdc34.Required to promote S phase of cell cycle [313] and G1-to-S-phase transition [314].	Cdk inhibitors p21WAF, p27KIP, and the activator cyclin D [315-317].
UBE2J1	35		Ubiquitin-conjugating enzyme E2, J1 (UBC6 homolog, yeast) (UBE2J1 homolog, mouse), involved in ER stress [318].	
UBE2G1	19		Ubiquitin-conjugating enzyme E2G 1 (UBC7 homolog, yeast) (UBE2G1 homolog, mouse), Ubiquitin-protein ligase G1. ER degradation [319].	
UBE2H	20		Ubiquitin-conjugating enzyme E2H/ E2-20K (UBC8 homolog, yeast) (UBE2H homolog, mouse) expressed in the rat and the human central nervous system [320], a candidate for involvement in autistic disorder [320].	

Table 2. Proteins identified from mass spectrometry

Band	Score	Mass (Da)	Name	Function	Comments
1	2984	312352	Progestin induced protein [Homo sapiens]/EDD	A ubiquitin-protein ligase	
2			Samples in this band were lost at the mass spectrometry center.		
3	41	101047	Progestin induced protein [Homo sapiens]		Degradation fragment of EDD
	39	134705	KIAA1695 protein [Homo sapiens]		An unknown protein
4	310	193187	Clathrin, heavy polypeptide (Hc)	Endocytosis	
	188	181602	MEK kinase 4 (MEKK4)	Signal transduction, activate p38 and JNK.	
	132	166867	Eukaryotic translation initiation factor 3 subunit 10	Regulation of translation in eukaryotic cells.	
5	526	150914	DEAD/H (Asp-Glu-Ala-Asp/His) box polypeptide 9	ATP-dependent RNA helicase A	
	433	143409	RNA Helicase A		
6	255	141853	Chondroitin sulfate proteoglycan 6 (Bamacan);	Extracelluar protein, a component of basal membrane	
	186	154318	Phosphoinositide-3-kinase, regulatory subunit 4, p150.	An adaptor protein of human Vps34 PI3 kinase, It associates specifically with PI3K and functions in vesicle formation and protein trafficking [321].	
	112	135236	DNA directed RNA polymerase II polypeptide B	RNA polymerase subunit 2, regulation of the rate of transcription initiation [322].	
	81	98924	Epidermal growth factor pathway substrate 15 (EPS15)	A substrate of the EGF receptor tyrosine kinase. It is monubiquitinated by Cbl and mediates endocytosis of EGFR [323].	
7	638	121471	ATP citrate lyase (ACL)	Required for acetyl CoA synthesis, lipid metabolizing enzymes [324].	
	369	116096	Serine/threonine protein kinase 31	A testis specific gene	A predicted kinase protein.
	207	91058	Squamous cell carcinoma antigen recognized by T-cells		A predicted protein.
	128	99436	CBL	A RING finger E3	
	51	104092	ERCC4	An endonuclease that functions in chromosome recombination in meiosis	
8	506	108122	General vesicular transport factor p115 (Transcytosis associated protein) (TAP)	A general fusion factor required for binding of vesicles to acceptor membranes	
	130	100895	CBL	A RING finger E3	
9	1185	99424	Miwi	A testis specific protein	
	188	83474	DEAD/H (Asp-Glu-Ala-Asp/His) box polypeptide 1	RNA helicase	
10	1240	7112	dnaK-type molecular chaperone hsp72-ps1	heat shock protein	
	1035	73494	PL10 protein	A member of the DEAD/H box family, a male germ cell specific RNA helicase 2720782.	
	928	73597	DEAD-Box protien, Helicase-like protein 2(HLP2)	RNA helicase	
	771	73103	Protein disulfide isomerase related protein	Catalyzation of protein folding, a chaperone protein [325].	
11	1233	69785	dnaK-type molecular chaperone hst70	Heat shock protein.	
	1085	70826	Poly A binding protein (PABP)		
	355	68911	Vacuolar H ATPase 70 kDa subunit.	The catalytic nucleotide binding subunit of the V-ATPase complex, an ATP-dependent proton pump involved in receptor-mediated endocytosis, intracellular membrane traffic, protein processing and degradation [326].	
12	234	69785	dnaK-type molecular chaperone hst70	Heat shock protein.	
13	1376	62638	CRMP-2 (TOAD-64/DRP-2)	Neuronal differentiation, expressed primarily in the neural system [327].	
	432	60705	Nuclear factor NF-κB p65 subunit	Transcriptional factor	
14, 16	, 17, 19		No significant results were found in these bands		
15, 18			Many ribosomal proteins		

Proteins that have been screened for substrates of EDD/Rat100 are indicated in bold text.

References

- 1. Coulombe, P., et al., *N-Terminal ubiquitination of extracellular signal-regulated kinase 3 and p21 directs their degradation by the proteasome.* Mol Cell Biol, 2004. **24**(14): p. 6140-50.
- Breitschopf, K., et al., A novel site for ubiquitination: the N-terminal residue, and not internal lysines of MyoD, is essential for conjugation and degradation of the protein.
 Embo J, 1998. 17(20): p. 5964-73.
- 3. Cadwell, K. and L. Coscoy, *Ubiquitination on nonlysine residues by a viral E3 ubiquitin ligase*. Science, 2005. **309**(5731): p. 127-30.
- 4. Jin, J., et al., Dual E1 activation systems for ubiquitin differentially regulate E2 enzyme charging. Nature, 2007. **447**(7148): p. 1135-8.
- 5. Pelzer, C., et al., *UBE1L2*, a novel E1 enzyme specific for ubiquitin. J Biol Chem, 2007. **282**(32): p. 23010-4.
- 6. Ozkan, E., H. Yu, and J. Deisenhofer, *Mechanistic insight into the allosteric activation of a ubiquitin-conjugating enzyme by RING-type ubiquitin ligases*. Proc Natl Acad Sci U S A, 2005. **102**(52): p. 18890-5.
- 7. Szczepanowski, R.H., R. Filipek, and M. Bochtler, *Crystal structure of a fragment of mouse ubiquitin-activating enzyme*. J Biol Chem, 2005. **280**(23): p. 22006-11.
- 8. Haas, A.L., et al., *Ubiquitin-activating enzyme. Mechanism and role in protein-ubiquitin conjugation.* J Biol Chem, 1982. **257**(5): p. 2543-8.
- 9. Haas, A.L. and I.A. Rose, *The mechanism of ubiquitin activating enzyme. A kinetic and equilibrium analysis.* J Biol Chem, 1982. **257**(17): p. 10329-37.

- 10. Raboy, B. and R.G. Kulka, *Role of the C-terminus of Saccharomyces cerevisiae ubiquitin-conjugating enzyme (Rad6) in substrate and ubiquitin-protein-ligase (E3-R) interactions.* Eur J Biochem, 1994. **221**(1): p. 247-51.
- 11. Sommer, T. and S. Jentsch, *A protein translocation defect linked to ubiquitin conjugation at the endoplasmic reticulum*. Nature, 1993. **365**(6442): p. 176-9.
- 12. Huang, D.T., et al., *Basis for a ubiquitin-like protein thioester switch toggling E1-E2 affinity*. Nature, 2007. **445**(7126): p. 394-8.
- 13. VanDemark, A.P. and C.P. Hill, *Two-stepping with E1*. Nat Struct Biol, 2003. **10**(4): p. 244-6.
- 14. VanDemark, A.P. and C.P. Hill, *E1 on the move*. Mol Cell, 2005. **17**(4): p. 474-5.
- 15. Xie, Y. and A. Varshavsky, *The E2-E3 interaction in the N-end rule pathway: the RING-H2 finger of E3 is required for the synthesis of multiubiquitin chain.* Embo J, 1999. **18**(23): p. 6832-44.
- 16. Huibregtse, J.M., et al., *A family of proteins structurally and functionally related to the E6-AP ubiquitin-protein ligase*. Proc Natl Acad Sci U S A, 1995. **92**(11): p. 5249.
- 17. Talis, A.L., J.M. Huibregtse, and P.M. Howley, *The role of E6AP in the regulation of p53 protein levels in human papillomavirus (HPV)-positive and HPV-negative cells.*J Biol Chem, 1998. **273**(11): p. 6439-45.
- 18. Huibregtse, J.M., M. Scheffner, and P.M. Howley, *E6-AP directs the HPV E6-dependent inactivation of p53 and is representative of a family of structurally and functionally related proteins*. Cold Spring Harb Symp Quant Biol, 1994. **59**: p. 237-45.

- 19. Salvat, C., et al., *The -4 phenylalanine is required for substrate ubiquitination catalyzed by HECT ubiquitin ligases*. J Biol Chem, 2004. **279**(18): p. 18935-43.
- 20. Huang, L., et al., *Structure of an E6AP-UbcH7 complex: insights into ubiquitination* by the E2-E3 enzyme cascade. Science, 1999. **286**(5443): p. 1321-6.
- 21. Verdecia, M.A., et al., *Conformational flexibility underlies ubiquitin ligation*mediated by the WWP1 HECT domain E3 ligase. Mol Cell, 2003. **11**(1): p. 249-59.
- 22. Zheng, N., *A closer look of the HECTic ubiquitin ligases*. Structure, 2003. **11**(1): p. 5-6.
- 23. Wang, G., J. Yang, and J.M. Huibregtse, *Functional domains of the Rsp5 ubiquitin- protein ligase*. Mol Cell Biol, 1999. **19**(1): p. 342-52.
- 24. Plant, P.J., et al., *The C2 domain of the ubiquitin protein ligase Nedd4 mediates*Ca2+-dependent plasma membrane localization. J Biol Chem, 1997. **272**(51): p. 32329-36.
- 25. Staub, O., et al., WW domains of Nedd4 bind to the proline-rich PY motifs in the epithelial Na+ channel deleted in Liddle's syndrome. Embo J, 1996. **15**(10): p. 2371-80.
- 26. Bedford, M.T., D.C. Chan, and P. Leder, *FBP WW domains and the Abl SH3 domain bind to a specific class of proline-rich ligands*. Embo J, 1997. **16**(9): p. 2376-83.
- 27. Shearwin-Whyatt, L., et al., *Regulation of functional diversity within the Nedd4* family by accessory and adaptor proteins. Bioessays, 2006. **28**(6): p. 617-28.
- 28. Cooper, B., et al., Requirement of E6AP and the features of human papillomavirus E6 necessary to support degradation of p53. Virology, 2003. **306**(1): p. 87-99.

- 29. Yoshida, M., et al., *Poly(A) binding protein (PABP) homeostasis is mediated by the stability of its inhibitor, Paip2*. Embo J, 2006. **25**(9): p. 1934-44.
- 30. Lim, N.S., et al., Comparative peptide binding studies of the PABC domains from the ubiquitin-protein isopeptide ligase HYD and poly(A)-binding protein. Implications for HYD function. J Biol Chem, 2006. **281**(20): p. 14376-82.
- 31. Joazeiro, C.A. and A.M. Weissman, *RING finger proteins: mediators of ubiquitin ligase activity*. Cell, 2000. **102**(5): p. 549-52.
- 32. Swanson, R., M. Locher, and M. Hochstrasser, *A conserved ubiquitin ligase of the nuclear envelope/endoplasmic reticulum that functions in both ER-associated and Matalpha2 repressor degradation*. Genes Dev, 2001. **15**(20): p. 2660-74.
- 33. Katoh, S., et al., *Active site residues and amino acid specificity of the ubiquitin carrier protein-binding RING-H2 finger domain.* J Biol Chem, 2005. **280**(49): p. 41015-24.
- 34. Joazeiro, C.A., et al., *The tyrosine kinase negative regulator c-Cbl as a RING-type, E2-dependent ubiquitin-protein ligase.* Science, 1999. **286**(5438): p. 309-12.
- 35. Zheng, N., et al., Structure of a c-Cbl-UbcH7 complex: RING domain function in ubiquitin-protein ligases. Cell, 2000. **102**(4): p. 533-9.
- 36. Kamura, T., et al., *Rbx1*, a component of the VHL tumor suppressor complex and *SCF ubiquitin ligase*. Science, 1999. **284**(5414): p. 657-61.
- 37. Skowyra, D., et al., *F-box proteins are receptors that recruit phosphorylated substrates to the SCF ubiquitin-ligase complex.* Cell, 1997. **91**(2): p. 209-19.
- 38. Winston, J.T., et al., *A family of mammalian F-box proteins*. Curr Biol, 1999. **9**(20): p. 1180-2.

- 39. Jackson, P.K., et al., *The lore of the RINGs: substrate recognition and catalysis by ubiquitin ligases*. Trends Cell Biol, 2000. **10**(10): p. 429-39.
- 40. Thrower, J.S., et al., *Recognition of the polyubiquitin proteolytic signal*. Embo J, 2000. **19**(1): p. 94-102.
- 41. Lam, Y.A., et al., *Editing of ubiquitin conjugates by an isopeptidase in the 26S proteasome*. Nature, 1997. **385**(6618): p. 737-40.
- 42. Leggett, D.S., et al., *Multiple associated proteins regulate proteasome structure and function*. Mol Cell, 2002. **10**(3): p. 495-507.
- 43. Finley, D., B. Bartel, and A. Varshavsky, *The tails of ubiquitin precursors are ribosomal proteins whose fusion to ubiquitin facilitates ribosome biogenesis*. Nature, 1989. **338**(6214): p. 394-401.
- 44. Wiborg, O., et al., *The human ubiquitin multigene family: some genes contain multiple directly repeated ubiquitin coding sequences.* Embo J, 1985. **4**(3): p. 755-9.
- 45. Turner, G.C. and A. Varshavsky, *Detecting and measuring cotranslational protein degradation in vivo*. Science, 2000. **289**(5487): p. 2117-20.
- 46. Amerik, A.Y., et al., *The Doa4 deubiquitinating enzyme is functionally linked to the vacuolar protein-sorting and endocytic pathways.* Mol Biol Cell, 2000. **11**(10): p. 3365-80.
- 47. McCullough, J., M.J. Clague, and S. Urbe, *AMSH is an endosome-associated ubiquitin isopeptidase*. J Cell Biol, 2004. **166**(4): p. 487-92.
- 48. Chung, C.H. and S.H. Baek, *Deubiquitinating enzymes: their diversity and emerging roles*. Biochem Biophys Res Commun, 1999. **266**(3): p. 633-40.

- 49. Wilkinson, K.D., Regulation of ubiquitin-dependent processes by deubiquitinating enzymes. Faseb J, 1997. **11**(14): p. 1245-56.
- 50. Baek, S.H., et al., New de-ubiquitinating enzyme, ubiquitin C-terminal hydrolase 8, in chick skeletal muscle. Biochem J, 1997. **325 (Pt 2)**: p. 325-30.
- 51. Baker, R.T., et al., *Identification, functional characterization, and chromosomal* localization of USP15, a novel human ubiquitin-specific protease related to the UNP oncoprotein, and a systematic nomenclature for human ubiquitin-specific proteases.

 Genomics, 1999. **59**(3): p. 264-74.
- 52. Wing, S.S., *Deubiquitinating enzymes--the importance of driving in reverse along the ubiquitin-proteasome pathway.* Int J Biochem Cell Biol, 2003. **35**(5): p. 590-605.
- 53. Hu, M., et al., Crystal structure of a UBP-family deubiquitinating enzyme in isolation and in complex with ubiquitin aldehyde. Cell, 2002. **111**(7): p. 1041-54.
- 54. Holowaty, M.N., et al., *Protein interaction domains of the ubiquitin-specific protease, USP7/HAUSP.* J Biol Chem, 2003. **278**(48): p. 47753-61.
- 55. Larsen, C.N., J.S. Price, and K.D. Wilkinson, Substrate binding and catalysis by ubiquitin C-terminal hydrolases: identification of two active site residues.

 Biochemistry, 1996. **35**(21): p. 6735-44.
- 56. Pickart, C.M. and I.A. Rose, *Ubiquitin carboxyl-terminal hydrolase acts on ubiquitin carboxyl-terminal amides*. J Biol Chem, 1985. **260**(13): p. 7903-10.
- 57. Johnston, S.C., et al., Structural basis for the specificity of ubiquitin C-terminal hydrolases. Embo J, 1999. **18**(14): p. 3877-87.
- 58. Misaghi, S., et al., Structure of the ubiquitin hydrolase UCH-L3 complexed with a suicide substrate. J Biol Chem, 2005. **280**(2): p. 1512-20.

- 59. King, R.C. and P.D. Storto, *The role of the otu gene in Drosophila oogenesis*. Bioessays, 1988. **8**(1): p. 18-24.
- 60. Balakirev, M.Y., et al., *Otubains: a new family of cysteine proteases in the ubiquitin pathway.* EMBO Rep, 2003. **4**(5): p. 517-22.
- 61. Evans, P.C., et al., *A novel type of deubiquitinating enzyme*. J Biol Chem, 2003. **278**(25): p. 23180-6.
- 62. Nanao, M.H., et al., *Crystal structure of human otubain 2*. EMBO Rep, 2004. **5**(8): p. 783-8.
- 63. Tzvetkov, N. and P. Breuer, *Josephin domain-containing proteins from a variety of species are active de-ubiquitination enzymes*. Biol Chem, 2007. **388**(9): p. 973-8.
- 64. Mao, Y., et al., *Deubiquitinating function of ataxin-3: insights from the solution structure of the Josephin domain.* Proc Natl Acad Sci U S A, 2005. **102**(36): p. 12700-5.
- 65. Nicastro, G., et al., *The solution structure of the Josephin domain of ataxin-3:*structural determinants for molecular recognition. Proc Natl Acad Sci U S A, 2005.

 102(30): p. 10493-8.
- 66. Winborn, B.J., et al., *The deubiquitinating enzyme ataxin-3, a polyglutamine disease protein, edits Lys63 linkages in mixed linkage ubiquitin chains.* J Biol Chem, 2008. **283**(39): p. 26436-43.
- 67. Eytan, E., et al., *Ubiquitin C-terminal hydrolase activity associated with the 26 S protease complex.* J Biol Chem, 1993. **268**(7): p. 4668-74.
- 68. Verma, R., et al., Role of Rpn11 metalloprotease in deubiquitination and degradation by the 26S proteasome. Science, 2002. **298**(5593): p. 611-5.

- 69. Yao, T. and R.E. Cohen, *A cryptic protease couples deubiquitination and degradation by the proteasome*. Nature, 2002. **419**(6905): p. 403-7.
- 70. Maytal-Kivity, V., et al., MPN+, a putative catalytic motif found in a subset of MPN domain proteins from eukaryotes and prokaryotes, is critical for Rpn11 function.

 BMC Biochem, 2002. 3: p. 28.
- 71. Yoshida, S., M. Sukeno, and Y. Nabeshima, *A vasculature-associated niche for undifferentiated spermatogonia in the mouse testis.* Science, 2007. **317**(5845): p. 1722-6.
- 72. Shetty, G. and M.L. Meistrich, *The missing niche for spermatogonial stem cells: do blood vessels point the way?* Cell Stem Cell, 2007. **1**(4): p. 361-3.
- 73. Lonnie D. Russell, R.A.E., Amiya P. Sinha Hikim, Eric D. Clegg, *Histological and Histopathological Evaluation of the Testis*. 1990: Cache River Press.
- 74. O'Connor, A.E. and D.M. De Kretser, *Inhibins in normal male physiology*. Semin Reprod Med, 2004. **22**(3): p. 177-85.
- 75. *The Sertoli Cell*, ed. L.D.R.M.D. Griswold. 1993, Clearwater: Cache River Press.
- 76. L.Carlos Junqueira, J.C.R.O.k., *Basic Histology*. 7th ed. 1992, Toronto: Appleton & Lange, A Publising Division of Prentice Hall (Prentice Hall Canada, Inc.).
- 77. Tipler, C.P., et al., *Purification and characterization of 26S proteasomes from human and mouse spermatozoa*. Mol Hum Reprod, 1997. **3**(12): p. 1053-60.
- 78. Wojcik, C., et al., *Proteasomes in human spermatozoa*. Int J Androl, 2000. **23**(3): p. 169-77.
- 79. Kwon, J., The new function of two ubiquitin C-terminal hydrolase isozymes as reciprocal modulators of germ cell apoptosis. Exp Anim, 2007. **56**(2): p. 71-7.

- 80. Sutovsky, P., et al., *Ubiquitin tag for sperm mitochondria*. Nature, 1999. **402**(6760): p. 371-2.
- 81. Thompson, W.E., J. Ramalho-Santos, and P. Sutovsky, *Ubiquitination of prohibitin* in mammalian sperm mitochondria: possible roles in the regulation of mitochondrial inheritance and sperm quality control. Biol Reprod, 2003. **69**(1): p. 254-60.
- 82. Sutovsky, P., et al., Early degradation of paternal mitochondria in domestic pig (Sus scrofa) is prevented by selective proteasomal inhibitors lactacystin and MG132. Biol Reprod, 2003. **68**(5): p. 1793-800.
- 83. Sutovsky, P., et al., *Ubiquitinated sperm mitochondria, selective proteolysis, and the regulation of mitochondrial inheritance in mammalian embryos*. Biol Reprod, 2000.63(2): p. 582-90.
- 84. Sutovsky, P., et al., *Degradation of paternal mitochondria after fertilization:*implications for heteroplasmy, assisted reproductive technologies and mtDNA

 inheritance. Reprod Biomed Online, 2004. 8(1): p. 24-33.
- 85. Sutovsky, P., et al., A putative, ubiquitin-dependent mechanism for the recognition and elimination of defective spermatozoa in the mammalian epididymis. J Cell Sci, 2001. **114**(Pt 9): p. 1665-75.
- 86. Mitchell, M.J., et al., *Homology of a candidate spermatogenic gene from the mouse Y chromosome to the ubiquitin-activating enzyme E1*. Nature, 1991. **354**(6353): p. 483-6.
- 87. Odorisio, T., et al., Transcriptional analysis of the candidate spermatogenesis gene

 Ubely and of the closely related Ubelx shows that they are coexpressed in

- spermatogonia and spermatids but are repressed in pachytene spermatocytes. Dev Biol, 1996. **180**(1): p. 336-43.
- 88. Kay, G.F., et al., A candidate spermatogenesis gene on the mouse Y chromosome is homologous to ubiquitin-activating enzyme E1. Nature, 1991. **354**(6353): p. 486-9.
- 89. Mitchell, M.J., et al., *The origin and loss of the ubiquitin activating enzyme gene on the mammalian Y chromosome*. Hum Mol Genet, 1998. **7**(3): p. 429-34.
- 90. Zhu, H., et al., *Identification and characteristics of a novel E1 like gene nUBE1L in human testis*. Acta Biochim Biophys Sin (Shanghai), 2004. **36**(3): p. 227-34.
- 91. Lawrence, C., *The RAD6 DNA repair pathway in Saccharomyces cerevisiae: what does it do, and how does it do it?* Bioessays, 1994. **16**(4): p. 253-8.
- 92. Koken, M.H., et al., Expression of the ubiquitin-conjugating DNA repair enzymes HHR6A and B suggests a role in spermatogenesis and chromatin modification. Dev Biol, 1996. **173**(1): p. 119-32.
- 93. Roest, H.P., et al., *Inactivation of the HR6B ubiquitin-conjugating DNA repair* enzyme in mice causes male sterility associated with chromatin modification. Cell, 1996. **86**(5): p. 799-810.
- 94. Koken, M.H., et al., Structural and functional conservation of two human homologs of the yeast DNA repair gene RAD6. Proc Natl Acad Sci U S A, 1991. **88**(20): p. 8865-9.
- 95. Baarends, W.M., et al., *Histone ubiquitination and chromatin remodeling in mouse spermatogenesis*. Dev Biol, 1999. **207**(2): p. 322-33.
- 96. Cenci, G., et al., *UbcD1*, a Drosophila ubiquitin-conjugating enzyme required for proper telomere behavior. Genes Dev, 1997. **11**(7): p. 863-75.

- 97. Rajapurohitam, V., et al., *Activation of a UBC4-dependent pathway of ubiquitin* conjugation during postnatal development of the rat testis. Dev Biol, 1999. **212**(1): p. 217-28.
- 98. Wing, S.S. and P. Jain, *Molecular cloning, expression and characterization of a ubiquitin conjugation enzyme (E2(17)kB) highly expressed in rat testis.* Biochem J, 1995. **305 (Pt 1)**: p. 125-32.
- 99. Wing, S.S., et al., A novel rat homolog of the Saccharomyces cerevisiae ubiquitinconjugating enzymes UBC4 and UBC5 with distinct biochemical features is induced during spermatogenesis. Mol Cell Biol, 1996. **16**(8): p. 4064-72.
- 100. Della, N.G., P.V. Senior, and D.D. Bowtell, *Isolation and characterisation of murine homologues of the Drosophila seven in absentia gene (sina)*. Development, 1993. **117**(4): p. 1333-43.
- 101. Carthew, R.W. and G.M. Rubin, seven in absentia, a gene required for specification of R7 cell fate in the Drosophila eye. Cell, 1990. **63**(3): p. 561-77.
- 102. Hu, G., et al., Characterization of human homologs of the Drosophila seven in absentia (sina) gene. Genomics, 1997. **46**(1): p. 103-11.
- Holloway, A.J., et al., Chromosomal mapping of five highly conserved murine homologues of the Drosophila RING finger gene seven-in-absentia. Genomics, 1997.
 41(2): p. 160-8.
- 104. Germani, A., et al., SIAH-1 interacts with alpha-tubulin and degrades the kinesin Kid by the proteasome pathway during mitosis. Oncogene, 2000. **19**(52): p. 5997-6006.

- 105. Hu, G., et al., Mammalian homologs of seven in absentia regulate DCC via the ubiquitin-proteasome pathway. Genes Dev, 1997. **11**(20): p. 2701-14.
- 106. Sourisseau, T., et al., *Alteration of the stability of Bag-1 protein in the control of olfactory neuronal apoptosis.* J Cell Sci, 2001. **114**(Pt 7): p. 1409-16.
- 107. Dickins, R.A., et al., *The ubiquitin ligase component Siah1a is required for completion of meiosis I in male mice*. Mol Cell Biol, 2002. **22**(7): p. 2294-303.
- 108. Liu, Z., R. Oughtred, and S.S. Wing, *Characterization of E3Histone, a novel testis ubiquitin protein ligase which ubiquitinates histones.* Mol Cell Biol, 2005. **25**(7): p. 2819-31.
- 109. Garcia-Gonzalo, F.R. and J.L. Rosa, *The HERC proteins: functional and evolutionary insights*. Cell Mol Life Sci, 2005. **62**(16): p. 1826-38.
- 110. Lehman, A.L., et al., A very large protein with diverse functional motifs is deficient in rjs (runty, jerky, sterile) mice. Proc Natl Acad Sci U S A, 1998. 95(16): p. 9436-41.
- 111. Ji, Y., et al., The ancestral gene for transcribed, low-copy repeats in the Prader-Willi/Angelman region encodes a large protein implicated in protein trafficking, which is deficient in mice with neuromuscular and spermiogenic abnormalities. Hum Mol Genet, 1999. **8**(3): p. 533-42.
- 112. Callaghan, M.J., et al., *Identification of a human HECT family protein with homology to the Drosophila tumor suppressor gene hyperplastic discs.* Oncogene, 1998. **17**(26): p. 3479-91.

- 113. Mansfield, E., et al., Genetic and molecular analysis of hyperplastic discs, a gene whose product is required for regulation of cell proliferation in Drosophila melanogaster imaginal discs and germ cells. Dev Biol, 1994. **165**(2): p. 507-26.
- 114. Henderson, M.J., et al., *EDD*, the human hyperplastic discs protein, has a role in progesterone receptor coactivation and potential involvement in DNA damage response. J Biol Chem, 2002. **277**(29): p. 26468-78.
- 115. Saunders, D.N., et al., *Edd, the murine hyperplastic disc gene, is essential for yolk sac vascularization and chorioallantoic fusion.* Mol Cell Biol, 2004. **24**(16): p. 7225-34.
- 116. Oughtred, R., et al., Characterization of rat100, a 300-kilodalton ubiquitinprotein ligase induced in germ cells of the rat testis and similar to the Drosophila hyperplastic discs gene. Endocrinology, 2002. **143**(10): p. 3740-7.
- 117. Wright, A., et al., Regulation of early wave of germ cell apoptosis and spermatogenesis by deubiquitinating enzyme CYLD. Dev Cell, 2007. **13**(5): p. 705-16.
- 118. Kim, Y.K., et al., *The expression of Usp42 during embryogenesis and spermatogenesis in mouse.* Gene Expr Patterns, 2007. **7**(1-2): p. 143-8.
- 119. Gousseva, N. and R.T. Baker, Gene structure, alternate splicing, tissue distribution, cellular localization, and developmental expression pattern of mouse deubiquitinating enzyme isoforms Usp2-45 and Usp2-69. Gene Expr, 2003. 11(3-4): p. 163-79.

- 120. Berruti, G. and E. Martegani, *mUBPy and MSJ-1, a deubiquitinating enzyme and a molecular chaperone specifically expressed in testis, associate with the acrosome and centrosome in mouse germ cells.* Ann N Y Acad Sci, 2002. **973**: p. 5-7.
- 121. Kwon, J., et al., Developmental regulation of ubiquitin C-terminal hydrolase isozyme expression during spermatogenesis in mice. Biol Reprod, 2004. **71**(2): p. 515-21.
- 122. Kwon, J., et al., Two closely related ubiquitin C-terminal hydrolase isozymes function as reciprocal modulators of germ cell apoptosis in cryptorchid testis. Am J Pathol, 2004. **165**(4): p. 1367-74.
- 123. Wang, Y.L., et al., *Overexpression of ubiquitin carboxyl-terminal hydrolase L1* arrests spermatogenesis in transgenic mice. Mol Reprod Dev, 2006. **73**(1): p. 40-9.
- 124. Kwon, J., et al., Ubiquitin C-terminal hydrolase L-1 is essential for the early apoptotic wave of germinal cells and for sperm quality control during spermatogenesis. Biol Reprod, 2005. **73**(1): p. 29-35.
- 125. L.Hiatt, L.P.G.J., *Color Textbook of Histology*. 1997, West Philadelphia: W. B. Saunders Company, *A Division of Harcourt Brace & Company*.
- 126. Tawa, N.E., Jr., R. Odessey, and A.L. Goldberg, *Inhibitors of the proteasome* reduce the accelerated proteolysis in atrophying rat skeletal muscles. J Clin Invest, 1997. **100**(1): p. 197-203.
- 127. Solomon, V., et al., Rates of ubiquitin conjugation increase when muscles atrophy, largely through activation of the N-end rule pathway. Proc Natl Acad Sci U S A, 1998. **95**(21): p. 12602-7.

- 128. Solomon, V., S.H. Lecker, and A.L. Goldberg, *The N-end rule pathway catalyzes a major fraction of the protein degradation in skeletal muscle*. J Biol Chem, 1998. **273**(39): p. 25216-22.
- 129. Bossola, M., et al., *Increased muscle ubiquitin mRNA levels in gastric cancer patients*. Am J Physiol Regul Integr Comp Physiol, 2001. **280**(5): p. R1518-23.
- 130. Tiao, G., et al., Sepsis stimulates nonlysosomal, energy-dependent proteolysis and increases ubiquitin mRNA levels in rat skeletal muscle. J Clin Invest, 1994. **94**(6): p. 2255-64.
- 131. Mansoor, O., et al., Increased mRNA levels for components of the lysosomal,

 Ca2+-activated, and ATP-ubiquitin-dependent proteolytic pathways in skeletal

 muscle from head trauma patients. Proc Natl Acad Sci U S A, 1996. 93(7): p. 2714
 8.
- 132. Price, S.R., *Increased transcription of ubiquitin-proteasome system components:*molecular responses associated with muscle atrophy. Int J Biochem Cell Biol, 2003.

 35(5): p. 617-28.
- 133. Medina, R., et al., Activation of the ubiquitin-ATP-dependent proteolytic system in skeletal muscle during fasting and denervation atrophy. Biomed Biochim Acta, 1991. **50**(4-6): p. 347-56.
- 134. Wing, S.S. and D. Banville, *14-kDa ubiquitin-conjugating enzyme: structure of the rat gene and regulation upon fasting and by insulin*. Am J Physiol, 1994. **267**(1 Pt 1): p. E39-48.

- 135. Wing, S.S., A.L. Haas, and A.L. Goldberg, *Increase in ubiquitin-protein conjugates concomitant with the increase in proteolysis in rat skeletal muscle during starvation and atrophy denervation*. Biochem J, 1995. **307 (Pt 3)**: p. 639-45.
- 136. Handley, P.M., et al., *Molecular cloning, sequence, and tissue distribution of the human ubiquitin-activating enzyme E1*. Proc Natl Acad Sci U S A, 1991. **88**(1): p. 258-62.
- 137. Lecker, S.H., et al., *Ubiquitin conjugation by the N-end rule pathway and mRNAs for its components increase in muscles of diabetic rats.* J Clin Invest, 1999. **104**(10): p. 1411-20.
- 138. Chrysis, D. and L.E. Underwood, *Regulation of components of the ubiquitin* system by insulin-like growth factor I and growth hormone in skeletal muscle of rats made catabolic with dexamethasone. Endocrinology, 1999. **140**(12): p. 5635-41.
- 139. Fang, C.H., et al., Burn injuries in rats upregulate the gene expression of the ubiquitin-conjugating enzyme E2(14k) in skeletal muscle. J Burn Care Rehabil, 2000. **21**(6): p. 528-34.
- 140. Hobler, S.C., et al., Sepsis is associated with increased ubiquitinconjugating enzyme E214k mRNA in skeletal muscle. Am J Physiol, 1999. **276**(2 Pt 2): p. R468-73.
- 141. Temparis, S., et al., *Increased ATP-ubiquitin-dependent proteolysis in skeletal muscles of tumor-bearing rats.* Cancer Res, 1994. **54**(21): p. 5568-73.
- 142. Adegoke, O.A., et al., *Ubiquitin-conjugating enzyme E214k/HR6B is dispensable* for increased protein catabolism in muscle of fasted mice. Am J Physiol Endocrinol Metab, 2002. **283**(3): p. E482-9.

- 143. Roest, H.P., et al., *The ubiquitin-conjugating DNA repair enzyme HR6A is a maternal factor essential for early embryonic development in mice*. Mol Cell Biol, 2004. **24**(12): p. 5485-95.
- 144. Fischer, D., et al., *The gene expression of ubiquitin ligase E3alpha is upregulated* in skeletal muscle during sepsis in rats-potential role of glucocorticoids. Biochem Biophys Res Commun, 2000. **267**(2): p. 504-8.
- 145. Bartel, B., I. Wunning, and A. Varshavsky, *The recognition component of the N-end rule pathway*. Embo J, 1990. **9**(10): p. 3179-89.
- 146. Kwon, Y.T., et al., Construction and analysis of mouse strains lacking the ubiquitin ligase UBR1 (E3alpha) of the N-end rule pathway. Mol Cell Biol, 2001. **21**(23): p. 8007-21.
- 147. Gomes, M.D., et al., *Atrogin-1, a muscle-specific F-box protein highly expressed during muscle atrophy.* Proc Natl Acad Sci U S A, 2001. **98**(25): p. 14440-5.
- 148. Bodine, S.C., et al., *Identification of ubiquitin ligases required for skeletal muscle atrophy*. Science, 2001. **294**(5547): p. 1704-8.
- 149. Dehoux, M.J., et al., *Induction of MafBx and Murf ubiquitin ligase mRNAs in rat skeletal muscle after LPS injection.* FEBS Lett, 2003. **544**(1-3): p. 214-7.
- 150. Borden, K.L. and P.S. Freemont, *The RING finger domain: a recent example of a sequence-structure family.* Curr Opin Struct Biol, 1996. **6**(3): p. 395-401.
- 151. Kedar, V., et al., Muscle-specific RING finger 1 is a bona fide ubiquitin ligase that degrades cardiac troponin I. Proc Natl Acad Sci U S A, 2004. **101**(52): p. 18135-40.

- 152. McElhinny, A.S., et al., Muscle-specific RING finger-1 interacts with titin to regulate sarcomeric M-line and thick filament structure and may have nuclear functions via its interaction with glucocorticoid modulatory element binding protein-1. J Cell Biol, 2002. **157**(1): p. 125-36.
- 153. Tintignac, L.A., et al., *Degradation of MyoD mediated by the SCF (MAFbx) ubiquitin ligase.* J Biol Chem, 2005. **280**(4): p. 2847-56.
- 154. Li, H.H., et al., *Atrogin-1/muscle atrophy F-box inhibits calcineurin-dependent cardiac hypertrophy by participating in an SCF ubiquitin ligase complex.* J Clin Invest, 2004. **114**(8): p. 1058-71.
- 155. Lagirand-Cantaloube, J., et al., *Inhibition of atrogin-1/MAFbx mediated MyoD*proteolysis prevents skeletal muscle atrophy in vivo. PLoS One, 2009. **4**(3): p. e4973.
- 156. Rajapurohitam, V., N. Bedard, and S.S. Wing, Control of ubiquitination of proteins in rat tissues by ubiquitin conjugating enzymes and isopeptidases. Am J Physiol Endocrinol Metab, 2002. 282(4): p. E739-45.
- 157. Lecker, S.H., et al., *Multiple types of skeletal muscle atrophy involve a common program of changes in gene expression*. Faseb J, 2004. **18**(1): p. 39-51.
- 158. Combaret, L., et al., *USP19 is a ubiquitin-specific protease regulated in rat skeletal muscle during catabolic states*. Am J Physiol Endocrinol Metab, 2005. **288**(4): p. E693-700.
- 159. Bassaglia, Y., et al., *Proteasomes are tightly associated to myofibrils in mature skeletal muscle*. Exp Cell Res, 2005. **302**(2): p. 221-32.

- 160. Combaret, L., et al., Glucocorticoids regulate mRNA levels for subunits of the 19 S regulatory complex of the 26 S proteasome in fast-twitch skeletal muscles.

 Biochem J, 2004. **378**(Pt 1): p. 239-46.
- 161. Combaret, L., et al., *Torbafylline (HWA 448) inhibits enhanced skeletal muscle ubiquitin-proteasome-dependent proteolysis in cancer and septic rats.* Biochem J, 2002. **361**(Pt 2): p. 185-92.
- 162. Hobler, S.C., et al., Sepsis-induced increase in muscle proteolysis is blocked by specific proteasome inhibitors. Am J Physiol, 1998. **274**(1 Pt 2): p. R30-7.
- 163. Attaix, D., et al., *The ubiquitin-proteasome system and skeletal muscle wasting*. Essays Biochem, 2005. **41**: p. 173-86.
- 164. Price, S.R., et al., Muscle wasting in insulinopenic rats results from activation of the ATP-dependent, ubiquitin-proteasome proteolytic pathway by a mechanism including gene transcription. J Clin Invest, 1996. **98**(8): p. 1703-8.
- 165. Combaret, L., et al., Manipulation of the ubiquitin-proteasome pathway in cachexia: pentoxifylline suppresses the activation of 20S and 26S proteasomes in muscles from tumor-bearing rats. Mol Biol Rep, 1999. **26**(1-2): p. 95-101.
- 166. Llovera, M., et al., *Anti-TNF treatment reverts increased muscle ubiquitin gene expression in tumour-bearing rats*. Biochem Biophys Res Commun, 1996. **221**(3): p. 653-5.
- 167. Du, J., et al., Glucocorticoids induce proteasome C3 subunit expression in L6 muscle cells by opposing the suppression of its transcription by NF-kappa B. J Biol Chem, 2000. **275**(26): p. 19661-6.

- 168. McFarlane, C., et al., Myostatin induces cachexia by activating the ubiquitin proteolytic system through an NF-kappaB-independent, FoxO1-dependent mechanism. J Cell Physiol, 2006. **209**(2): p. 501-14.
- 169. Auclair, D., et al., *Activation of the ubiquitin pathway in rat skeletal muscle by catabolic doses of glucocorticoids*. Am J Physiol, 1997. **272**(3 Pt 1): p. C1007-16.
- 170. Dardevet, D., et al., Sensitivity and protein turnover response to glucocorticoids are different in skeletal muscle from adult and old rats. Lack of regulation of the ubiquitin-proteasome proteolytic pathway in aging. J Clin Invest, 1995. **96**(5): p. 2113-9.
- 171. Wing, S.S. and A.L. Goldberg, *Glucocorticoids activate the ATP-ubiquitin-dependent proteolytic system in skeletal muscle during fasting*. Am J Physiol, 1993. **264**(4 Pt 1): p. E668-76.
- 172. Hall-Angeras, M., et al., *Effect of the glucocorticoid receptor antagonist RU*38486 on muscle protein breakdown in sepsis. Surgery, 1991. **109**(4): p. 468-73.
- 173. May, R.C., R.A. Kelly, and W.E. Mitch, *Metabolic acidosis stimulates protein degradation in rat muscle by a glucocorticoid-dependent mechanism.* J Clin Invest, 1986. 77(2): p. 614-21.
- 174. Marinovic, A.C., et al., *Ubiquitin (UbC) expression in muscle cells is increased* by glucocorticoids through a mechanism involving Sp1 and MEK1. J Biol Chem, 2002. **277**(19): p. 16673-81.
- 175. Lecker, S.H., *Ubiquitin-protein ligases in muscle wasting: multiple parallel pathways?* Curr Opin Clin Nutr Metab Care, 2003. **6**(3): p. 271-5.

- 176. Jagoe, R.T. and A.L. Goldberg, *What do we really know about the ubiquitin- proteasome pathway in muscle atrophy?* Curr Opin Clin Nutr Metab Care, 2001. **4**(3): p. 183-90.
- 177. Cai, D., et al., *IKKbeta/NF-kappaB activation causes severe muscle wasting in mice*. Cell, 2004. **119**(2): p. 285-98.
- 178. Li, Y.P., et al., *TNF-alpha increases ubiquitin-conjugating activity in skeletal muscle by up-regulating UbcH2/E220k.* Faseb J, 2003. **17**(9): p. 1048-57.
- 179. Llovera, M., et al., *Ubiquitin gene expression is increased in skeletal muscle of tumour-bearing rats.* FEBS Lett, 1994. **338**(3): p. 311-8.
- 180. Garcia-Martinez, C., et al., *Tumour necrosis factor-alpha increases the ubiquitinization of rat skeletal muscle proteins.* FEBS Lett, 1993. **323**(3): p. 211-4.
- 181. Lorite, M.J., et al., Activation of ATP-ubiquitin-dependent proteolysis in skeletal muscle in vivo and murine myoblasts in vitro by a proteolysis-inducing factor (PIF). Br J Cancer, 2001. **85**(2): p. 297-302.
- 182. Lorite, M.J., P. Cariuk, and M.J. Tisdale, *Induction of muscle protein degradation* by a tumour factor. Br J Cancer, 1997. **76**(8): p. 1035-40.
- 183. McPherron, A.C. and S.J. Lee, *Double muscling in cattle due to mutations in the myostatin gene*. Proc Natl Acad Sci U S A, 1997. **94**(23): p. 12457-61.
- 184. McPherron, A.C., A.M. Lawler, and S.J. Lee, *Regulation of skeletal muscle mass in mice by a new TGF-beta superfamily member*. Nature, 1997. **387**(6628): p. 83-90.
- 185. Rolfe, M., et al., Reconstitution of p53-ubiquitinylation reactions from purified components: the role of human ubiquitin-conjugating enzyme UBC4 and E6-associated protein (E6AP). Proc Natl Acad Sci U S A, 1995. **92**(8): p. 3264-8.

- 186. Scheffner, M., J.M. Huibregtse, and P.M. Howley, *Identification of a human* ubiquitin-conjugating enzyme that mediates the E6-AP-dependent ubiquitination of p53. Proc Natl Acad Sci U S A, 1994. **91**(19): p. 8797-801.
- 187. Jensen, J.P., et al., *Identification of a family of closely related human ubiquitin conjugating enzymes*. J Biol Chem, 1995. **270**(51): p. 30408-14.
- 188. Nuber, U., et al., Cloning of human ubiquitin-conjugating enzymes UbcH6 and UbcH7 (E2-F1) and characterization of their interaction with E6-AP and RSP5. J Biol Chem, 1996. **271**(5): p. 2795-800.
- 189. Bedard, N., et al., *Mice lacking the UBC4-testis gene have a delay in postnatal testis development but normal spermatogenesis and fertility.* Mol Cell Biol, 2005. **25**(15): p. 6346-54.
- 190. Mendis-Handagama, S.M., J.B. Kerr, and D.M. de Kretser, *Experimental cryptorchidism in the adult mouse: I. Qualitative and quantitative light microscopic morphology.* J Androl, 1990. **11**(6): p. 539-47.
- 191. Shikone, T., H. Billig, and A.J. Hsueh, *Experimentally induced cryptorchidism increases apoptosis in rat testis*. Biol Reprod, 1994. **51**(5): p. 865-72.
- 192. Huibregtse, J.M., et al., *A family of proteins structurally and functionally related* to the E6-AP ubiquitin-protein ligase. Proc Natl Acad Sci U S A, 1995. **92**(7): p. 2563-7.
- 193. Muller, D., et al., Molecular characterization of a novel rat protein structurally related to poly(A) binding proteins and the 70K protein of the U1 small nuclear ribonucleoprotein particle (snRNP). Nucleic Acids Res, 1992. **20**(7): p. 1471-5.

- 194. Oughtred, R., et al., *Identification of amino acid residues in a class I ubiquitin- conjugating enzyme involved in determining specificity of conjugation of ubiquitin to proteins.* J Biol Chem, 1998. **273**(29): p. 18435-42.
- 195. Martin, P., A. Martin, and A. Shearn, *Studies of l(3)c43hs1 a polyphasic,*temperature-sensitive mutant of Drosophila melanogaster with a variety of imaginal disc defects. Dev Biol, 1977. **55**(2): p. 213-32.
- 196. Lee, J.D., et al., *The ubiquitin ligase Hyperplastic discs negatively regulates* hedgehog and decapentaplegic expression by independent mechanisms.

 Development, 2002. **129**(24): p. 5697-706.
- 197. Fuja, T.J., et al., Somatic mutations and altered expression of the candidate tumor suppressors CSNK1 epsilon, DLG1, and EDD/hHYD in mammary ductal carcinoma. Cancer Res, 2004. **64**(3): p. 942-51.
- 198. Clancy, J.L., et al., *EDD*, the human orthologue of the hyperplastic discs tumour suppressor gene, is amplified and overexpressed in cancer. Oncogene, 2003. **22**(32): p. 5070-81.
- 199. Ohshima, R., et al., *Putative tumor suppressor EDD interacts with and up*regulates APC. Genes Cells, 2007. **12**(12): p. 1339-45.
- 200. Henderson, M.J., et al., *EDD mediates DNA damage-induced activation of CHK2*. J Biol Chem, 2006. **281**(52): p. 39990-40000.
- 201. Munoz, M.A., et al., *The E3 ubiquitin ligase EDD regulates S-phase and G(2)/M DNA damage checkpoints.* Cell Cycle, 2007. **6**(24): p. 3070-7.

- 202. Gupta, N., et al., *Cloning and identification of EDD gene from ultraviolet- irradiated HaCaT cells.* Photodermatol Photoimmunol Photomed, 2006. **22**(6): p. 278-84.
- 203. Honda, Y., et al., Cooperation of HECT-domain ubiquitin ligase hHYD and DNA topoisomerase II-binding protein for DNA damage response. J Biol Chem, 2002.
 277(5): p. 3599-605.
- 204. Maddika, S. and J. Chen, *Protein kinase DYRK2 is a scaffold that facilitates assembly of an E3 ligase*. Nat Cell Biol, 2009. **11**(4): p. 409-19.
- 205. Makiniemi, M., et al., *BRCT domain-containing protein TopBP1 functions in DNA replication and damage response.* J Biol Chem, 2001. **276**(32): p. 30399-406.
- 206. Kozlov, G., et al., *Structural basis of ubiquitin recognition by the ubiquitin-associated (UBA) domain of the ubiquitin ligase EDD*. J Biol Chem, 2007. **282**(49): p. 35787-95.
- 207. Kessler, S.H. and A.B. Sachs, *RNA recognition motif 2 of yeast Pab1p is required* for its functional interaction with eukaryotic translation initiation factor 4G. Mol Cell Biol, 1998. **18**(1): p. 51-7.
- 208. Deo, R.C., et al., *Recognition of polyadenylate RNA by the poly(A)-binding protein.* Cell, 1999. **98**(6): p. 835-45.
- 209. Mangus, D.A., M.C. Evans, and A. Jacobson, *Poly(A)-binding proteins:*multifunctional scaffolds for the post-transcriptional control of gene expression.

 Genome Biol, 2003. **4**(7): p. 223.
- 210. Tasaki, T., et al., A family of mammalian E3 ubiquitin ligases that contain the UBR box motif and recognize N-degrons. Mol Cell Biol, 2005. **25**(16): p. 7120-36.

- 211. Khaleghpour, K., et al., *Translational repression by a novel partner of human poly(A) binding protein, Paip2*. Mol Cell, 2001. **7**(1): p. 205-16.
- 212. Johnston, N.L. and R.E. Cohen, *Uncoupling ubiquitin-protein conjugation from ubiquitin-dependent proteolysis by use of beta, gamma-nonhydrolyzable ATP analogues.* Biochemistry, 1991. **30**(30): p. 7514-22.
- 213. Hershko, A. and I.A. Rose, *Ubiquitin-aldehyde: a general inhibitor of ubiquitin-recycling processes*. Proc Natl Acad Sci U S A, 1987. **84**(7): p. 1829-33.
- Wilkinson, K.D., et al., Synthesis and characterization of ubiquitin ethyl ester, a new substrate for ubiquitin carboxyl-terminal hydrolase. Biochemistry, 1986.
 25(21): p. 6644-9.
- 215. Elbashir, S.M., et al., *Analysis of gene function in somatic mammalian cells using small interfering RNAs.* Methods, 2002. **26**(2): p. 199-213.
- 216. Fukata, Y., et al., *CRMP-2 binds to tubulin heterodimers to promote microtubule assembly.* Nat Cell Biol, 2002. **4**(8): p. 583-91.
- 217. Craig, A.W., et al., *Interaction of polyadenylate-binding protein with the eIF4G homologue PAIP enhances translation*. Nature, 1998. **392**(6675): p. 520-3.
- 218. Deo, R.C., N. Sonenberg, and S.K. Burley, *X-ray structure of the human hyperplastic discs protein: an ortholog of the C-terminal domain of poly(A)-binding protein.* Proc Natl Acad Sci U S A, 2001. **98**(8): p. 4414-9.
- 219. Arimura, N., et al., *Role of CRMP-2 in neuronal polarity*. J Neurobiol, 2004. **58**(1): p. 34-47.

- 220. Gu, Y., N. Hamajima, and Y. Ihara, Neurofibrillary tangle-associated collapsin response mediator protein-2 (CRMP-2) is highly phosphorylated on Thr-509, Ser-518, and Ser-522. Biochemistry, 2000. **39**(15): p. 4267-75.
- 221. Gu, Y. and Y. Ihara, Evidence that collapsin response mediator protein-2 is involved in the dynamics of microtubules. J Biol Chem, 2000. **275**(24): p. 17917-20.
- 222. Ayad, N.G., et al., *Identification of ubiquitin ligase substrates by in vitro* expression cloning. Methods Enzymol, 2005. **399**: p. 404-14.
- 223. Gocke, C.B. and H. Yu, *Identification of SUMO targets through in vitro* expression cloning. Methods Mol Biol, 2009. **497**: p. 51-61.
- 224. Mok, J., H. Im, and M. Snyder, *Global identification of protein kinase substrates* by protein microarray analysis. Nat Protoc, 2009. **4**(12): p. 1820-7.
- 225. MacBeath, G., *Protein microarrays and proteomics*. Nat Genet, 2002. **32 Suppl**: p. 526-32.
- 226. Baracos, V.E., et al., *Activation of the ATP-ubiquitin-proteasome pathway in skeletal muscle of cachectic rats bearing a hepatoma*. Am J Physiol, 1995. **268**(5 Pt 1): p. E996-1006.
- 227. Tisdale, M.J., *Cachexia in cancer patients*. Nat Rev Cancer, 2002. **2**(11): p. 862-71.
- 228. Argiles, J.M. and F.J. Lopez-Soriano, *The role of cytokines in cancer cachexia*. Med Res Rev, 1999. **19**(3): p. 223-48.
- Mahony, S.M. and M.J. Tisdale, *Induction of weight loss and metabolic alterations by human recombinant tumour necrosis factor*. Br J Cancer, 1988. 58(3):
 p. 345-9.

- 230. Tisdale, M.J., Loss of skeletal muscle in cancer: biochemical mechanisms. Front Biosci, 2001. **6**: p. D164-74.
- 231. Lu, Y., et al., USP19 deubiquitinating enzyme supports cell proliferation by stabilizing KPC1, a ubiquitin ligase for p27Kip1. Mol Cell Biol, 2009. **29**(2): p. 547-58.
- 232. Hassink, G.C., et al., *The ER-resident ubiquitin-specific protease 19 participates* in the UPR and rescues ERAD substrates. EMBO Rep, 2009. **10**(7): p. 755-61.
- 233. Kubo, Y., Comparison of initial stages of muscle differentiation in rat and mouse myoblastic and mouse mesodermal stem cell lines. J Physiol, 1991. **442**: p. 743-59.
- 234. Sultan, K.R., et al., *Quantification of hormone-induced atrophy of large myotubes* from C2C12 and L6 cells: atrophy-inducible and atrophy-resistant C2C12 myotubes.

 Am J Physiol Cell Physiol, 2006. **290**(2): p. C650-9.
- 235. Evinger-Hodges, M.J., et al., *Inhibition of myoblast differentiation in vitro by a protein isolated from liver cell medium.* J Cell Biol, 1982. **93**(2): p. 395-401.
- 236. Andres, V. and K. Walsh, *Myogenin expression, cell cycle withdrawal, and* phenotypic differentiation are temporally separable events that precede cell fusion upon myogenesis. J Cell Biol, 1996. **132**(4): p. 657-66.
- 237. Jaynes, J.B., et al., *Transcriptional regulation of the muscle creatine kinase gene and regulated expression in transfected mouse myoblasts*. Mol Cell Biol, 1986. **6**(8): p. 2855-64.
- 238. Edmondson, D.G. and E.N. Olson, *Helix-loop-helix proteins as regulators of muscle-specific transcription*. J Biol Chem, 1993. **268**(2): p. 755-8.

- 239. Acharyya, S., et al., *Cancer cachexia is regulated by selective targeting of skeletal muscle gene products.* J Clin Invest, 2004. **114**(3): p. 370-8.
- 240. Tessitore, L., P. Costelli, and F.M. Baccino, *Humoral mediation for cachexia in tumour-bearing rats*. Br J Cancer, 1993. **67**(1): p. 15-23.
- 241. Solomon, V. and A.L. Goldberg, *Importance of the ATP-ubiquitin-proteasome* pathway in the degradation of soluble and myofibrillar proteins in rabbit muscle extracts. J Biol Chem, 1996. **271**(43): p. 26690-7.
- 242. Rudnicki, M.A. and R. Jaenisch, *The MyoD family of transcription factors and skeletal myogenesis*. Bioessays, 1995. **17**(3): p. 203-9.
- 243. Duprey, P. and C. Lesens, Control of skeletal muscle-specific transcription: involvement of paired homeodomain and MADS domain transcription factors. Int J Dev Biol, 1994. 38(4): p. 591-604.
- 244. Benezra, R., et al., *The protein Id: a negative regulator of helix-loop-helix DNA binding proteins*. Cell, 1990. **61**(1): p. 49-59.
- 245. Florini, J.R., D.Z. Ewton, and S.A. Coolican, *Growth hormone and the insulin-like growth factor system in myogenesis*. Endocr Rev, 1996. **17**(5): p. 481-517.
- 246. Ross, J., *mRNA stability in mammalian cells*. Microbiol Rev, 1995. **59**(3): p. 423-50.
- 247. Hatakeyama, S., et al., *U box proteins as a new family of ubiquitin-protein ligases*. J Biol Chem, 2001. **276**(35): p. 33111-20.
- 248. Suzumori, N., et al., *RFPL4 interacts with oocyte proteins of the ubiquitin- proteasome degradation pathway.* Proc Natl Acad Sci U S A, 2003. **100**(2): p. 550-5.

- 249. Clermont, Y., *Kinetics of spermatogenesis in mammals: seminiferous epithelium cycle and spermatogonial renewal.* Physiol Rev, 1972. **52**(1): p. 198-236.
- 250. Zhou, J. and E.N. Olson, *Dimerization through the helix-loop-helix motif*enhances phosphorylation of the transcription activation domains of myogenin. Mol
 Cell Biol, 1994. **14**(9): p. 6232-43.
- 251. Lin, H., et al., Divergent N-terminal sequences target an inducible testis deubiquitinating enzyme to distinct subcellular structures. Mol Cell Biol, 2000. **20**(17): p. 6568-78.
- 252. Seufert, W., J.P. McGrath, and S. Jentsch, *UBC1 encodes a novel member of an essential subfamily of yeast ubiquitin-conjugating enzymes involved in protein degradation*. Embo J, 1990. **9**(13): p. 4535-41.
- 253. Rotin, D., O. Staub, and R. Haguenauer-Tsapis, *Ubiquitination and endocytosis of plasma membrane proteins: role of Nedd4/Rsp5p family of ubiquitin-protein ligases.*J Membr Biol, 2000. **176**(1): p. 1-17.
- 254. Bays, N.W., et al., *Hrd1p/Der3p is a membrane-anchored ubiquitin ligase* required for ER-associated degradation. Nat Cell Biol, 2001. **3**(1): p. 24-9.
- 255. Medintz, I., H. Jiang, and C.A. Michels, *The role of ubiquitin conjugation in glucose-induced proteolysis of Saccharomyces maltose permease*. J Biol Chem, 1998. **273**(51): p. 34454-62.
- 256. Dohmen, R.J., et al., *The N-end rule is mediated by the UBC2(RAD6) ubiquitin-conjugating enzyme.* Proc Natl Acad Sci U S A, 1991. **88**(16): p. 7351-5.

- 257. Byrd, C., G.C. Turner, and A. Varshavsky, *The N-end rule pathway controls the import of peptides through degradation of a transcriptional repressor*. Embo J, 1998. **17**(1): p. 269-77.
- 258. Takeda, K. and M. Yanagida, *Regulation of nuclear proteasome by Rhp6/Ubc2* through ubiquitination and destruction of the sensor and anchor Cut8. Cell, 2005. **122**(3): p. 393-405.
- 259. Yamashita, K., M. Shinohara, and A. Shinohara, *Rad6-Bre1-mediated histone*H2B ubiquitylation modulates the formation of double-strand breaks during meiosis.

 Proc Natl Acad Sci U S A, 2004. **101**(31): p. 11380-5.
- 260. Game, J.C., et al., The RAD6/BRE1 histone modification pathway in Saccharomyces confers radiation resistance through a RAD51-dependent process that is independent of RAD18. Genetics, 2006. 173(4): p. 1951-68.
- 261. Hoege, C., et al., *RAD6-dependent DNA repair is linked to modification of PCNA by ubiquitin and SUMO*. Nature, 2002. **419**(6903): p. 135-41.
- 262. Gardner, R.G., Z.W. Nelson, and D.E. Gottschling, *Degradation-mediated protein quality control in the nucleus*. Cell, 2005. **120**(6): p. 803-15.
- 263. Deffenbaugh, A.E., et al., Release of ubiquitin-charged Cdc34-S Ub from the RING domain is essential for ubiquitination of the SCF(Cdc4)-bound substrate Sic1. Cell, 2003. 114(5): p. 611-22.
- 264. Verma, R., R.M. Feldman, and R.J. Deshaies, *SIC1 is ubiquitinated in vitro by a pathway that requires CDC4, CDC34, and cyclin/CDK activities.* Mol Biol Cell, 1997. **8**(8): p. 1427-37.

- 265. Skowyra, D., et al., *Reconstitution of G1 cyclin ubiquitination with complexes containing SCFGrr1 and Rbx1*. Science, 1999. **284**(5414): p. 662-5.
- 266. Flick, K., et al., *Proteolysis-independent regulation of the transcription factor*Met4 by a single Lys 48-linked ubiquitin chain. Nat Cell Biol, 2004. **6**(7): p. 634-41.
- 267. Kaiser, P., et al., Regulation of transcription by ubiquitination without proteolysis: Cdc34/SCF(Met30)-mediated inactivation of the transcription factor Met4. Cell, 2000. **102**(3): p. 303-14.
- 268. Chen, P., et al., *Multiple ubiquitin-conjugating enzymes participate in the in vivo degradation of the yeast MAT alpha 2 repressor*. Cell, 1993. **74**(2): p. 357-69.
- 269. Seufert, W. and S. Jentsch, *Ubiquitin-conjugating enzymes UBC4 and UBC5*mediate selective degradation of short-lived and abnormal proteins. Embo J, 1990.

 9(2): p. 543-50.
- 270. Laney, J.D., E.F. Mobley, and M. Hochstrasser, *The short-lived Matalpha2* transcriptional repressor is protected from degradation in vivo by interactions with its corepressors *Tup1* and *Ssn6*. Mol Cell Biol, 2006. **26**(1): p. 371-80.
- 271. Roth, A.F. and N.G. Davis, *Ubiquitination of the yeast a-factor receptor*. J Cell Biol, 1996. **134**(3): p. 661-74.
- 272. Kolling, R. and C.P. Hollenberg, *The first hydrophobic segment of the ABC-transporter, Ste6, functions as a signal sequence.* FEBS Lett, 1994. **351**(2): p. 155-8.
- 273. Horak, J. and D.H. Wolf, *Glucose-induced monoubiquitination of the Saccharomyces cerevisiae galactose transporter is sufficient to signal its internalization.* J Bacteriol, 2001. **183**(10): p. 3083-8.

- 274. Gitan, R.S. and D.J. Eide, *Zinc-regulated ubiquitin conjugation signals*endocytosis of the yeast ZRT1 zinc transporter. Biochem J, 2000. **346 Pt 2**: p. 32936.
- 275. Parag, H.A., et al., Selective ubiquitination of calmodulin by UBC4 and a putative ubiquitin protein ligase (E3) from Saccharomyces cerevisiae. FEBS Lett, 1993.

 325(3): p. 242-6.
- 276. Biederer, T., C. Volkwein, and T. Sommer, *Degradation of subunits of the Sec61p complex, an integral component of the ER membrane, by the ubiquitin-proteasome pathway.* Embo J, 1996. **15**(9): p. 2069-76.
- 277. Biederer, T., C. Volkwein, and T. Sommer, *Role of Cue1p in ubiquitination and degradation at the ER surface*. Science, 1997. **278**(5344): p. 1806-9.
- 278. Hampton, R.Y. and H. Bhakta, *Ubiquitin-mediated regulation of 3-hydroxy-3-methylglutaryl-CoA reductase*. Proc Natl Acad Sci U S A, 1997. **94**(24): p. 12944-8.
- 279. Gauss, R., T. Sommer, and E. Jarosch, *The Hrd1p ligase complex forms a linchpin between ER-lumenal substrate selection and Cdc48p recruitment.* Embo J, 2006. **25**(9): p. 1827-35.
- 280. Qin, S., et al., Cloning and characterization of a Saccharomyces cerevisiae gene encoding a new member of the ubiquitin-conjugating protein family. J Biol Chem, 1991. **266**(23): p. 15549-54.
- 281. Schule, T., et al., *Ubc8p functions in catabolite degradation of fructose-1, 6-bisphosphatase in yeast.* Embo J, 2000. **19**(10): p. 2161-7.

- 282. Eckert, J.H. and N. Johnsson, *Pex10p links the ubiquitin conjugating enzyme*Pex4p to the protein import machinery of the peroxisome. J Cell Sci, 2003. **116**(Pt 17): p. 3623-34.
- 283. Collins, C.S., et al., *The peroxisome biogenesis factors pex4p, pex22p, pex1p, and pex6p act in the terminal steps of peroxisomal matrix protein import.* Mol Cell Biol, 2000. **20**(20): p. 7516-26.
- 284. Townsley, F.M. and J.V. Ruderman, *Functional analysis of the Saccharomyces cerevisiae UBC11 gene.* Yeast, 1998. **14**(8): p. 747-57.
- 285. Hiraishi, H., M. Mochizuki, and H. Takagi, *Enhancement of stress tolerance in Saccharomyces cerevisiae by overexpression of ubiquitin ligase Rsp5 and ubiquitin-conjugating enzymes*. Biosci Biotechnol Biochem, 2006. **70**(11): p. 2762-5.
- 286. Gangavarapu, V., et al., *Mms2-Ubc13-dependent and -independent roles of Rad5 ubiquitin ligase in postreplication repair and translesion DNA synthesis in Saccharomyces cerevisiae*. Mol Cell Biol, 2006. **26**(20): p. 7783-90.
- 287. Haracska, L., et al., Opposing effects of ubiquitin conjugation and SUMO modification of PCNA on replicational bypass of DNA lesions in Saccharomyces cerevisiae. Mol Cell Biol, 2004. **24**(10): p. 4267-74.
- 288. Baarends, W.M., et al., Loss of HR6B ubiquitin-conjugating activity results in damaged synaptonemal complex structure and increased crossing-over frequency during the male meiotic prophase. Mol Cell Biol, 2003. **23**(4): p. 1151-62.
- 289. Kavakebi, P., et al., *The N-end rule ubiquitin-conjugating enzyme, HR6B, is up-*regulated by nerve growth factor and required for neurite outgrowth. Mol Cell
 Neurosci, 2005. **29**(4): p. 559-68.

- 290. Kaiser, P., et al., *A human ubiquitin-conjugating enzyme homologous to yeast UBC8*. J Biol Chem, 1994. **269**(12): p. 8797-802.
- 291. Kamynina, E., et al., *A novel mouse Nedd4 protein suppresses the activity of the epithelial Na+ channel.* Faseb J, 2001. **15**(1): p. 204-214.
- 292. Honda, R., H. Tanaka, and H. Yasuda, *Oncoprotein MDM2 is a ubiquitin ligase*E3 for tumor suppressor p53. FEBS Lett, 1997. **420**(1): p. 25-7.
- 293. Younger, J.M., et al., A foldable CFTR{Delta}F508 biogenic intermediate accumulates upon inhibition of the Hsc70-CHIP E3 ubiquitin ligase. J Cell Biol, 2004. **167**(6): p. 1075-85.
- 294. Spencer, E., J. Jiang, and Z.J. Chen, *Signal-induced ubiquitination of IkappaBalpha by the F-box protein Slimb/beta-TrCP*. Genes Dev, 1999. **13**(3): p. 284-94.
- 295. Hakli, M., et al., *Transcriptional coregulator SNURF (RNF4) possesses ubiquitin E3 ligase activity.* FEBS Lett, 2004. **560**(1-3): p. 56-62.
- 296. Albert, T.K., et al., *Identification of a ubiquitin-protein ligase subunit within the CCR4-NOT transcription repressor complex.* Embo J, 2002. **21**(3): p. 355-64.
- 297. Dominguez, C., et al., Structural model of the UbcH5B/CNOT4 complex revealed by combining NMR, mutagenesis, and docking approaches. Structure, 2004. **12**(4): p. 633-44.
- 298. Saville, M.K., et al., *Regulation of p53 by the ubiquitin-conjugating enzymes UbcH5B/C in vivo.* J Biol Chem, 2004. **279**(40): p. 42169-81.
- 299. Huang, J., et al., *High-throughput screening for inhibitors of the e3 ubiquitin ligase APC*. Methods Enzymol, 2005. **399**: p. 740-54.

- 300. Polanowska, J., et al., *A conserved pathway to activate BRCA1-dependent ubiquitylation at DNA damage sites*. Embo J, 2006. **25**(10): p. 2178-88.
- 301. Yamada, H.Y. and G.J. Gorbsky, *Tumor suppressor candidate TSSC5 is regulated* by *UbcH6 and a novel ubiquitin ligase RING105*. Oncogene, 2006. **25**(9): p. 1330-9.
- 302. Zhu, B., et al., *Monoubiquitination of human histone H2B: the factors involved and their roles in HOX gene regulation*. Mol Cell, 2005. **20**(4): p. 601-11.
- 303. Anan, T., et al., *Human ubiquitin-protein ligase Nedd4: expression, subcellular localization and selective interaction with ubiquitin-conjugating enzymes.* Genes Cells, 1998. **3**(11): p. 751-63.
- 304. Kumar, S., W.H. Kao, and P.M. Howley, *Physical interaction between specific E2* and Hect E3 enzymes determines functional cooperativity. J Biol Chem, 1997.

 272(21): p. 13548-54.
- 305. Imai, Y., M. Soda, and R. Takahashi, *Parkin suppresses unfolded protein stress-induced cell death through its E3 ubiquitin-protein ligase activity.* J Biol Chem, 2000. **275**(46): p. 35661-4.
- 306. Ardley, H.C., et al., *Genomic organization of the human ubiquitin-conjugating* enzyme gene, UBE2L6 on chromosome 11q12. Cytogenet Cell Genet, 2000. **89**(1-2): p. 137-40.
- 307. Fortier, J.M. and J. Kornbluth, *NK lytic-associated molecule, involved in NK cytotoxic function, is an E3 ligase*. J Immunol, 2006. **176**(11): p. 6454-63.
- 308. Zhang, Y., et al., Parkin functions as an E2-dependent ubiquitin- protein ligase and promotes the degradation of the synaptic vesicle-associated protein, CDCrel-1. Proc Natl Acad Sci U S A, 2000. **97**(24): p. 13354-9.

- 309. Gabellini, D., et al., Early mitotic degradation of the homeoprotein HOXC10 is potentially linked to cell cycle progression. Embo J, 2003. **22**(14): p. 3715-24.
- 310. Townsley, F.M., et al., *Dominant-negative cyclin-selective ubiquitin carrier* protein E2-C/UbcH10 blocks cells in metaphase. Proc Natl Acad Sci U S A, 1997. **94**(6): p. 2362-7.
- 311. Deng, L., et al., Activation of the IkappaB kinase complex by TRAF6 requires a dimeric ubiquitin-conjugating enzyme complex and a unique polyubiquitin chain.

 Cell, 2000. **103**(2): p. 351-61.
- 312. Schulman, B.A. and Z.J. Chen, *Protein ubiquitination: CHIPping away the symmetry*. Mol Cell, 2005. **20**(5): p. 653-5.
- 313. Lisztwan, J., et al., Association of human CUL-1 and ubiquitin-conjugating enzyme CDC34 with the F-box protein p45(SKP2): evidence for evolutionary conservation in the subunit composition of the CDC34-SCF pathway. Embo J, 1998.

 17(2): p. 368-83.
- 314. Liu, Q., et al., *Ubiquitin-conjugating enzyme 3 delays human lens epithelial cells in metaphase*. Invest Ophthalmol Vis Sci, 2006. **47**(4): p. 1302-9.
- 315. Sutterluty, H., et al., *p45SKP2 promotes p27Kip1 degradation and induces S phase in quiescent cells.* Nat Cell Biol, 1999. **1**(4): p. 207-14.
- 316. Charrasse, S., et al., Degradation of B-Myb by ubiquitin-mediated proteolysis: involvement of the Cdc34-SCF(p45Skp2) pathway. Oncogene, 2000. **19**(26): p. 2986-95.

- 317. Pagano, M., et al., Role of the ubiquitin-proteasome pathway in regulating abundance of the cyclin-dependent kinase inhibitor p27. Science, 1995. **269**(5224): p. 682-5.
- 318. Oh, R.S., X. Bai, and J.M. Rommens, *Human homologs of Ubc6p ubiquitin-conjugating enzyme and phosphorylation of HsUbc6e in response to endoplasmic reticulum stress*. J Biol Chem, 2006. **281**(30): p. 21480-90.
- 319. Kim, B.W., et al., Endoplasmic reticulum-associated degradation of the human type 2 iodothyronine deiodinase (D2) is mediated via an association between mammalian UBC7 and the carboxyl region of D2. Mol Endocrinol, 2003. 17(12): p. 2603-12.
- 320. Vourc'h, P., et al., *Mutation screening and association study of the UBE2H gene on chromosome 7q32 in autistic disorder*. Psychiatr Genet, 2003. **13**(4): p. 221-5.
- 321. Panaretou, C., et al., Characterization of p150, an adaptor protein for the human phosphatidylinositol (PtdIns) 3-kinase. Substrate presentation by phosphatidylinositol transfer protein to the p150.Ptdins 3-kinase complex. J Biol Chem, 1997. 272(4): p. 2477-85.
- 322. Hekmatpanah, D.S. and R.A. Young, *Mutations in a conserved region of RNA polymerase II influence the accuracy of mRNA start site selection.* Mol Cell Biol, 1991. **11**(11): p. 5781-91.
- 323. de Melker, A.A., G. van der Horst, and J. Borst, *c-Cbl directs EGF receptors into* an endocytic pathway that involves the ubiquitin-interacting motif of Eps15. J Cell Sci, 2004. **117**(Pt 21): p. 5001-12.

- 324. Elshourbagy, N.A., et al., *Rat ATP citrate-lyase. Molecular cloning and sequence analysis of a full-length cDNA and mRNA abundance as a function of diet, organ, and age.* J Biol Chem, 1990. **265**(3): p. 1430-5.
- 325. Freedman, R.B., P. Klappa, and L.W. Ruddock, *Protein disulfide isomerases* exploit synergy between catalytic and specific binding domains. EMBO Rep, 2002. **3**(2): p. 136-40.
- 326. Forgac, M., *The vacuolar H+-ATPase of clathrin-coated vesicles is reversibly inhibited by S-nitrosoglutathione*. J Biol Chem, 1999. **274**(3): p. 1301-5.
- 327. Minturn, J.E., et al., *Early postmitotic neurons transiently express TOAD-64, a neural specific protein.* J Comp Neurol, 1995. **355**(3): p. 369-79.